Temperature and soil nutrient availability shape tree responses to elevation in the Australian Wet Tropics: growth, physiology, and chemistry

Arun Singh Ramesh, MRes

Supervisors: A/Prof Lucas Cernusak,
Prof Darren Crayn and Dr Alexander Cheesman

Submitted in complete fulfilment of the requirements for the degree of Doctor of Philosophy in Natural Sciences

College of Science and Engineering, James Cook University

[March–2023]

To mumma and papa, Sunanda and Ramesh Singh, my dear in-laws, Tushar Prabhu and Sunetra Giridhar, and my beloved, Apoorva Prabhu, with love.....

Acknowledgements

The work presented in this thesis was only possible with the support of individuals and groups to whom I am grateful. I would firstly like to acknowledge and thank the traditional owners of the land, the Kuku-yalanji, Durbalngan, and Djabuganjdji people, and pay my respects to the elders of the land on which my research was conducted.

I would like to specifically thank my primary supervisor A/Prof Lucas Cernusak who has been a great mentor and with whom I have established a good student-supervisor relationship over the past five years. His routine meetings and periodic brainstorming discussions have led to some brilliant ideas in exploring the ecophysiology of tropical mountaintop trees. My co-supervisors Prof Darren Crayn and Dr Alexander Cheesman have been a great asset, my thanks to them for their patience, and providing me with all the constructive criticism and motivation at times when it was most needed.

I am thankful to Dr Habacuc Flores-Moreno for his advice relating to the statistical approach for chapters 3 and 4 of this PhD and providing me with suggestions on technical aspects that have improved the thesis greatly. Dr Noel Preece and Dr Penny van Oosterzee are acknowledged for helping facilitate seed collection of target tree species from their Thiaki property in the Atherton Tablelands. Dr Jen Whan and Dr Yi Hu at JCU are acknowledged for assistance with isotope and elemental analysis of leaf and soil samples that were generated as part of this PhD. Dr Edita Ritmejeryte is acknowledged for assisting with phenolics and antioxidant assays from experimental leaf samples and for technical advice in chapter 4 of the thesis. Prof Mike Liddell, Prof Susan Laurance and Prof Paul Nelson are also acknowledged for helping me with technical aspects and providing creative ideas.

I would like to thank Prof Bill McDonald and Dr Lousie Ashton for allowing the use of Mt Lewis study sites and sharing the tree basal area measurements that were used in Chapter 2 of this thesis. Dr Ana Palma and the Australian Tropical Herbarium staff, especially Stuart Worboys, are acknowledged for their support during the initial stages of my field work component. The staff of the Daintree Rainforest Observatory, Dr Michele Schiffer and Andrew Thompson, and the Daintree Discovery Centre, Abi Ralph, are acknowledged for providing access and resources during my visits to the Daintree rainforest. Broadcast Australia and station operator, Spiro Buhagiar, are acknowledged for providing cable car access to Mt Bellenden Ker. I am also thankful to the plant propagators at Yuruga Nursery,

Ty and Ted, and Cathy at Kuranda nursery, for assisting with mountaintop plant propagation through cuttings of tree material that were initially selected for experimental studies.

This thesis would not have been possible without the constant support of my family, especially Apoorva Prabhu, Prof Tushar Prabhu, Prof Sunetra Giridhar, mom, and dad to whom I am indebted, and my deepest acknowledgements and gratitude go to these pillars of strength.

I would like to thank several research colleagues, friends and network of ecologists and scientists with whom I have enjoyed this PhD journey. I am grateful to A/Prof John Dwyer, Prof Rod Fensham and Prof Margaret Mayfield at the University of Queensland for hosting me when I needed research space during my stint in Brisbane. I would like to thank Dr Siddeswara Guru for supporting me with a casual contract at TERN, Brisbane. Dr Nara Vogado and Jayden Engert for being wonderful company throughout my PhD and for being kind hosts whenever I need a space during my visits to Cairns. Dr Yoko Ishida and Andrew Gray-Spence are acknowledged for being great company and helping create a friendly atmosphere at the Centre for Tropical Environmental and Sustainability Sciences (TESS) and IT support when needed. There are several postgraduate students at JCU who are worth mentioning here: Pauline, Kali, Lizzy, Russel, Ryan, Rachel, Nahid, Linda, Damian, Lauren, Lain, Jane, Cos and the amazing network of students and staff at TESS with whom I shared memories during this candidature.

Lastly, I would like to thank the College of Science and Engineering, James Cook University, for providing me with an international postgraduate research scholarship, the staff at JCU academic services for assistance with academic paperwork, and the staff at Graduate Research School for providing me with candidature extensions for loss of time due to COVID-19. Prof Hilary Whitehouse is also acknowledged for her support during difficult times (such as the COVID-19, and personal reasons). I would like to acknowledge the Department of Environment and Science, Queensland National Parks, and the Rangers, Mossman for allowing access to conduct scientific research in the National Parks.

I am grateful to the funding bodies that provided financial aid for this thesis, The Skyrail Rainforest Foundation, The Wet Tropics Management Authority, and The Ian Potter Foundation that helped with field work travel, analytical and experimental costs.

Statement of Original Authorship

The work contained in this thesis has not been previously submitted to meet requirements for an award at this or any other higher education institution. To the best of my knowledge and belief, the thesis contains no material previously published or written by another person except where due reference is made.

Signature: _____

Date: 12 March 2023

Statement of the Contributions

The thesis was initially conceived and designed by me, Arun Singh (AS) and over time was developed and improved under the supervision of Lucas Cernusak (LC), Alexander Cheesman (AC) and Darren Crayn (DC). AS conducted field work, experimental data collection and wrote the thesis draft with inputs from LC, AC and DC. Editorial assistance throughout the thesis chapters was provided by all my supervisors.

During the initial phase, AS consulted the Australian Tropical Herbarium and conducted field work with Stuart Worboys and target species selection was developed in consultation with DC. AS and AC also collaborated with Prof Bill McDonald for identifying study plots along an elevation transect in Mt Lewis National Park. Dr Noel Preece, Dr Penny van Oosterzee and Dr Ana Palma assisted with seed collection. Jayden Engert and Iftakharul (Russel) Alam assisted with soil sample collection and sensor deployment, respectively, in the Mt Lewis transect. Damian Settle and Jayden Engert assisted with experimental plant harvests. Dr Jen Whan and Dr Yi Hu assisted with leaf and soil nutrient analysis and Dr Edita Ritmejeryte with phenolics and antioxidant assays.

Statistical advice for chapters 3 and 4 was provided by Dr Habacuc Flores-Moreno and LC. All research communications and journal publications published so far have been co-authored by my supervisors and where appropriate I have included external collaborators.

Financial support for this thesis was provided by the following:

- The Skyrail Rainforest Foundation:
  AUD $5,000 (Round-1: 2018 – 2019)
  AUD $5,000 (Round-2: 2019 – 2020)
- The Wet Tropics Management Authority:
  AUD $3,920.80 (2019 – 2020)

In addition, the bulk of experimental consumables, analytical fees and journal research publication costs were provided by The Ian Potter Foundation to the principal investigator, DC and co-investigators LC and AC. JCU also supported conference travel fees and PhD related consumables throughout my candidature under the HDR student support fees (AUD 1,000 per annum) for the duration of my candidature (2018 – 2022). The Terrestrial Ecosystem Research Network (TERN), Ecosystem Processes team supported field work costs for microclimate data retrieval during the final phase of my PhD (2022).

Chapter number	Title and status of publication	Author contributions and statement of support
1	General Introduction	Arun Singh (AS) wrote the initial draft of this chapter. Editorial assistance was provided by Alexander Cheesman (AC), Lucas Cernusak (LC) and Darren Crayn (DC).
2	Singh Ramesh, A., Cheesman, A.W., McDonald, W.J.F., Crayn, D.M. and Cernusak, L.A. (2023). *Microclimate, soil nutrients and soil stable isotope composition in relation to elevation in the Australian Wet Tropics* (In preparation for journal submission)	AS, AC and LC conceived the chapter. AS conducted field data collection, analysis and wrote the initial draft. Advice on statistical approach was provided by AC and LC. Writing assistance was provided by AC, LC and DC. Study site selection was conducted by AS, AC and LC in consultation with Prof Bill McDonald. Jen Whan and Yi Hu assisted with nutrient and isotope analysis from field soil samples. Field exploration for soil nutrients and sensor deployment was conducted by AS with assistance from Jayden Engert and Iftakharul (Russel) Alam respectively (specifically in Mt Lewis sites).
3	Singh Ramesh, A., Cheesman A.W., Flores-Moreno H., Preece, N.D., Crayn, D.M. and Cernusak, L.A. (2023). *Temperature, nutrient availability, and species traits interact to shape elevation responses of Australian tropical trees.* Front. For. Glob. Change 6:1089167. DOI: 10.3389/ffgc.2023.1089167 (published January 2023)	AS and LC conceived the chapter with inputs from AC and Habacuc Flores-Moreno (HFM). AS conducted field data collection and experimental work under the supervision of LC and AC. AS conducted statistical analysis with assistance from HFM and LC. DC helped develop species selection and Noel Preece facilitated seed collection. Data on stem diameter growth in the field was from the CSIRO permanent long-term forest monitoring plots. AS wrote the initial manuscript draft with writing assistance from all co-authors on the publication. Two anonymous reviewers also provided writing suggestions that greatly improved this manuscript.
4	Singh Ramesh, A., Ritmejeryte, E., Cheesman, A.W., Flores-Moreno, H., Crayn, D.M. and Cernusak, L.A. (2023). *Foliar chemistry in tropical rainforest trees is regulated by the temperature responses of leaf photosynthetic capacities.* (In preparation for journal submission)	AS and LC conceived the chapter with input from AC. AS conducted data collection and experimental leaf gas exchange under the guidance of LC and AC. Edita Ritmejeryte assisted with the plant phenolics assay and Jen Whan assisted with nutrient analysis from field and experimental leaf samples. AS conducted the statistical analysis with assistance from HFM and LC. AS wrote the initial manuscript draft with writing assistance from all co-authors in the chapter.
5	General discussion	AS wrote this chapter and all supervisors assisted with editing.

List of Publications

Research articles

Chapter 2

Singh Ramesh, A., Cheesman, A.W., McDonald, W.J.F., Crayn, D.M. and Cernusak, L.A. *Microclimate, soil nutrients and soil stable isotope composition in relation to elevation in the Australian Wet Tropics* (In preparation for submission to the journal Agricultural and Forest Meteorology).

Chapter 3

Singh Ramesh, A., Cheesman, A.W., Flores-Moreno, H., Preece, N.D., Crayn, D.M. and Cernusak, L.A. (2023). *Temperature, nutrient availability, and species traits interact to shape elevation responses of Australian tropical trees*. Frontiers in Forests and Global Change 6:1089167. DOI: 10.3389/ffgc.2023.1089167 (published January 2023)

Chapter 4

Singh Ramesh A., Ritmejeryte, E., Cheesman, A.W., Flores-Moreno, H., Crayn, D.M. and Cernusak, L.A. *Foliar chemistry in tropical rainforest trees is regulated by the temperature responses of leaf photosynthetic capacities*. (In preparation for submission to the journal Plant, Cell & Environment)

Conference presentations

- **Singh Ramesh, A.**, Cheesman, A.W., Crayn, D.M., and Cernusak, L.A. (November 2020). *Leaf thermoregulation among congeners across elevation gradients from wet tropics of Far North Queensland.* Ecological Society of Australia (online).
- **Singh Ramesh, A.**, Cheesman, A.W., Crayn, D.M., and Cernusak, L.A. (February 2022). *Are tropical mountaintop trees constrained in their distributions by physiological limitations: Thermal adaptation and acclimation to climate change.* Early career researcher conference by the Royal Society of Queensland (online)
- **Singh Ramesh, A.**, Cheesman, A.W., Crayn, D.M., and Cernusak, L.A. (November 2022). *Temperature response of tropical rainforest tree seedlings: did the tropical*

mountaintop tree survive experimental warming? Ecological Society of Australia.

Data and abstract publications

- **Singh Ramesh, A.,** Cheesman, A. & Cernusak, L. (2022): Far North Queensland Microclimate Data. Version 1.0. Terrestrial Ecosystem Research Network. (Dataset). https://portal.tern.org.au/metadata/TERN/56be85d3-94fa-4e8b-b249-e4862fa3b5a6
- **Singh Ramesh, A.**, Cheesman, A.W., Crayn, D.M., and Cernusak, L.A. (February 2022). *Are tropical mountaintop trees constrained in their distributions by physiological limitations: Thermal adaptation and acclimation to climate change*. 131. https://doi.org/10.53060/prsq.2022-08

Keywords

Australian Wet Tropics, biomass allocation, climate warming, $\delta^{13}C$, $\delta^{15}N$, elevation gradient, J_{max}/V_{cmax}, leaf chlorophyll, leaf phenolics, leaf N, LMA, microclimate, relative growth rates, root- to-shoot biomass ratio, soil C:N, soil $\delta^{15}N$, soil nutrient availability, soil temperature, stem diameter growth, wet tropical mountaintops

Abbreviations

A_{net} – Net leaf photosynthetic rate

a.s.l. – Above sea level

ATR – Annual temperature range

AWT – Australian Wet Tropics World Heritage Area

C:N – Carbon-to-nitrogen ratio

DBH – Diameter at breast height

DTR – Diel temperature range

$\Delta T_{soil-air}$ – Soil-to-air temperature difference

$\Delta T_{wet-dry}$ – Temperature difference between wettest and driest quarters of the year

$\delta^{13}C$ – Carbon stable isotope composition ($^{13}C/^{12}C$) with respect to a standard

$\delta^{15}N$ – Nitrogen stable isotope composition ($^{15}N/^{14}N$) with respect to a standard

FvCB – Farqhuar-von Caemmerer-Berry photosynthesis model (Farquhar *et al*. 1980)

GA – Gallic acid

J_{max} – Maximum rate of electron transport

LMA – Leaf dry mass per unit leaf area

MAP – Mean annual precipitation

MAT – Mean annual temperature

NR – Nutrient-rich soil type

NP – Nutrient-poor soil type

PAR – Photosynthetically active radiation

RGR – Relative growth rates

RuBisCO – Ribulose-1,5-bisphosphate carboxylase

T_{growth} – Growth temperature

T_{leaf} – Leaf temperature

V_{cmax} – Maximum rate of carboxylation

VPD – Vapour pressure deficit

Abstract

Tropical rainforest ecosystems are projected to become warmer by *ca* 4°C by the end of this century. Such an increase in surface air temperatures will likely have consequences on tropical tree growth, physiology, and biochemistry. This is especially concerning for tree species that are currently restricted to a narrow range of environmental conditions, such as those found on tropical mountaintops, where species operate under resource-poor conditions and specific thermal regimes - now subject to change. Such vulnerable systems can be found across the Australian Wet Tropics (AWT) World Heritage Area, where bioclimatic models suggest a decline in habitat suitability for most tree species restricted to the tropical mountaintops (>1000 meters a.s.l.). With no available alternative habitat to migrate toward under projected climate warming, these systems are likely facing tree species loss and ecosystem degradation. Therefore, understanding how tropical trees will respond to increased warming is a necessary first step in conservation and management of these fragile ecosystems. This knowledge is currently constrained due to the paucity of data on the temperature responses of tree growth, physiology, and biochemistry for species from the AWT.

In this thesis, I address this important knowledge-gap by asking, a) whether mountaintop tree species are constrained in their distributions due to physiological limitations; and b) whether species display physiological tolerances and growth performance with an ability to acclimate to climate warming.

I first studied (**Chapter 2**) *in-situ* microclimate (i.e., Soil, near Surface air, and above ground Air temperatures) and soil properties (i.e., C:N ratio, organic matter, pH) to understand how they co-vary across an elevation gradient in the AWT. Here, I identified trends across elevation in the temperature difference between soil and above ground air ($\Delta T_{soil-air}$), as well as in the diel and annual temperature ranges. I found that $\Delta T_{soil-air}$ increased with elevation, and soils were cooler than air during the day and warmer during the night across sites. The diel and annual temperature range for both soil and air was higher for a mountaintop site compared to the lowland sites. I also observed that soil C:N ratio and organic matter content increased with elevation and were correlated with climatic variables, suggesting an interaction of climate and edaphic conditions experienced by the seedlings in the rainforest understory. These results are important because of the direct impacts these predictors have on below canopy processes, such as seed germination and sapling growth, that shape tree

communities. This chapter demonstrates that environmental variables other than temperature need to be considered when examining species physiological responses across elevation gradients and may be fundamental to predicting responses to future changes in climate.

Chapters 3 and **4** report on a combination of field and experimental glasshouse studies that examined the interactive impacts of soil nutrient availability and temperature on plant growth, leaf traits, physiology, and biochemistry. In **Chapter 3**, I evaluated stem diameter growth rates and functional leaf traits of a rainforest tree genus, *Flindersia*, across an elevation gradient in the AWT. I then conducted a controlled-environment glasshouse experiment to evaluate the relative roles that nutrient availability and temperature play in shaping those observations. For this work, I investigated a tropical mountaintop restricted tree species, *F. oppositifolia*, and three widespread congeners distributed across a relatively wide elevational range in the AWT, namely, *F. ifflana*, *F. bourjotiana,* and *F. brayleyana,* with seeds sourced from a Lowland, Mid-elevation and an Upland rainforest site respectively. The results from the field-based study displayed trends in species' growth and leaf functional traits in relation to elevation, such that stem diameter growth and leaf $\delta^{15}N$ decreased and leaf dry mass per leaf area trait and leaf $\delta^{13}C$ increased with elevation, suggesting controls from either climate, soil nutrient availability, and/or species turnover across elevation. However, under experimental conditions I observed that species displayed specific growth functional strategies and leaf traits that were impacted by an interaction of temperature and soil nutrients. There were instances when certain leaf traits such as leaf $\delta^{13}C$ displayed opposing trends from those observed in the field, indicating the importance of other covarying drivers that could not be reproduced in the glasshouse. The distinguishing feature of the mountaintop restricted species (*F. oppositifolia*) was a proportionally higher allocation of resources to roots under conditions approximating its mountaintop environment (nutrient-poor soil and cold growth temperature). I concluded from these results that species' traits interact with temperature and soil nutrient availability to drive observed functional patterns in the field in response to elevation in the AWT.

In **Chapter 4**, I used the same experimental set-up as in chapter 3 but evaluated species' physiological performances and relative allocation in foliar biochemistry. Specifically, I tested species' physiological limitations by studying the temperature response of leaf photosynthetic capacities (i.e., maximum rates of carboxylation- V_{cmax} and maximum rates of electron transport- J_{max}) obtained by fitting the Farqhuar-von Cammemaer-Berry (FvCB) model of C_3 photosynthesis to light saturated net carbon dioxide assimilation (A–C_i) curves. Here, I found the ratio of J_{max}/V_{cmax} to decline with leaf temperature, and with

differing slopes in plants grown at higher temperatures. I also found that leaf phenolics strongly declined with warming and were positively related to J_{max}/V_{cmax} measured at the chamber growth temperature. Thermal generalists (widely distributed congeners) were able to take advantage of increased N availability to increase their leaf chlorophyll concentrations under warmer growth temperatures, whereas the mountaintop restricted thermal specialist displayed limited plasticity in leaf chlorophyll. The results from this chapter suggest species-specific physiological controls on the flexibility of foliar chemistry, with implications for tree growth and defense under future climate warming.

Overall, the thesis has found important results in terms of environmental drivers that need to be considered while examining the physiology and growth responses of tree species in the tropics. The thesis fills an important knowledge-gap on the temperature and soil nutrient effects on the ecophysiology of tropical rainforest tree species along an elevation gradient in the AWT World Heritage Area, and in particular, the temperature sensitivity and physiological limitations of mountaintop restricted tree species. The overarching results from this thesis on species' specific growth and physiological responses to temperature and soil nutrients opens further opportunities for future projects on climate change impacts, plant-soil interactions and conservation planning of endemic tree species in the tropics.

Chapter 1 of the thesis is a general introduction and **Chapter 5** is a general discussion and conclusion of my thesis' findings.

Table of Contents

Acknowledgements ..... *i*

Statement of Original Authorship ..... *iii*

Statement of the Contributions ..... *iv*

List of Publications ..... *vi*

Keywords ..... *viii*

Abbreviations ..... *ix*

Abstract ..... *x*

Table of Contents ..... *xiii*

Chapter 1. General introduction… 14

Chapter 2. Microclimate, soil nutrients and soil stable isotopes in relation to elevation in the Australian Wet Tropics 19

Chapter 3. Temperature, nutrient availability, and species traits interact to shape elevation responses of Australian tropical trees… 51

Chapter 4. Foliar chemistry in tropical rainforest trees is regulated by the temperature responses of leaf photosynthetic capacities 77

Chapter 5. General discussion and conclusion… 106

Bibliography 115

Chapter 1: General Introduction

1.1 Background

Tropical rainforests occupy less than 12% of the global land area but act as a major atmospheric carbon sink, accounting for about half of terrestrial photosynthesis (Malhi and Grace, 2000; Saatchi et al., 2011). Climate models under the Representative Concentration Pathways (RCP) adopted by the IPCC predict a rise in global mean surface air temperatures for the period 2081 – 2100 relative to 1986 – 2005 in the following ranges: *ca* 1.1 to 2.6°C (RCP 4.5), and 2.6 to 4.8°C (RCP 8.5), when atmospheric CO_2 concentrations are predicted to stabilize at *ca* 550 and 940 ppm respectively (McInnes et al., 2015; Burke et al., 2018). This is of major concern as such temperatures have not been experienced since the Pliocene (*ca* 3.3 – 3.0 Mya) in the case of RCP 4.5, or Eocene (*ca* 50 Mya) in the case of RCP 8.5 projections (Burke et al., 2018).

Under such conditions, species may have to rapidly migrate or adapt to novel climate scenarios to avoid the risk of extinction (Alonso-Amelot, 2008). Paleoclimate studies have shown that angiosperm dominated tropical forests persisted through historical climate change, for example through the Palaeocene – Eocene (*ca* 55 Mya) transition (Jaramillo et al., 2010), where temperatures were *ca* 10°C higher than that recorded in the Holocene (*ca* 11,700 years ago) (Huber and Caballero, 2011; Malhi, 2012), indicating that plants may have a capacity to adapt to predicted warming (Malhi, 2012). However, given the rate and intensity of anthropogenic induced climate change compared to paleoclimatic transitions, questions remain as to species' potential to adapt to such rapid shifts.

Tropical montane ecosystems constitute a vast expanse of (relatively) undisturbed landscapes, which harbor complex biodiversity and regionally endemic taxa (Bruijnzeel et al., 2011; Fahey et al., 2016). However, species restricted to these biomes are considered particularly vulnerable to projected climate change because they often occupy specialized thermal regimes based on their observed climatic niches, making them susceptible to any disruption (Alonso-Amelot, 2008). It has been implicitly assumed that climatic factors, such as increase in temperatures or decrease in moisture at lower elevations, are primarily responsible for restricting species to the tropical mountaintops (Williams et al., 2003; Oliveira et al., 2014; Costion et al., 2015). However, there is growing evidence to suggest that species restricted to these biomes are also influenced by additional biophysical and edaphic factors,

such as topography and soil nutrient availability (Vitousek, 1998; Bellingham and Tanner, 2000; Condit et al., 2013; Bunyan et al., 2015; Elsen and Tingley, 2015); and biotic interactions and dispersal limitations (Schemske et al., 2009; Rehm and Feeley, 2015; Ensslin et al., 2018; Freeman et al., 2018).

Range shifts of tropical montane species and altered community structure have been detected in Costa Rica (Colwell et al., 2008); and upslope migration of lowland plant communities across elevation gradients has been observed in the tropical Andes, Borneo and Madagascar (Colwell et al., 2008; Laurance et al., 2011; Freeman et al., 2018). These observations suggest that climate may be the predominant factor that controls or restricts species current distributions; however, this does not necessarily reflect a species' fundamental climatic niche, or their capacity to adapt to novel climate regimes (Bush et al., 2018). Although many studies have highlighted temperature as an important factor limiting tropical mountaintop species distributions, experimental evaluation of this is rare (Cavaleri et al., 2015). The potential for disparities between species' realized and potential thermal limits may cause bioclimatic models based upon observed distributions to underestimate species' capacities to persist *in-situ* (Bush et al., 2018). Studies involving a combination of examining *in-situ* responses along elevation gradients and controlled targeted experiments might help us better understand species' responses to changing environmental conditions. This detailed understanding is necessary to inform both ecosystem-wide protection and the targeting of efforts to prevent species-level extinctions (Costion et al., 2015).

1.2 Thesis rationale and objectives

1.2.1 Rationale

The Australian Wet Tropics (AWT) region of far north Queensland represents an important area (*ca* 10,000 km^2) of tropical forest, which is home to more than 3300 vascular plants, 700 vertebrates, and more than 500 species of other life forms (Weber et al., 2021; Williams et al., 2016). This small portion (~0.12%) of the Australian continent was declared a World Heritage Area in the year 1988 and has since been managed by the Wet Tropics Management Authority. Within the AWT, montane areas (herein defined as above ~1000 m a.s.l.) constitute just 5% (~500 km^2) of the land area (Figure 1), but contribute significantly to regional ecosystem functioning, productivity and services (McJannet et al., 2006; Williams et al., 2003); and biodiversity, containing the entire home range of more than 80 vascular plant species (Metcalfe, 2009; D.M. Crayn pers. comm. 2023).

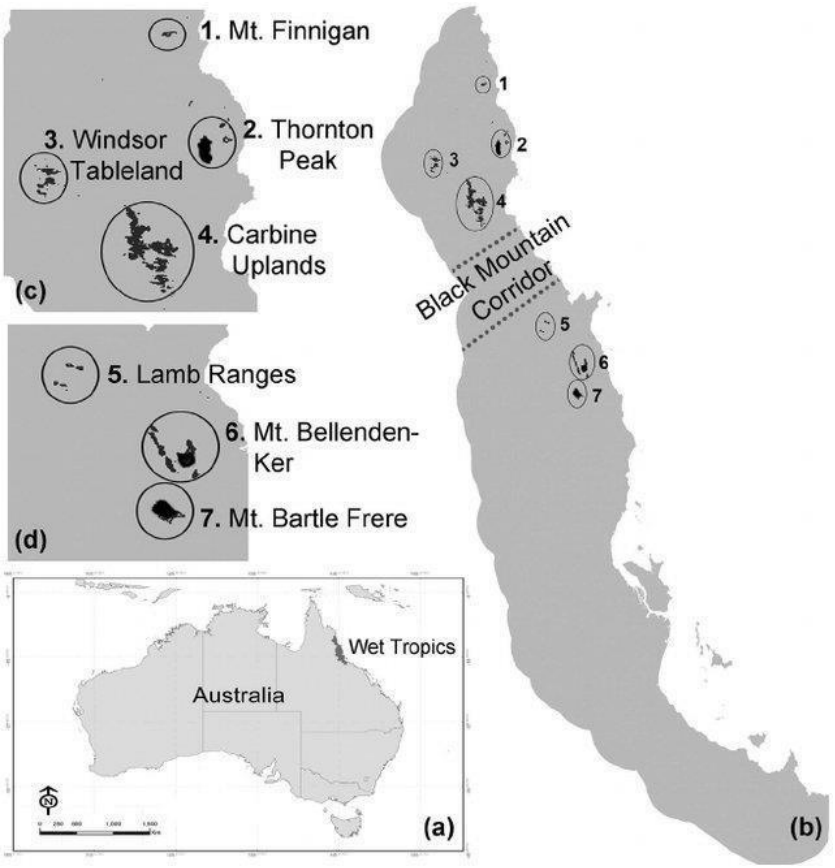

Figure 1. Reproduced from Costion et al. (2015). The Australian Wet Tropics bioregion of northeast Queensland highlighted (a); region overview (b); and centers of species diversity for the mountaintop endemic flora zoomed in for regions north (c) and south (d) of the Black Mountain Corridor.

The assembly of the Australian flora has been strongly influenced by two biogeographical processes since the Sahul paleocontinent broke from Antarctica in the Oligocene (*ca* 33.9 – 23 Mya) and drifted northward, colliding with the Sunda shelf in the mid Miocene (*ca* 23 – 5.3 Mya): Gondwanan vicariance and Asian immigration (Yap et al., 2018). Lineages deriving from these two processes tend to have different climate tolerances. A greater proportion of the lowland forests in the AWT consist of species from the Sunda continental shelf (southeast Asian origin) that favor a warm humid climate, while plants from the Sahul continental shelf (Australia and the island of New Guinea) occupy cooler upland refugia (Crayn et al., 2015; Joyce et al., 2020). Paleo records and biogeographic studies have also suggested that patterns of community structure and assembly in the AWT have been shaped over time by climatic factors such as aridity (Bowman and McDonough, 1991; Thornhill et al., 2016). Pleistocene contraction of lowland rainforest extent, and the isolation of cool moist upland refugia, has resulted in regionally endemic, cold-adapted species on the

mountaintops (Williams et al., 2003).

Bioclimatic modelling for 19 vascular taxa endemic to the mountaintops of the AWT predicted that habitat suitability will decline by 17% to 100% by 2040, with only 3 species likely to survive beyond 2080 (Costion et al., 2015). A subsequent re-modelling study incorporating an improved species occurrence dataset for 37 mountaintop endemic taxa, utilizing the maximum entropy (MAXENT) modelling approach under emission scenarios (RCP 4.5 and RCP 8.5) for the years 2035, 2065 and 2085 shows similar trends, where most species are predicted to experience a decline in their suitable habitat under the conservative emission scenario (RCP 4.5) and no areas with currently high species richness (i.e., the Carbine Uplands, Figure 1) to retain suitable habitat beyond 2085 (Roeble, 2018). However, these modelling studies were based upon an incomplete understanding of species' physiological tolerances. It has been suggested that experimental studies on individual species' physiological limitations and thermal tolerances need to be conducted for us to draw definitive conclusions on their likely responses to future climatic scenarios (Costion et al., 2015).

It is also important to note that while temperature trends across elevation are the most invoked to shape species distributions, other abiotic factors need to be considered. Physiognomic studies in the AWT (Webb, 1959) suggest that vegetation structure is strongly driven by precipitation gradients (<1000 to >7000 mm/year (McJannet et al., 2007)). This is apparent for tropical montane cloud forest, a significant portion of the area found >1000 m a.s.l., where up to 30% of the ecosystem water budget is derived through occult deposition (cloud stripping) (McJannet et al., 2007; Wallace and McJannet, 2013). The availability of nutrients in montane (and especially cloud forest) soils is significantly lower than many lowland soils encouraging adaptations, such as the formation of adventitious roots above ground (e.g., *Ceratopetalum virchowii* F. Muell.) (Herwitz, 1986; 1991). Such adaptations to montane edaphic conditions may also have contributed to shaping the regionally endemic biota, in addition to direct impact of temperature regimes.

1.2.2 Objectives

With this thesis, I aim to address an important knowledge-gap by using species of the genus *Flindersia,* an important component of the Australian Wet Tropics (Bradford et al., 2014), to test whether: (a) tropical mountaintop endemic species are constrained in their distributions by physiological limitations; and (b) whether widespread congeneric species

display a broad temperature tolerance, with an ability to acclimate to projected climate warming. To achieve this, I identified the following objectives:

Objective 1: To understand how microclimate and soil nutrients vary across elevation gradients.

Objective 2: To understand the relationship between trends observed in Objective 1 and variation in plant functional traits of both a mountaintop endemic species, and its more broadly distributed sister taxa (congeners distributed across various sites along the elevation gradient).

Objective 3: To study potential thermal tolerances by comparing growth, physiology, and biochemistry, of species studied in Objective 2 under climate-controlled glasshouse conditions across a range of temperatures.

In addressing these objectives, I endeavored to conduct research that could be directly transferable to conservation efforts across the tropics, being fundamental to understanding the ecophysiology of tropical mountaintop restricted species and their adaptation or acclimation potential under future climate change scenarios. I developed this PhD project aiming for a broad relevance towards 'Environmental Change and Conservation', which is one of the 'National Strategic Research Priorities' (Australian Government – Science, 2018). My goals are also in line with the Wet Tropics Management Authority Board's priorities, which include to "*Pursue climate change adaptation and mitigation strategies to protect and conserve the integrity of the Wet Tropics World Heritage Area (WTWHA- Role 1, Goals 1 & 6)*".

Chapter 2: Microclimate, soil nutrients and soil stable isotopes in relation to elevation in the Australian Wet Tropics

This chapter is in preparation for submission to the journal *Agricultural and Forest Meteorology*.

The Temperature and Soil Moisture Sensor (model TMS-4, TOMST, Prague, Czech Republic) recording microclimate from a study site (~1000 m a.s.l.) in the Australian Wet Tropics (**Top)**; Soil sample collected from the same study site being processed in the laboratory (**Bottom)**.

Abstract

Microclimate, such as soil and surface air temperatures, and edaphic factors, such as soil organic matter content and nutrient availability, are important attributes of the below-canopy environment that shape vegetation communities. In this chapter, I present high-resolution (15-min frequency), ~3-year record (December 2019 – September 2022) of microclimate data from across 20 rainforest sites in the Australian Wet Tropics (AWT), spanning an elevation range from 40 to 1550 meters a.s.l., along with analyses of soil chemical properties from the same sites. I found that with increasing elevation, the decline in soil temperature was less steep than the decline for above-ground air temperature. There was a linear increase in the mean soil-to-air temperature difference ($\Delta T_{soil–air}$) with increasing elevation, such that soils in the lowlands were cooler than air and those at higher elevation sites were generally warmer than air. Also, soils were cooler during the day and warmer than air during the night at all sites. The difference in mean temperature between the wettest quarter (summer months) and the driest quarter (winter months) for soil and air also increased with elevation. Diel and annual temperature range were larger for the mountaintop site compared to lowland sites. Soil C:N ratio increased with elevation, in concert with a decline in soil pH; these two trends also coincided with an increase in soil organic matter content with elevation. Together, these variables displayed a strong correlation with climatic variables, suggesting an interaction of temperature and soil properties with elevation. Finally, soil nitrogen isotopic composition, $\delta^{15}N$, was found to decline with elevation, suggesting a tighter N cycle in high elevation soils. These observations show that both microclimate and edaphic properties vary with elevation in the AWT. Capturing long-term trends in microclimate in conjunction with environmental variables will enhance our understanding of important below-canopy processes in the context of projected climate warming.

2.1 Introduction

Over the past decades, the temperature sensitivity of tropical rainforests has garnered attention due to its impact on key ecological processes that govern not only the performance of individual species but also the functioning of the entire ecosystem (Doughty and Goulden, 2008; Cavaleri et al., 2015; Hursh et al., 2017). For example, the effects of surface air and soil temperatures when considered in the context of soil nutrient and water availability, have a direct impact on seed germination and sapling growth (Baltzer et al., 2005; Ho et al., 2019; Alonso-Rodríguez et al., 2022). Likewise, small fluctuations in microclimate across the understory can result in temperature difference in soil to above ground air ($\Delta T_{soil–air}$), which impacts both above and below ground ecological processes (Lembrechts et al., 2018). For instance, soils in tropical rainforests are reported to often be cooler than air temperatures and vary across spatial gradients, such as elevation, whereas soils in temperate ecosystems are several degrees warmer than air (Lembrechts et al., 2021). Yet, studies involving the observations of such microclimate differences in tropical rainforest ecosystems are rare, and studies assessing how these microclimates may change in response to modern climate change even more so. Elevation gradients can provide an ideal natural laboratory to understand how climate and soil properties vary in response to changing environmental conditions (Tito et al., 2020).

Bioclimatic predictors that incorporate temperature anomalies, seasonality, diel and annual temperature ranges are as important as average conditions in understanding species' growth patterns and physiological limitations (Booth, 2018; Noce et al., 2020). These predictors are known to capture biologically relevant trends such as carbon assimilation rates, night-time respiration, plant phenology and are often used in model forecasts of species' potential distributions (Schmitt et al., 2013; Lembrechts et al., 2021). Nevertheless, most studies calculate these bioclimatic predictors using historical climate datasets, with information captured from weather station records located outside the native range of a study system (Kearney, 2018; Lembrechts et al., 2018); and are typically of a coarse spatial (>1 km) and temporal resolution (>10 – 30 minute) (Fick and Hijmans, 2017; Kearney, 2018). For species that are restricted to narrow thermal regimes, such as the ones endemic to the tropical mountaintops, model predictions may benefit from direct measurements of both soil and surface air temperatures at a higher resolution in space and time (Jarvis and Mulligan, 2011; Hamilton et al., 2012).

Soils in intact tropical forests are generally cooler, relative to above-ground air temperatures (Lembrechts et al., 2021), and show reduced variation in temperature with increasing soil depth (Gao et al., 2008; Singh and Sharma, 2017). This is because soils exhibit thermal inertia, with temperatures that remain stable as compared to diel fluctuations in coincident air temperatures (Jackson and Forster, 2010; Panwar et al., 2020). This stability is generally pronounced in the shaded understory, yet will be influenced by site topography, water flow, humidity, and solar incidence (Gao et al., 2008; Frenne et al., 2019; Jang et al., 2022). Examining variation in $\Delta T_{soil-air}$ along environmental gradients, such as elevation, can enhance our understanding of the impacts of climate change on below-ground ecological processes (Lembrechts et al., 2021), a key component of predicting species and ecosystem responses.

Soil moisture content is a key parameter in determining soil thermal properties (Haskell et al., 2010; Schjønning, 2021). Moist soils conduct heat more efficiently and maintain a stable vertical heat gradient along the soil profile, whereas drier soils at the surface heat-up more rapidly on sunny days and cool more quickly at night, thereby causing a large diel temperature difference (Haskell et al., 2010; Panwar et al., 2020). Soil nutrient availability can also affect soil thermal conductivity through its impact on soil physical properties, such as via formation of pore spaces that can alter moisture holding capacity and influence heat transfer rates (Usowicz et al., 2013). Likewise, increases in soil organic matter content (OMC) impacts thermal diffusivity and soils tend to absorb and store more heat where OMC is highest (Abu-Hamdeh and Reeder, 2000).

Nutrients in soils are derived from a) dissolution of mineral content, b) deposition from hydrologic or aeolian inputs, c) mineralization of organic matter, or d) biological activities, such as nitrogen fixation from the atmosphere (Cavelier et al., 2000; Pajares and Bohannan, 2016). Tropical forest soils are typified by the rapid cycling of organic matter, which often comes to dominate the nutrient cycling process (Vitousek, 1984; Gleason et al., 2010). With increasing elevation, slower decomposition rates typically lead to the accumulation of more organic matter (Schuur and Matson, 2001; Werner and Homeier, 2015) and soils becoming increasingly acidic — with implications for nutrient availability (Kauffman et al., 1998). These conditions can also lead to slower soil N and P mineralization rates, causing a further decline in nutrient availability on tropical mountaintops (Vitousek et al., 1982; Vitousek, 1998; Fahey et al., 2016).

The use of the stable nitrogen isotope ratio, $\delta^{15}N$, provides an important proxy to help

understand nutrient cycling and dynamics in tropical forest soils (Craine et al., 2015). The $\delta^{15}N$ composition in soils generally declines with increasing elevation in the tropics and is a result of several factors such as temperature, precipitation and changes in plant and soil microbial communities (Sah and Brumme, 2003; Baumgartner et al., 2021).
Soil properties such as pH and nutrient availability can also influence changes in the cycling of nitrogen, impacting the $\delta^{15}N$ signature in soils (Liu et al., 2017; Peng et al., 2022). Understanding this important integrator in soils can add value to our understanding of key ecosystem processes, which is a result of nitrogen cycling via litterfall, soil mineralization, nitrification, leaching, and gaseous losses into the atmosphere over millennia (Amundson et al., 2003).

Predictor variables such as soil and air temperature changes with elevation in tropical rainforests are often mentioned in literature for their direct impacts on ecological processes. However, temperature difference in soil, surface air and above ground air temperatures that are important for both above and below-ground biological processes and their effects on edaphic properties with elevation in the AWT is poorly understood. In this study, I explored trends in microclimate, which include the soil, near-surface air and above-ground air temperatures, and soil moisture content, from across an elevation gradient in the AWT World Heritage Area. I used high temporal resolution data to calculate key bioclimatic predictors (e.g., Mean Annual Temperature (MAT), Diel Temperature Range (DTR), Annual Temperature Range (ATR), Isothermality, and Temperature Seasonality) which are commonly used in species distribution modelling (Fick and Hijmans, 2017; Booth, 2018). I also examined other environmental attributes, such as tree basal area and edaphic properties to understand how these attributes co-vary across elevation and evaluated their relation with microclimate.

I hypothesized that: 1) above-ground air temperatures would display a steeper decline with elevation than soil temperatures, resulting in a change in temperature difference ($\Delta T_{soil-air}$) across elevation; 2) summary statistics for bioclimatic variables for soil and air will differ with elevation, particularly differentiating the mountain-top environment from lower elevations; 3) soil nutrient availability will vary with elevation and in relation to soil pH, and soil organic matter content; and 4) soil $\delta^{15}N$ will decline with elevation, indicating a progressively more closed nitrogen cycle as elevation increases.

2.2 Methods

2.2.1 Study sites and microclimate measurements

The study was conducted in the AWT World Heritage Area (Figure 3.1). The AWT is spread over an area of more than 10,000 km^2 along the northeast coast and is an important bioclimatic refuge for species of Gondwanan origin (Weber et al., 2021). Forest types in the AWT have been described based on their vegetation communities and are observed to change with elevation (Webb, 1959). Lowlands (from near sea level to ~400 m a.s.l.) are dominated by complex mesophyll (large-leaved) vine forests, with a transition into a simple notophyll (moderate leaf size) vine forest type in the mid-elevation (~400 to 800 m a.s.l.) and the uplands (~1000 to 1200 m a.s.l.). This eventually grades into a simple microphyll (small-leaved) vine forest and vine thickets on the wet tropical mountaintops (greater than ~1300 m a.s.l.) (Webb, 1959). I studied microclimate in the understory of intact tropical rainforests at 21 sites from across the AWT ranging in elevation from 40 to 1550 m a.s.l.

Measurements included temperature of a) air (~ +15 cm above ground), b) surface (less than 1 cm above ground) and c) soil (~ –8 cm below ground), and d) the soil moisture content (less than 10 cm below ground). Data was captured using temperature soil moisture sensor units (TMS-4; TOMST, Prague, Czech Republic). The TMS-4 temperature sensors utilize MAXIM/DALLAS Semiconductor DS7505U+, with a resolution of 0.0625°C and with an accuracy of ± 0.5°C. Soil moisture captured by the TMS-4 is internally recorded and sensed with a time-domain transmission sensor (Wild et al., 2019) that records soil moisture counts, ranging from count 500 (completely dry) to 3500 (100% saturation). Soil moisture content was calibrated following a modified protocol suggested by the manufacturer (Wild et al., 2019). A representative regional soil from one of the study sites (~1000 m a.s.l., Mt Lewis National Park) was air dried, sieved and packed in a vertical PVC column (~20 cm height, 8.5 cm diameter) fitted on the bottom with a 90 mm Rain Harvesting Mozzie Stoppa filter (Rain Harvesting, Blue Mountain & Co) and with two TMS-4 sensors installed. A range in moisture content was developed by wetting the soils in the column to field capacity and allowing it to drain while recording the weight of the column alongside recording data from the sensor. The change in weight as the soil dried was used to calculate the soil volumetric water content (VMC, cm^3 cm^{-3}) and related to the raw moisture counts using a quadratic curve (Eqn. 1).

$$\mathrm{VWC} = (6e^{-09} \times soil\ moisture\ count^2) + (1.7e^{-04} \times soil\ moisture\ count) - 0.0914 \quad \text{Eqn. 1}$$

Microclimate measurements commenced in November 2019 and are currently ongoing, with sensors programmed to record at a 15-minute resolution. The averages in Soil and Air temperatures presented in this study were the average taken from 01 December 2019 to 01 September 2022. The ~3 years of climatic datasets are available on the Terrestrial Ecosystem Research Network – Data Discovery Portal (Singh Ramesh et al., 2022).

2.2.2 Bioclimatic variables and soil-to-air temperature difference

Bioclimatic variables such as temperature of the wettest quarter (summer months, January – March), the driest quarter (winter months, July – September) and the temperature difference between the summer-to-winter ($\Delta T_{wet–dry}$) months were examined in relationship to elevation from the microclimate data for Soil and above ground Air temperature. I also calculated Mean Annual Temperature (MAT), Diel Temperature Range (DTR), Annual Temperature Range (ATR), Isothermality and Temperature Seasonality (Table 2.1). For this, I used the 15-minute microclimate data from the measurement period 2020/January/01 to 2021/December/31 and calculated bioclimatic variables for each month, and then averaged for the two-year period (i.e., 2020 and 2021) for which complete data existed. In addition, temperature difference between soil-to-air ($\Delta T_{soil–air}$) for daytime (7:00 to 17:00), night-time (17:15 to 06:45) and 24-hour average for the long-term data set was examined in relation to elevation.

2.2.3 Tree basal area measurements

To understand how vegetation structure might impact trends in microclimate, I paired long-term climate data with tree basal area measurements calculated at the plot level. I used stem diameter at breast height measurements (DBH) of trees greater than or equal to 10 cm from study plots established by Ashton et al. (2016) (17 sites, 20 x 20 meters, ~400 to 1200 m a.s.l.), Torello Raventos (2014) (1 site, 50 x 20 meters, 1550 m a.s.l.) and Bauman et al. (2022a) (2 sites, 100 x 50 meters, 40 and 80 m a.s.l.). Basal area was calculated by converting the diameter of individual trees to the area of a circle, and summing these per unit ground area, scaled up to plot level in square meters per hectare.

2.2.4 Soil nutrient and isotope composition

Soil nutrients and isotope composition were measured in composite soil samples

collected from the study sites (*n*=21) where microclimate is being monitored. At each site I collected five soil cores using an auger (~10 cm deep) after removing leaf litter consisting of recognizable leaf fragments. Samples were bulked and homogenized for each site prior to analysis. Soil pH in H_2O and in 0.01M $CaCl_2$ were measured on fresh soil using an ISFET pH pen (Model 24006 DeltaTrak). Samples were then oven-dried at *ca* 105°C for up to 72h and powdered using a Benchtop Ring Mill. Total soil elemental analysis for phosphorus (P) was conducted using microwave-assisted acid digestion of the oven dried samples, followed by ionization detection using the Inductively Coupled Plasma-Atomic Emission Spectrometer (ICP-AES) at the Advanced Analytical Centre, JCU - Townsville.

Soil carbon (%C) and nitrogen (%N) were measured using a Costech elemental analyser (EA) (Milan, Italy) fitted with a zero-blank auto-sampler at the Advanced Analytical Centre, JCU - Cairns. This was used to calculate the C:N ratio. The stable nitrogen isotope ratio (expressed as $\delta^{15}N$) of the samples was measured using a ThermoFinnigan Delta^{plus} XL isotope ratio mass spectrometer (ThermoFinnigan GmbH, Bremen, FRG), linked to the EA via a ConFlo III interface. Stable isotope results are reported as per mil (‰) deviations from the AIR reference standard scale for $\delta^{15}N$. Precisions (SD) on internal standards were better than ± 0.2‰. Soil organic matter content (OMC) was calculated via loss of mass on ignition (360°C for 2h) (Schulte and Hopkins, 1996).

2.2.5 Statistical analysis

Raw information on microclimate obtained from data loggers are recorded in UTC timestamps. This was converted into Australian Eastern Standard time (AEST, +10 hours). Temperature averages and diel ranges were summarized in R studio (Team, 2021) and bioclimatic variables were then calculated based on monthly averages for the years 2020 and 2021. Upon initial data exploration, one site in Mt Lewis National Park, at ~600 m a.s.l. displayed erroneous readings for a substantial portion of monitoring in the year 2020 and was therefore dropped from subsequent analyses, such that these were based on data from 20 rainforest sites.

To understand how temperature for Soil and Air varied with elevation, an ordinary least squares regression (OLS) analysis was computed for each of the variables against elevation. Model outputs were checked for normality of residuals, and homogeneity of variance using visual checks on the OLS model residuals with the package ‘see’ in R (Team, 2021).

I conducted an additional analysis to test for discontinuous effects of elevation by delineating the elevation profile into categories based on their vegetation communities (following Webb, 1959). Specifically, I delineated all sites into one of the four categories, lowland (<400 m; *n*=2 sites), mid-elevation (>400 to 900 m; *n*=9 sites), upland (>900 to 1300 m; *n*=8 sites) and the mountaintop (>1300 m a.s.l., *n*=1 site). A linear model was fitted with elevation-category as a fixed effect, followed by a type II Analysis of Variance (ANOVA). I performed a post-hoc comparison of means between these elevation-categories using the 'tukey' method with the help of the 'emmeans' package in R.

Finally, to understand how environmental variables (i.e., microclimate and soil properties) are interrelated across elevation, a principal component analysis (PCA) was performed using the package 'factoextra' in R (Kassambara and Mundt, 2017). A scree plot was used to determine the number of principal components to retain, based on which the first two principal components were retained that contributed to most of the variation.

2.3 Results

2.3.1 Trends in microclimate with elevation

Across the entire dataset, the long-term average for Soil and above-ground Air temperatures were highest for the lowland site, Daintree Rainforest Observatory (DRO) (*ca* 23.1°C and 23.3°C respectively, at 40 m a.s.l.) and lowest for the mountaintop site, Mt Bellenden Ker (*ca* 14.8°C for both Soil and Air, at 1550 m a.s.l.). The highest mean monthly maximum temperature for Soil was recorded during the month of February 2020 (at 27.6°C) for the lowland site, DRO. The highest mean monthly maximum temperature for Air (at 34.1°C) was for the month of October 2021 in a mid-elevation site in Mt Lewis National Park (~780 m a.s.l.). The lowest mean monthly minimum temperatures for Soil and above-ground Air were for the month of July 2021 in the mountaintop site, Mt Bellenden Ker (7.2°C and 4.8°C respectively). Trends with elevation for Soil, Surface and above-ground Air temperatures all showed highly significant declines with elevation (Figure 2.2); and became steeper in the following order: Air> Surface> Soil, as hypothesized. Soil temperature declined by *ca* –5.7°C, Surface by –5.8°C, and above ground Air temperature by –5.9°C per km of elevation (Figure 2.2; Table 2.2). There were no significant difference observed in the slopes for daytime (07:00 to 17:00 AEST) and night-time (17:15 to 06:45 AEST) Soil temperature with elevation (*ca* – 5.7°C km^{-1} and –5.6°C km^{-1} respectively) (Figure 2.2A & B), whereas the

slopes for Surface (–5.9°C km^{-1}) (Figure 2.2D) and above ground Air temperature (*ca* –6°C km^{-1}) were significantly higher ($F_{(1, 36)} = 152$, $p<0.001$ and $F_{(1, 36)} = 217$, $p<0.001$ respectively) during the daytime (Figure 2.2G), but were nearly identical during the night time with elevation (–5.7°C km^{-1}) (Figure 2.2E & H).

2.3.2 Trends in bioclimatic descriptors across sites

The temperature of the wettest quarter (summer months, i.e., January, February and March), and the driest quarter (winter months, i.e., July, August and September) displayed a decline across the elevation range and the slopes for driest quarter were steeper for both soil ($F_{(1, 36)} = 2492$, $p<0.001$) and air ($F_{(1, 36)} = 2561$, $p<0.001$). For example, the slopes for soil ($R^2= 0.98$, $p<0.001$) and air temperatures ($R^2= 0.98$, $p<0.001$) declined in a linear fashion with elevation during the wettest quarter by –5.3°C km^{-1} and –5.4°C km^{-1} respectively (Figure 2.3A & B), whereas the slopes for the driest quarter declined by –5.8°C km^{-1} and –5.9°C km^{-1} with elevation for soil ($R^2= 0.98$, $p<0.001$) and air temperatures ($R^2= 0.98$, $p<0.001$) respectively (Figure 2.3C & D). On the other hand, the temperature difference between the wettest and driest quarters ($\Delta T_{wet–dry}$) increased with elevation for both soil ($R^2= 0.46$, $p<0.001$) and air temperatures ($R^2= 0.4$, $p<0.001$) and were of similar slopes (by 4.8°C km^{-1}) (Figure 2.3E & F).

Bioclimatic descriptors such as the mean Diel Temperature Range (DTR) for air significantly differed between the mountaintop and the lowland sites ($F_{(3,16)} = 9.53$, $p<0.001$), with highest DTR observed for the mountaintop site (~12.0°C), i.e., nearly 32% higher than the lowland sites (~8.2°C, averaged from n=2 sites) (Figure 2.4A; Table 2.3). Similarly, the Annual Temperature Range (ATR) was significantly higher for soil ($F_{(3,16)} = 3.50$, $p<0.005$) and air ($F_{(3,16)} = 9.87$, $p<0.001$) in the mountaintop site (12.0° C and 23.4°C respectively), compared to the lowland sites (8.7°C and 16.5°C respectively, average from n=2 sites) (Figure 2.4G & H; Table 2.3). There was also a significant increase in temperature seasonality (coefficient of variation) for both soil ($F_{(3,16)}= 35.2$, $p<0.001$) and air ($F_{(3,16)}= 28.9$, $p<0.001$) with increasing elevation profile, such that the mountaintop site displayed the highest seasonality (15.1% and 15.6% respectively), which was nearly 50% higher than the lowland sites (7.5% and 7.9% respectively, average from n=2 sites) (Figure 2.4E & F; Table 2.3). There was no significant trend observed for Isothermality across the elevation gradient.

2.3.3 Soil-to-Air temperature difference with elevation

Across the elevation range, soil was generally cooler than air during the day (Figure 2.5A) and warmer during night (Figure 2.5B). The maximum difference in $\Delta T_{soil-air}$ during the daytime was found in a mid-elevation site, in Mt Lewis National Park (*ca* –0.98°C, at ~580 m a.s.l.), and during the night-time was recorded in another mid-elevation site, Mt Lewis National Park (*ca* 1.02°C, at ~780 m a.s.l.).

Long-term daily (24-hours) averaged $\Delta T_{soil-air}$ displayed a significant increase (R^2= 0.32, p<0.001) with increasing elevation such that the lowland and mid-elevation soils were relatively cooler or tracking the above-ground air temperatures, whereas the upland and mountaintop soils were warmer than air (Figure 2.5C). The largest difference in mean 24-hour $\Delta T_{soil-air}$ was observed in an upland site (*ca* 1.02°C, at ~ 1215 m a.s.l.) and the least in a mid- elevation site (*ca* –0.26°C, at ~580 m a.s.l.) in Mt Lewis National Park.

2.3.4 Tree Basal Area with elevation

The tree Basal Area (BA) increased significantly with increasing elevation (R^2= 0.63, p<0.001) by *ca* 32 m^2 ha^{-1} km^{-1} (Figure 2.6F). The highest BA (87.33 m^2 ha^{-1}) was recorded in an upland site, in Mt Lewis National Park at ~1200 m a.s.l. and the lowest (27.10 m^2 ha^{-1}) was recorded for the lowland site Daintree Rainforest Observatory at 40 m a.s.l. that was nearly 57% lower than the mountaintop site (*ca* 63.5 m^2 ha^{-1}) (Table 2.3).

2.3.5 Soil properties: nutrients, and isotope composition with elevation

Soil C:N ratio (R^2=0.41 p<0.01) and organic matter content (OMC) (R^2=0.74 p<0.001) significantly increased with elevation (Figure 2.6B & E respectively), whereas soil pH declined (R^2=0.48 p<0.001) with elevation (Figure 2.6D). Soil OMC as high as 3.7 % was recorded on the upland site, Mt Lewis National Park (~1200 m a.s.l.) and as low as 1.35% in the Rex Range (~420 m a.s.l.). Soil pH as high as 6 was recorded in a mid-elevation site, Mt Lewis National Park (~654 m a.s.l.) and as low as 3.7 was recorded on the mountaintop site (1550 m a.s.l.).

Soil $\delta^{15}N$ significantly declined with elevation (R^2=0.60 p<0.001) (Figure 2.6F). On average, I found that the $\delta^{15}N$ decreased with elevation by ~ –3.6‰ per km of elevation gain, and the difference in the composition from the lowland site, DRO (40 m a.s.l.) to the mountaintop site, Mt Bellenden Ker (1550 m a.sl.) was *ca* –5.7‰.

2.3.6 Correlations among environmental variables

PCA analysis of environmental observations from the study sites was conducted on standardized z-scores for Soil and Air temperature, soil pH, OMC, C:N ratio and total P, and BA (Table 2.5). The first (63.92%) and the second (17.35%) principal component contributed to most (~80%) of the variation (Figure 2.7; Supplementary Table 2.1B). The first principal component displayed high positive loadings for Soil and Air temperature and soil pH and negative loadings for soil OMC, C:N ratio and BA. Together, these variables contributed to most (~99%) of the variation in PC1. The second principal component showed the highest positive loading for total P (Figure 2.8; Supplementary Table 2.1B), contributing more than 70% of the variation in PC2. An ANOVA test indicated no significant differences among the elevation categories on the PCA. Furthermore, when $\delta^{15}N$ isotope composition was regressed against PC1 scores from the respective study sites it displayed a linear positive relationship (R^2=0.64 p<0.001) (Figure 2.8). The $\delta^{15}N$ is an integrator of ecosystem nitrogen cycling related to multiple processes (Robinson, 2001), and therefore it was independently examined in response to PC1.

2.4 Discussion

This study explored trends in microclimate such as Soil (–8cm), Surface (<1cm) and above ground Air (+15cm) temperatures and edaphic properties such as soil C:N, OMC and pH across an elevation gradient in the Australian Wet Tropics World Heritage Area (AWT). I calculated bioclimatic variables, such as temperature of the wettest and driest quarters, using the monthly temperature averages for Soil and Air with elevation, and explored trends in temperature seasonality, and diel and annual temperature ranges across the elevation gradient. I also evaluated the temperature difference, $\Delta T_{soil–air}$ for day, night and the 24-hour average. Finally, I explored how microclimate, edaphic characteristics and tree basal area are correlated in a coordinate space using a principal component analysis.

2.4.1 Microclimate across elevation

In the AWT, existing meteorological records are sparse and often associated with urban centers, making it difficult to examine temperature trends experienced by natural forests, because they fail to capture soil and surface air temperatures where key below-canopy ecological processes occur (Lembrechts et al., 2018). In this study, I observed only a marginal difference between the near Surface and above ground Air temperatures, hence I have drawn my comparisons with related studies primarily based on the Soil and above-ground Air

temperatures.

Microclimate in the AWT was explored previously in a long-term study (2004 – 2010) involving temperatures along a vertical gradient that encompass above-ground air (~1.5 m), surface soil and beneath a log of wood across 25 sites from near sea level to ~1500 m a.s.l. (Williams, 2013). Another study involving top-soil (–10 cm) temperatures along a gradient from 40 – 1540 m a.s.l. in the AWT reported a decline of *ca* –5.6°C km^{-1} (Zimmermann et al., 2015), which is similar to what I observed in this study, a decline of –5.7°C km^{-1} along a gradient from 40 – 1550 m a.s.l. (Figure 2.2F), suggesting stability in slopes with elevation. In the Neotropics, a study found top-soil temperature to decline by –4.9°C km^{-1} with elevation (Salinas et al., 2011), a smaller decline than what I observed in the AWT.

Long-term temperature trends in air temperature (~1.5 m above ground) in the AWT report nearly –1°C decline for every 200 m increase in elevation (Shoo et al., 2005). This decline is similar to what I observed in this study, *ca* –5.9°C km^{-1} of elevation (Figure 2.2C). Likewise, air temperature across a vertical canopy gradient (0.5 m to ~20 m above ground) in a recent study showed a decline of *ca* –5.2°C km^{-1} for the above-ground (0.5 m) and *ca* –5.6°C km^{-1} for canopy air (20 m) during the daytime (8:00 – 17:00) (Leahy et al., 2021). Although trends in air temperature across canopy appear to be different, they may not be large enough in terms of biological processes. In this study I found a larger decline in the slopes between daytime and night-time above ground air temperatures (Figure 2.2A). This difference may have implications on plant physiological processes such as night-time respiration rates across elevation for example. Spatiotemporal variability in Soil and Air temperatures has been reported to change in relation to diurnal length, topography (slope, aspect), tree canopy height and leaf area index at higher ecotones (Liu and Luo, 2011). Therefore, it is necessary to monitor long-term measures of higher spatiotemporal microclimate paired with some of these environmental attributes to make reasonable comparisons across sites in tropical rainforest ecosystems.

2.4.2 Bioclimatic trends and soil-to-air temperature difference across elevation

Bioclimatic trends such as the temperature of the wettest (summer) and driest (winter) quarter followed a similar pattern as above with elevation, i.e., soil temperature declined less steeply (Figure 2.3A & C) compared to above ground air temperatures (Figure 2.3B & D) for the two quarters, suggesting that above ground air temperatures display much larger variability than soil temperatures, as has been reported in previous studies (Bader et al.,

2007; Lembrechts et al., 2021). Furthermore, the slopes in both soil and air were much steeper with elevation during the driest quarter (Figure 2.3B & D). This difference is in line with meteorological process, where adiabatic lapse rate is generally higher in dry than in air saturated with water vapour (Jones, 2013). The temperature difference in soil and air across seasons with elevation could play an important role in determining plant phenological or growth stages, such as, seed dormancy, germination and sapling growth (Jaganathan and Biddick, 2021; Liyanage et al., 2022). This difference could have been driven by environmental factors such as higher solar incidence, reduced soil moisture and higher evaporation during the dry season (Körner and Paulsen, 2004). Combined observations with some of these environmental attributes will be necessary to better evaluate their influence on microclimate in the long-term on some of the ecological processes.

I found differences in other bioclimatic variables such as the DTR, ATR and temperature seasonality when averaged across the broad elevation profiles (Figure 2.4). The DTR and ATR for Air were larger compared to Soils throughout the measurement period. Studies have noted that inter-annual and diel temperature range in soil temperatures is generally small (Gao et al., 2008; Liu and Luo, 2011). The DTR is an important predictor in biological context, especially because of the nature of biological processes. For instance, increased daytime temperatures relative to night-time can increase the vapor pressure deficit (VPD) causing fluctuations in the DTR in the long-term that has an impact on stomatal activity (Grossiord et al., 2020). Likewise, increased night-time temperatures can affect plant respiration rates and alter the net ecosystem CO_2 exchange (Goulden et al., 2004). Diel and annual temperature fluctuations for soil and air can also alter the physiological activity of other taxonomic groups, such as ground-dwelling or nocturnal animals for example (Vallejo-vargas, 2022), suggesting the importance of understanding DTR and ATR in the long-term.

Next, I found that soils in lower elevation sites were relatively cooler and/or tracking the above ground air, whereas the upland and mountaintop soils were warmer than air. The $\Delta T_{soil-air}$ is an important attribute emphasized in previous studies comparing global meteorological data, and this difference is much larger in temperate ecosystems, where soils are warmer than air by several degrees (Lembrechts et al., 2021). Stable soil temperatures relative to air may be driven by soil thermal properties, which depend on soil texture, composition, and bulk density, to name a few contributing factors (Farouki, 1981; Li et al., 2019). Although I did not measure some of these attributes, I did find a trend between $\Delta T_{soil-air}$ and soil organic matter content (Supplementary Figure 2.1B). Soil organic matter is

generally a poor thermal conductor compared to mineral components of soil (Jang et al., 2022; Schjønning, 2021). This means that soils of high OMC tend to retain heat at the soil surface, which could be a reason why I observed warmer soils relative to air in higher elevations. Alternately, this could also be driven by exposure to sunlight during the early part of the day or late evenings leading to substantial heating of the ground causing soil to remain warm as the air cools above ground (Körner and Paulsen, 2004).

Tree basal area (BA) also increased with elevation at the same study sites where microclimate was monitored (Figure 2.6F). BA generally increases with elevation in the tropics, and this trend has been attributed to variation in stand age, turnover rates and disturbance from cyclones along elevation gradients (Malizia et al., 2020; Venter et al., 2017). Increases in BA can contribute to a decrease in below-canopy temperatures because of increased shading that can reduce the amount of direct sunlight reaching the ground. Although this may indicate a concerted decline in Soil and Air temperatures with elevation in this study, it does not explain why soil was warmer than air with increasing elevation. Increases in BA also do not necessarily mean an increase in tree canopy leaf area because tree canopy architecture may change with elevation (Unger et al., 2013). It is therefore necessary to pair variables such as tree canopy architecture, leaf area index and related biophysical attributes to better understand the effects of covarying drivers on microclimate with elevation (Bendix et al., 2006; Frenne et al., 2019; Schjønning, 2021).

2.4.3 Soil properties: nutrients and isotope composition

With increasing elevation in the tropics, soil nitrogen availability is generally reduced (Tanner et al., 1998; Vitousek, 1998; Soethe et al., 2008). In this study I observed a decline in soil nitrogen that was shown as an increase in soil C:N ratio with elevation. This observation compares well with what has been observed in other tropical montane environments (Fahey et al., 2016; Gong et al., 2020; Dai et al., 2022). Likewise, soil organic matter content also increased with elevation, as has been observed in some other studies (Tanner et al., 1998; Strong et al., 2011). Soil organic matter and soil C:N status are correlated, possibly because of slower litter decomposition with elevation in the tropics (Girardin et al., 2010; Parsons et al., 2014). This is because lower temperatures at higher elevation sites could play an important role in slowing litter decomposition and soil mineralization rates leading to an increased organic matter in soils. Slow decay of organic matter over time can result in

acidification by weak organic acids (Ross, 1993). This could be another reason for the decline in soil pH with increasing elevation in this study (Jiang et al., 2015; He et al., 2016). Moreover, decline in soil pH can further limit soil N availability and impact mineralization rates on mountaintop sites. Studies have shown that raising pH levels in soils can increase soil N-mineralization rates and release the labile organic matter (Curtin et al., 1998).

I found a strong negative trend in soil $\delta^{15}N$ with elevation, as has been reported in other studies in the tropics (Sah and Brumme, 2003; Ma et al., 2012; Baumgartner et al., 2021). This is an important integrator of many processes such as nutrient cycling and biogeochemical activity in the system (Amundson et al., 2003). A higher $\delta^{15}N$ in the lowland soils would indicate an increase in N availability and faster decomposition with increased microbial activity under higher soil temperatures (Sah and Brumme, 2003). Increased N_2O emissions have been observed with warmer soil temperatures in some lowland rainforest sites in the AWT and coincident increase in emissions with soil moisture content across the two seasons (Kiese and Butterbach-Bahl, 2002). Increased mineralization and leaching of N can lead to discrimination against ^{15}N and high loss of lighter ^{14}N would result in enrichment of ^{15}N in the system (Amundson et al., 2003). On the contrary, the decline in $\delta^{15}N$ with elevation likely coincides with a decline in soil N availability on mountaintop sites. This may be driven by lower soil mineralization from reduced microbial activity and net nitrification rates on tropical mountaintop sites (Sah and Brumme, 2003). This reduces losses of N from the ecosystem by processes that fractionate against ^{15}N (Martinelli et al., 1999) making the system more closed with tighter N cycling.

2.4.4 Correlations among environmental variables

The first principal component was strongly, positively loaded with soil temperature and pH and negatively loaded with edaphic properties such as soil OMC and C:N ratio (Supplementary Table 2.1B). Soil acidity and its nutrient status generally reflect the climatic conditions interacting with these properties, with soil pH and temperature generally being correlated (Ratier Backes et al., 2021). Soil temperatures and pH can have a direct effect on soil nutrient availability due to changes in leaf litter decomposition and due to the nature of microbial activity in the soils (Parsons et al., 2014; Nottingham et al., 2015). For example, with increasing elevation, difference in temperature sensitivities of soil organic matter have been reported to alter plant and microbial communities (Nottingham et al., 2015). Warmer soils accelerate mineralization and decomposition, releasing more nutrients for plants to

absorb (Nottingham et al., 2015). In the AWT, increased leaf litterfall has been observed during dry winters and increased decomposition during the wet summers, with slower decomposition associated with cooler temperatures (Parsons et al., 2014). These differences in biological activities across seasons may also be a reason why I saw an increase in soil OMC under higher elevation sites with larger seasonal temperature ranges (Nottingham et al., 2015).

I observed a strong linear positive response of soil $\delta^{15}N$ isotope composition with PC1 scores which may be indicative of changes in soil N availability across changes in PC1. N cycling in tropical rainforests is influenced by climate and soil nitrogen availability (Craine et al., 2015; Pajares and Bohannan, 2016). Therefore, at higher elevation sites under lower temperatures and reduced soil N availability there is likely a reduction in N-loss pathways that discriminate against ^{15}N, leading to a decrease in soil $\delta^{15}N$ as observed in this study. On the other hand, the second principal component was strongly positively loaded with soil total P. Soil total P being independently loaded on the second principal component suggests soil heterogeneity across sites in the AWT predominantly due to the origin of these soils from their parent rock, i.e., granitic or derived from basalt (Gleason et al., 2010).

2.5 Conclusion

Climate change is having a significant impact on tropical ecosystems, but the full extent of these effects is still not well understood. Studies characterizing the effects of microclimate and soil properties in combination in tropical rainforests are rare (Liu and Luo, 2011). This study has provided a snapshot into how microclimate and bioclimatic predictors, along with edaphic properties co-vary across elevation in the Australian Wet Tropics, an important knowledge gap. My results show that it is important to consider changes in other environmental variables beyond temperature when using elevation as a proxy to understand species response to climate change.

The bioclimatic and edaphic variables studied here can help us to better understand species' long-term growth patterns, functional traits, phenology and related ecophysiological processes, both above and below ground (Gardner et al., 2019; Parsons et al., 2014). As the earth surface warms, studying how bioclimatic variables and temperature difference between soil and air change along elevation gradients in the tropics may help to predict the future forest composition. Incorporating these trends in species distribution models can better

inform limitations on species' home ranges and could be useful to improve model forecasts (Costion et al., 2015; Evans et al., 2015; Lembrechts et al., 2018b; Gardner et al., 2019).

Table 2.1 Bioclimatic predictors calculated for soil and air studied for the years 2020 and 2021 and the measurement equation and inputs used to calculate these predictors.

Bioclimatic predictors	Equation	Inputs
Mean Annual Temperatures (MAT)	$\frac{\sum_{i=1}^{i=12} Tavg}{12}$	The average temperature for each month (T_{avg}) Units: °C
Annual Mean Diel Temperature Range (DTR)	$\frac{\sum_{i=1}^{i=12}(Tmax_i - Tmin_i)}{12}$	Monthly maximum temperatures (T_{max}°C) and monthly minimum temperatures (T_{min}°C) Units: °C
Annual Temperature Range (ATR)	T_{max} of the warmest month – T_{min} of the coldest month	The maximum temperature of the warmest month and minimum temperature of the coldest month. Units: °C
Isothermality	$\frac{DTR}{ATR}\ x\ 100$	Annual mean diurnal temperature range and Annual temperature range. Units: %
Temperature Seasonality – coefficient of variation	$\frac{SD\ (Tavg1 \dots \dots Tavg12)}{MAT}\ x\ 100$	The average temperature for each month (T_{avg}) and the annual mean temperature, standard deviation (SD) Units: %

Table 2.2 Summary table of linear regressions of microclimate (soil, near-surface and above-ground air temperatures) and soil moisture content with elevation in the Australian Wet Tropics. Based on the long-term averages from the measurement period between 01 December 2019 and 01 September 2022.

	Soil temperature			near Surface air temperature			Air temperature		
Predictors	***Estimates***	***CI***	***p***	***Estimates***	***CI***	***p***	***Estimates***	***CI***	***p***
(Intercept)	23.577	(23.300, 23.854)	**<0.001**	23.699	(23.397, 24.001)	**<0.001**	23.713	(23.414, 24.013)	**<0.001**
Elevation	-0.0057	(-0.0059, -0.0053)	**<0.001**	-0.0058	(-0.006, -0.005)	**<0.001**	-0.0059	(-0.006, -0.005)	**<0.001**
Observations	**20**			**20**			**20**		
R^2 / R^2 adjusted	**0.988 / 0.988**			**0.987 / 0.986**			**0.987 / 0.987**		

Table 2.3. Summary table of linear regressions of each of the bioclimatic predictors against the elevation categories showing the 95% CI and significant *p* values in bold.

	DTR (soil)			DTR (air)			Seasonality (soil)			Seasonality (air)			ATR (soil)		ATR (air)		
Predictors	***Estimates***	***CI***	***p***	***Estimates***	***CI***	***p***	***Estimates***	***CI***	***p***	***Estimates***	***CI***	***p***	***CI***	***p***	***Estimates***	***CI***	***p***
(Intercept)	3.38	2.65 – 4.11	**<0.001**	8.27	7.37 – 9.17	**<0.001**	7.49	6.46 – 8.52	**<0.001**	7.93	6.74 – 9.12	**<0.001**	7.42 – 10.02	**<0.001**	16.56	14.64 – 18.48	**<0.001**
Elevation profile [Mid-elevation]	0.21	-0.59 – 1.02	0.584	0.75	-0.25 – 1.75	0.130	2.26	1.12 – 3.40	**0.001**	2.72	1.40 – 4.04	**<0.001**	-0.78 – 2.09	0.348	1.64	-0.48 – 3.77	0.120
Elevation profile [Mountaintop]	1.46	0.20 – 2.73	**0.026**	3.79	2.23 – 5.35	**<0.001**	7.62	5.83 – 9.41	**<0.001**	7.64	5.57 – 9.70	**<0.001**	1.09 – 5.60	**0.006**	6.91	3.58 – 10.24	**<0.001**
Elevation profile [Upland]	0.30	-0.51 – 1.12	0.440	0.68	-0.32 – 1.69	0.169	3.85	2.70 – 5.01	**<0.001**	4.50	3.17 – 5.84	**<0.001**	-0.68 – 2.23	0.276	-0.01	-2.16 – 2.14	0.992
Observations		20			20			20			20		20			20	
R^2 / R^2 adjusted	0	0.297 / 0.165		0	0.641 / 0.574			0.868 / 0.844			0.845 / 0.815		0.397 / 0.284			0.649 / 0.584	

Table 2.4. Summary table of long-term averages (January 2020 to December 2021) of Mean Annual Temperatures (MAT) for Soil and Air temperatures and bioclimatic predictors averaged for the year 2020 and 2021 and tree Basal Area measured from across the study sites in the Australian Wet Tropics World Heritage Area. The abbreviations 'DTR', 'ATR' and 'BA' refer to Diel Temperature Range, Annual Temperature Range, and tree Basal Area, respectively.

Site	Elevation Profile	Elevation (m a.s.l.)	MAT (°C)		DTR (°C)		Isothermality (%)		Seasonality (%)		ATR (°C)		BA (m^2 ha^{-1})
			Soil	Air	Soil	Air	Soil	Air	Soil	Air	Soil	Air	
#DRO	Lowland	40	23.1	23.3	3.3	8	40.8	51.5	7.2	7.5	8.3	15.8	27.1
±DDC		80	23	23.1	3.3	8.4	37.8	58.6	7.7	8.3	9.1	17	34.3
Rex Range	Mid-elevation	422	21.2	21.2	3.6	9.5	40.3	51.7	8.8	9.5	9.2	18.6	46.6
Mt Lewis National Park		578	20.5	20.7	3.7	9.1	40	49.3	9.7	10.2	9.4	18.6	40.9
		600	20.2	20.2	4.3	8.4	43.3	51.8	9	9.6	10.1	16.2	43.3
		625	19.9	19.8	4.3	9.8	39.6	48.6	10.4	11.2	11.1	20.3	50
		654	20	20	3.1	9.2	37.3	53.1	9.1	10.2	8	17.4	60.2
		780	19.8	19.5	2.7	10	33.5	48.9	9.2	10.3	8.1	20	73.6
		802	19	19	3	7.9	35.7	48.9	10	11.2	8.5	16.4	58
		830	18.8	18.6	3.4	8.7	36.2	49.9	10.7	12	9.4	17.7	50
		831	18.5	18.9	3.8	8.4	39.5	48.1	10.6	11.2	9.8	17.9	46.9
	Upland	902	18.1	17.9	3.1	9.2	36.9	55.1	10.3	11.5	11.5	16.9	46.3
		960	17.5	17.4	3.5	8.3	38.2	54.9	11.3	12.4	9.2	15.4	53
		992	17.8	17.7	4.1	9.7	37.4	52.4	10.4	11.1	11.1	18.6	78
		1072	17.5	17.3	3.7	9.5	40.0	56.2	11.1	12.2	9.2	17.0	62.5
		1157	16.9	16.8	3.5	8.9	38.7	55.7	11.9	13.3	9.1	16.1	66
		1195	16.9	16.8	3.8	8.6	39.5	55.4	11.9	13.2	9.6	15.7	69
		1215	16.7	16.4	3.5	8.3	38.8	52.6	11.5	12.9	9.0	16.1	79
		1232	16.7	16.6	4.3	8.9	42.5	53.8	12.2	12.7	10.2	16.6	87.3
Mt Bellenden Ker	Mountaintop	1550	14.9	14.8	4.8	12.1	40.9	51.5	15.1	15.6	12.1	23.4	63.5

DRO Daintree Rainforest Observatory ± Daintree Discovery Center

Table 2.5. Summary table of environmental descriptors standardized as z-scores for each study site listed for Soil and Air temperature, soil pH, Organic Matter Content (OMC), C:N ratio and total P and Basal Area (BA) along with PCA scores. Soil $\delta^{15}N$ from the respective study sites is also presented.

Site	Elevation Profile	Elevation	PC1	PC2	PC3	sum-z	z-T_{soil}	z-T_{air}	z-Soil pH	z-Soil OMC	z-C:N ratio	z-BA	z-Total P	Soil $\delta^{15}N$
#DRO	Lowland	40	-1.76	1.04	0.21	-0.11	-0.93	-0.9	-0.78	0.93	0.11	0.78	0.69	7.3
±DDC		80	-3.21	-0.36	0.84	-4.09	-1.87	-1.81	-1.78	0.71	0.98	0.42	-0.75	6.8
Rex Range	Mid-elevation	422	1.38	-0.55	-1.87	2.39	0.53	0.52	2.02	-1	0.39	0.22	-0.29	4.1
Mt Lewis National Park		578	-1.92	-1.3	0.26	-0.33	-0.63	-0.64	-0.78	0.73	2.04	-0.24	-0.82	5.6
		600	-1.84	-0.17	-0.16	-0.55	-0.91	-0.93	-0.45	0.72	0.8	0.59	-0.36	7.0
		625	-0.68	-1.23	0.72	-0.77	-0.06	0.05	-0.62	0.74	0.75	-0.63	-1.01	6.7
		654	-2.63	-0.12	0.41	-1.84	-1.01	-1.07	-1.61	1.01	0.18	1.41	-0.75	4.8
		780	0.17	-0.35	0.42	-1.54	-0.03	-0.07	-0.12	-0.05	-0.35	-0.43	-0.49	4.8
		802	1.53	-0.31	-0.94	0.93	0.49	0.47	1.53	-0.79	-0.17	-0.43	-0.16	3.5
		830	-1.7	-0.09	-0.79	1.8	-0.43	-0.47	-0.29	0.67	1.08	1.35	-0.1	4.2
		831	-2.78	0.18	-0.58	0.85	-1.02	-0.99	-0.78	1.4	0.66	1.94	-0.36	2.0
	Upland	902	2.96	-0.26	0.66	0	1.98	1.93	0.7	0	-1.02	-1.43	0.23	5.6
		960	1.42	-0.96	0.16	-0.03	0.74	0.85	0.37	-0.8	0.25	-1.01	-0.42	2.0
		992	3.3	0.76	0.29	-2.01	1.09	1.07	0.54	-2.4	-2.29	-0.65	0.62	–
		1072	0.02	-0.75	-0.05	-0.9	0.05	0.09	-0.12	-0.36	0.11	0.08	-0.75	4.5
		1157	2.15	-0.11	-0.47	-0.02	0.63	0.64	1.53	-0.81	-1	-0.86	-0.16	2.7
		1195	3.91	-0.29	0.99	-0.18	1.96	2.02	0.54	-1.49	-1.55	-1.89	0.23	4.0
		1215	-0.01	-0.15	-0.86	1.95	0.42	0.31	0.21	-0.19	0.25	1.05	-0.1	2.3
		1232	-0.19	1.24	1	-0.75	-0.34	-0.38	-0.62	0.3	-0.31	-0.67	1.27	3.2
Mt Bellenden Ker	Mountaintop	1550	-0.12	3.76	-0.23	2.81	-0.66	-0.68	0.54	0.67	-0.9	0.37	3.49	1.6

DRO Daintree Rainforest Observatory ± Daintree Discovery Center

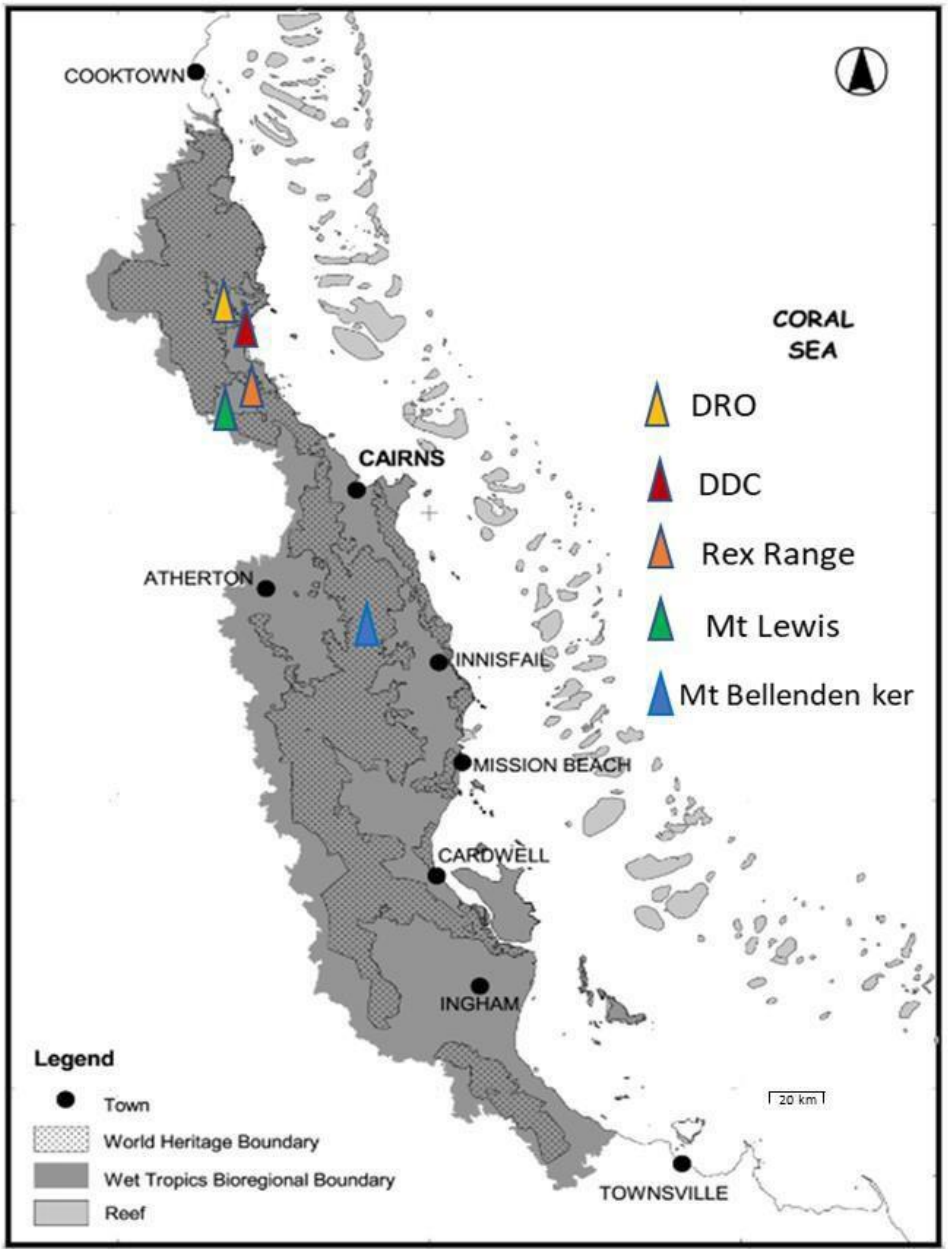

Figure 2.1. The Australian Wet Tropics World Heritage Area, with five rainforest monitoring sites where data loggers were deployed. The northernmost sites comprise the Daintree Rainforest Observatory (DRO ~40 m a.s.l. (yellow triangle)) and the Daintree Discovery center (DDC ~80 m a.s.l. (red triangle)), and the southernmost site is Mt Bellenden Ker (~1550 m a.s.l. (blue triangle)). The Rex Range (orange triangle) and Mt Lewis sites (green triangles) comprise of the mid-elevation and upland sites respectively, with 17 data loggers deployed across an elevation range from between ~400 m to ~1200 m a.s.l. Site triangles have been added on a map developed by Peter Bannink (Australian Tropical Herbarium).

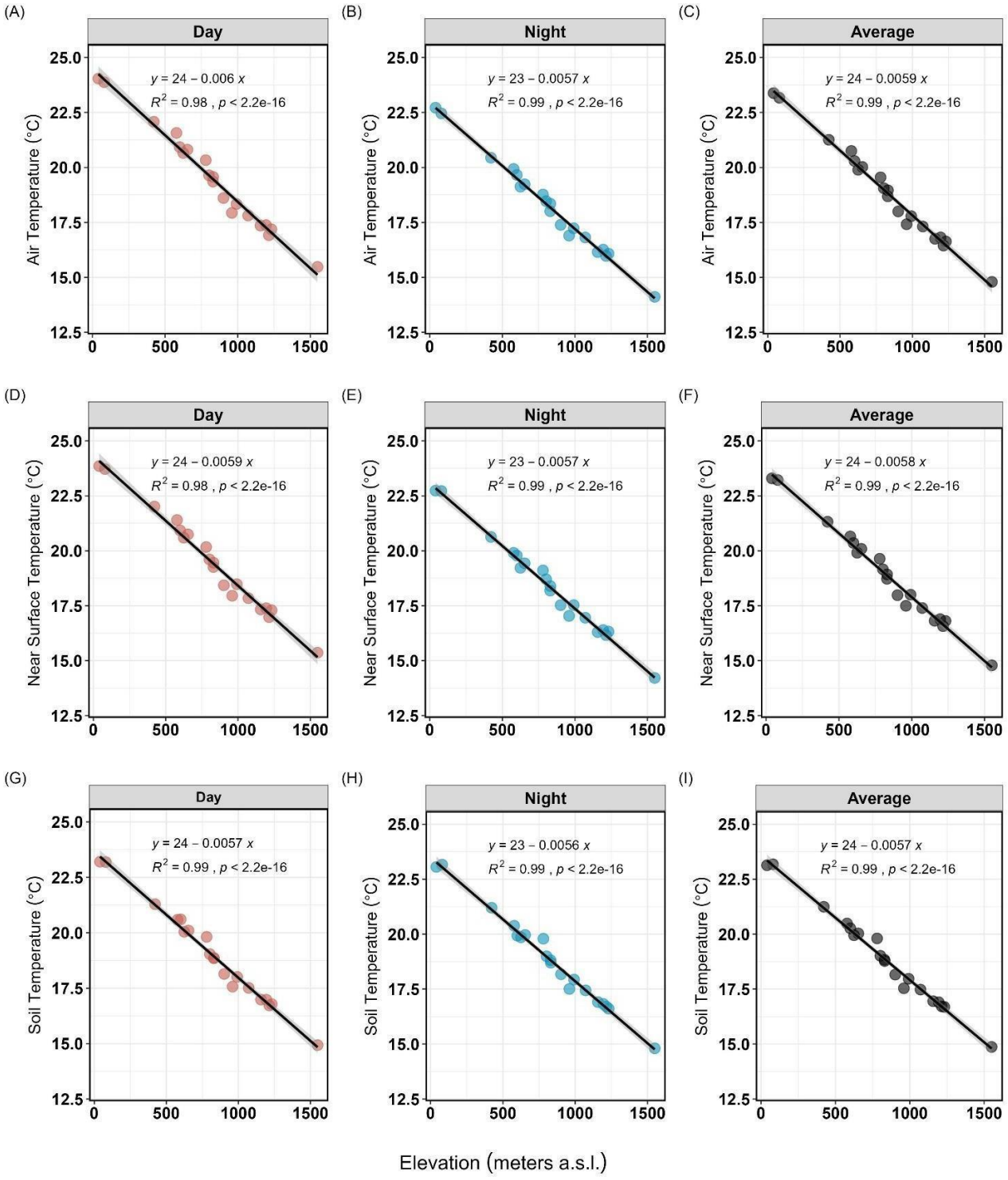

Figure 2.2. Trends in temperature during the Day (7:00 – 17:00 AEST), Night (17:15 to 06:45 AEST) and 24-hour average for the measurement period, December 2019 - September 2022. Temperature measurements are for above ground Air **(A), (B) & (C)** (*n*= 20)**,** Near Surface **(D)**, **(E)** & **(F)** (*n*= 20), and Soil **(G)**, **(H)** & **(I)** (*n*= 20) from study sites across the elevation range (40 to 1550 m a.s.l.) in the Australian Wet Tropics world heritage area.

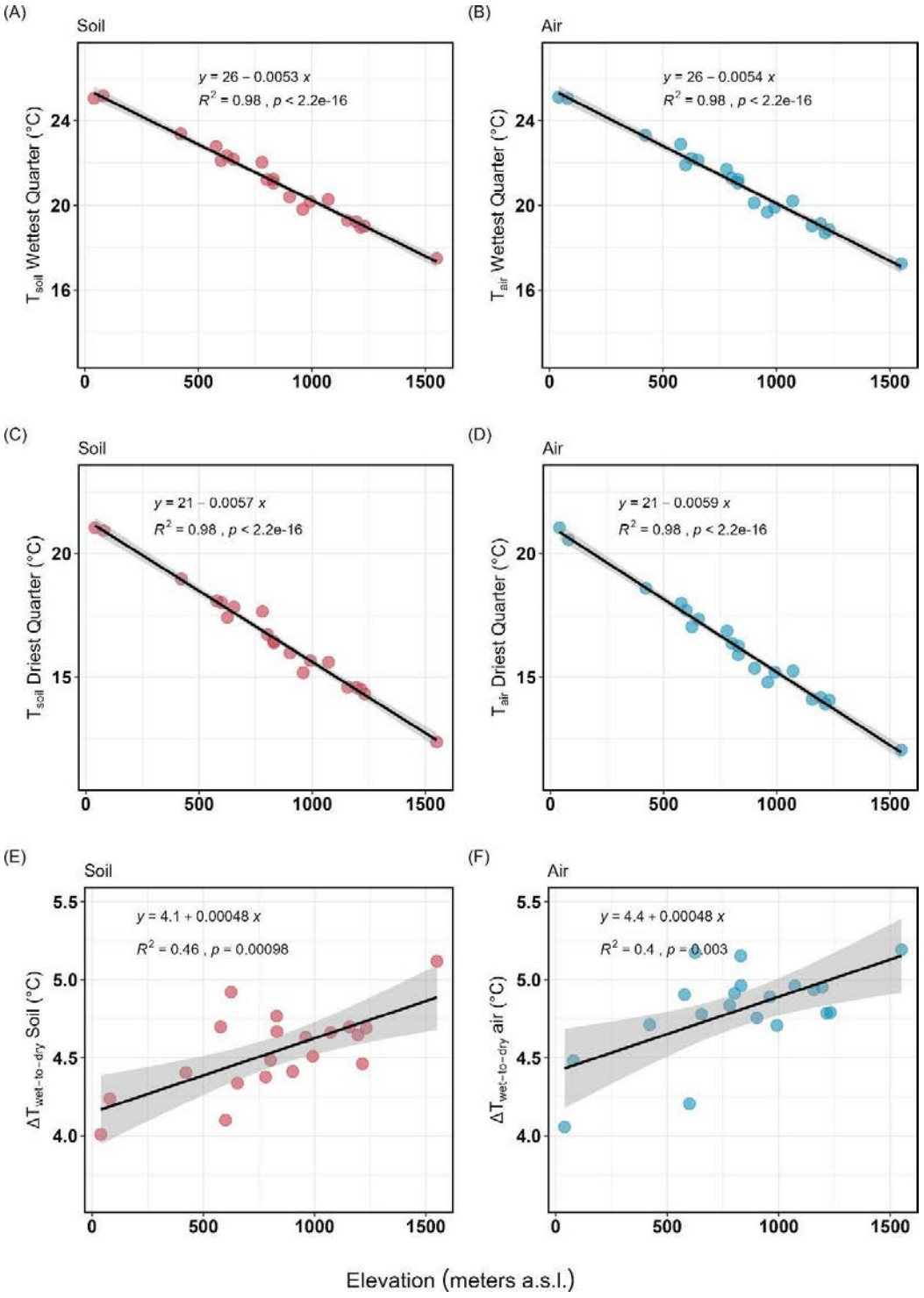

Figure 2.3. Temperature trends across elevation in the Australian Wet Tropics (*n*=20 sites). **Top**: Temperature recorded during the wettest quarter (summer months, January – March) for Soil **(A)** and Air (**B)**; Middle: and the driest quarter (winter months, July – September) **(C)** & **(D)**; **Bottom:** Temperature difference between the two quarters ($\Delta T_{wet\text{-}to\text{-}dry}$) for Soil **(E)** and Air **(F)**.

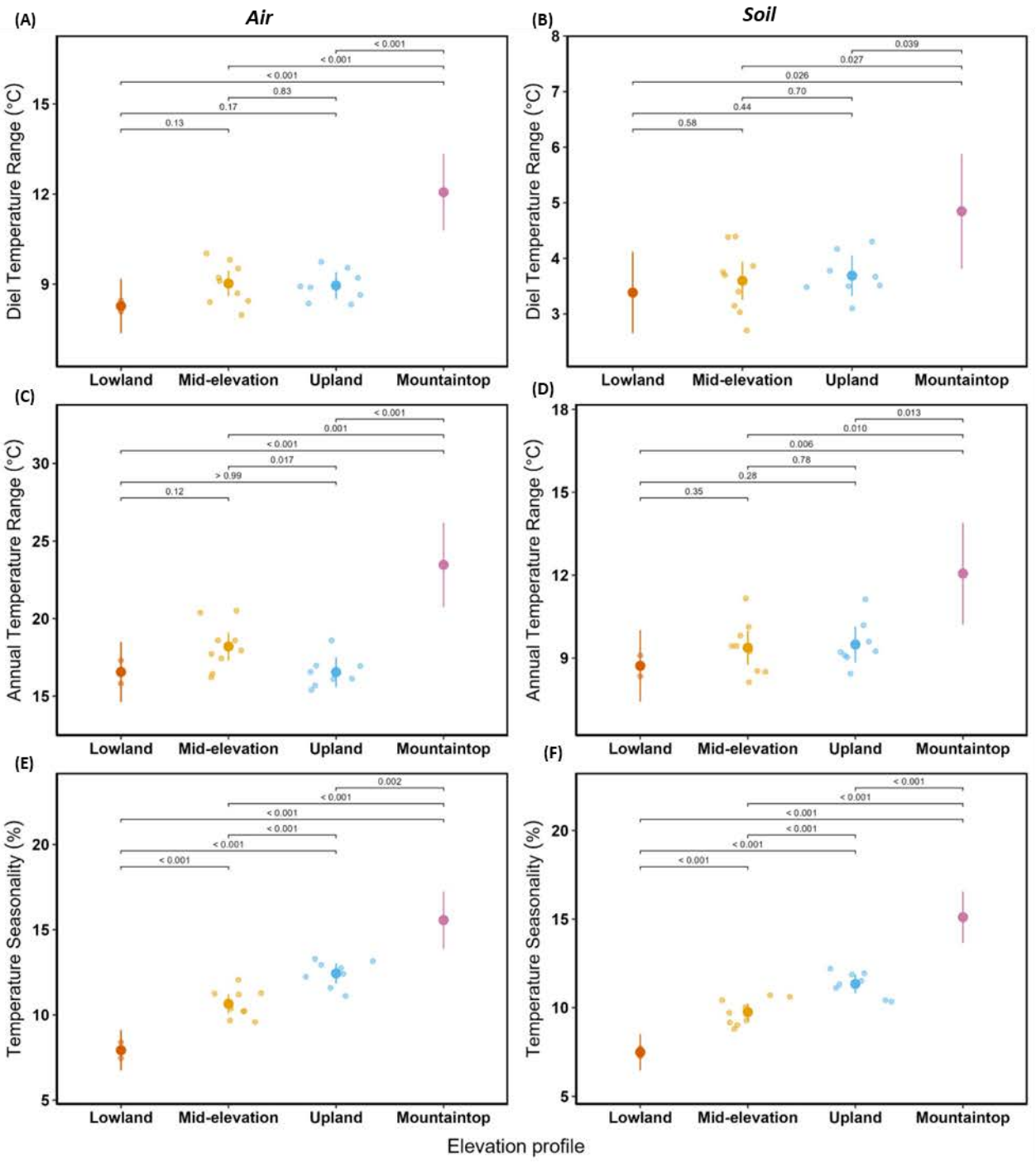

Figure 2.4. A plot of bioclimatic predictors for soil and above ground air across the elevation profile (as defined by (Webb, 1959)), averaged for the years 2020 and 2021. **Top:** Diel Temperature Range (DTR) for Air **(A)** and Soil **(B)**; **Middle:** Annual Temperature Range (ATR) for Air (**C)** and Soil **(D)**; **Bottom:** Temperature seasonality (coefficient of variation) for Air (BIO4) **(E)** and Soil **(F)**. Data point is an estimate of least square means with lower and upper confidence intervals shown as error bar for each elevation category, i.e., Lowland – two sites in the Daintree National Park (orange dot points); Mid-elevation – nine sites in the Mt Lewis National Park (yellow dot points; Upland – eight sites in the Mt Lewis National Park (blue dot points); and Mountaintop represents only one site on Mt Bellenden Ker (purple). Significant effects are for those *p-values* (<0.05, 0.01, and 0.001).

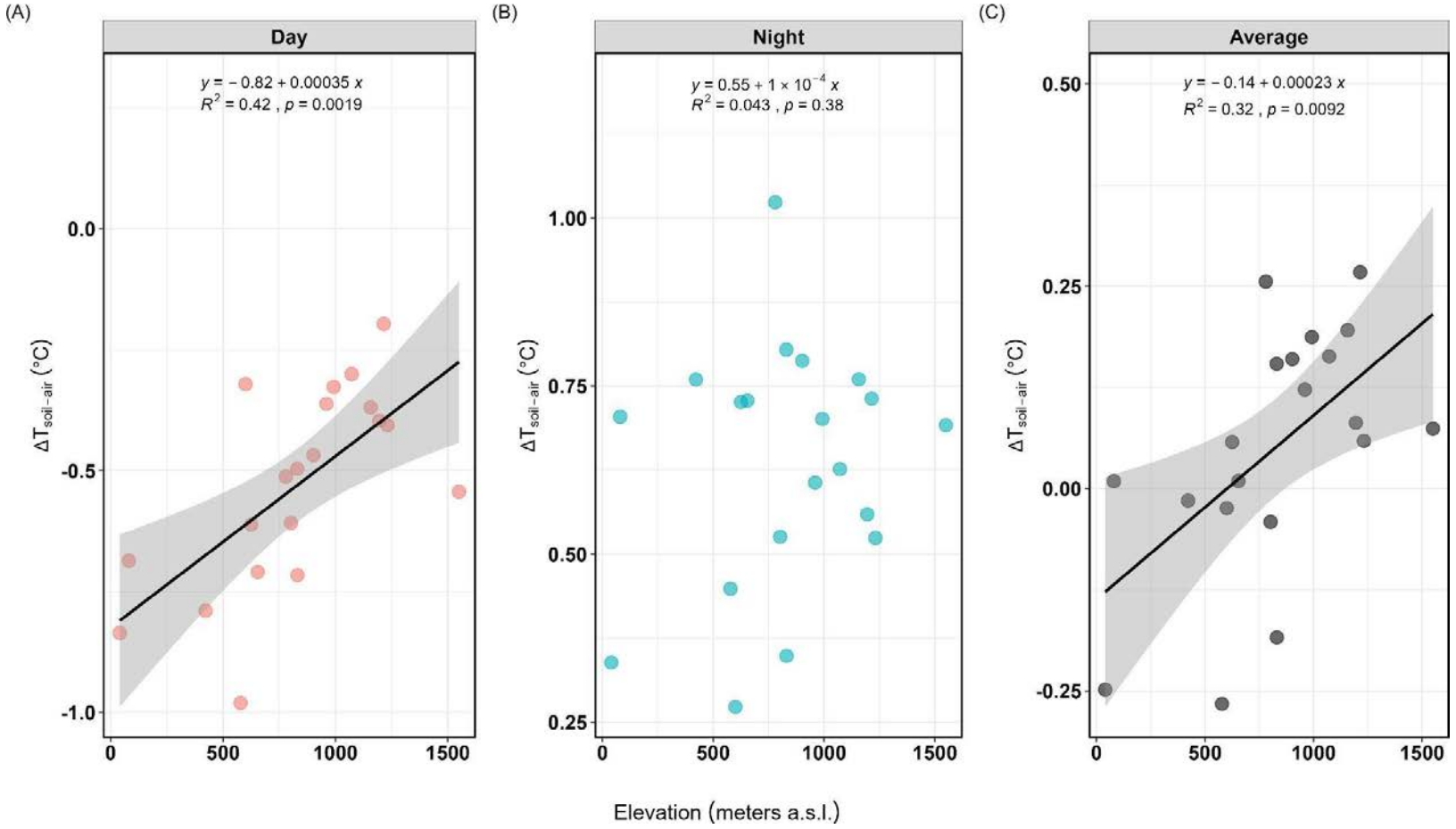

Figure 2.5. Trends in the temperature difference between soil and above-ground air ($\Delta T_{soil\text{-}air}$) with elevation in the Australian Wet Tropics (n=20 sites), observed during the daytime (7:00 – 17:00 AEST) **(A)**; observed during the night-time (17:15 to 06:45 AEST) **(B)**; and averaged across the 24-hour daily measurement period from between December 2019 and September 2022 **(C)**.

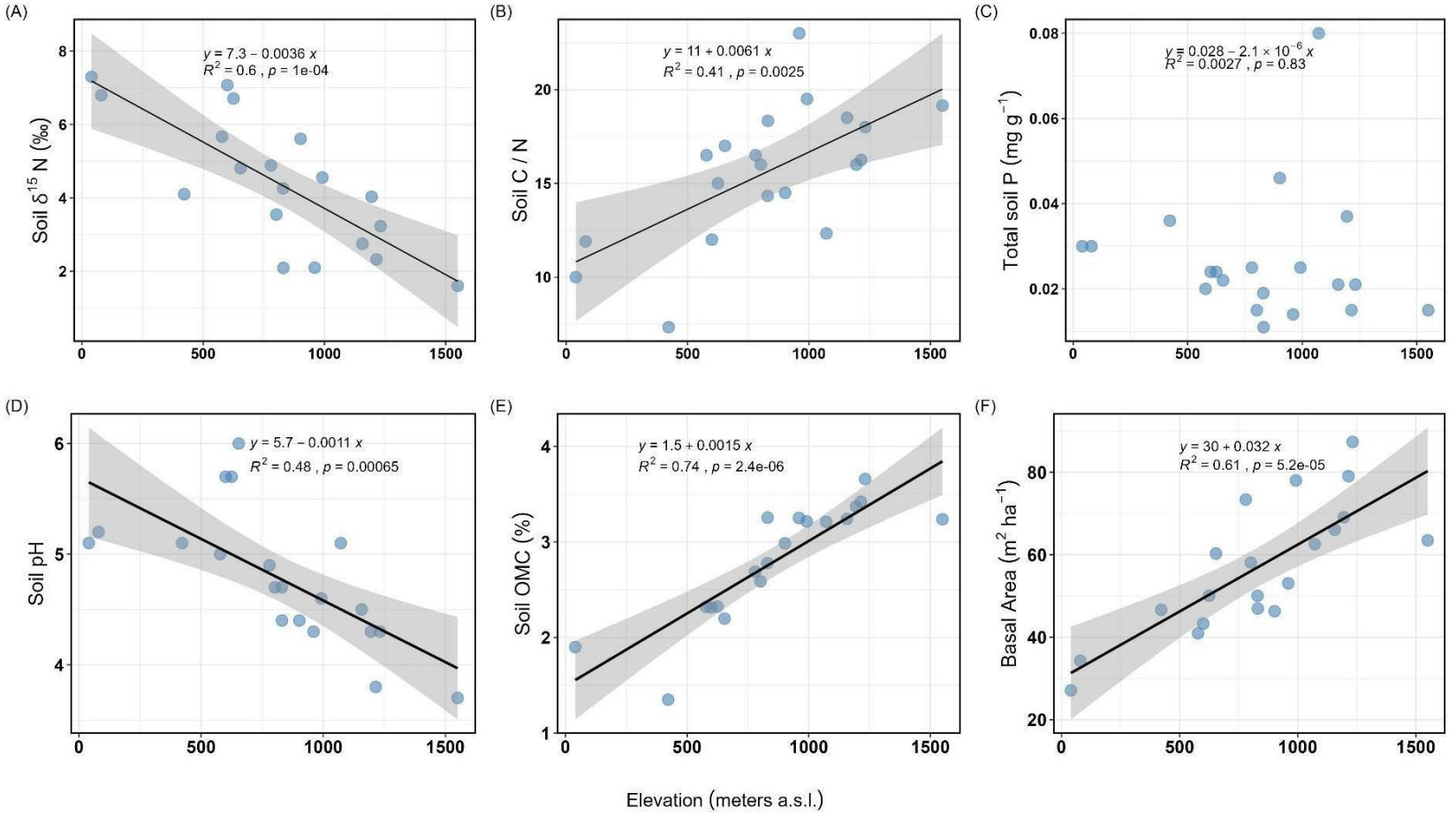

Figure 2.6. Top: Soil stable $\delta^{15}N$ isotope composition (*n*=19 sites) **(A),** soil C/N ratio (*n*=20 sites) **(B)** and total soil P content (*n*=20 sites) (**C**); **Bottom:** Soil pH (*n*=20 sites) (**D),** soil organic matter content (OMC) (*n*=20 sites) (**E)** and tree basal area (*n*=20 sites) **(F)** along an elevation gradient in the Australian Wet Tropics.

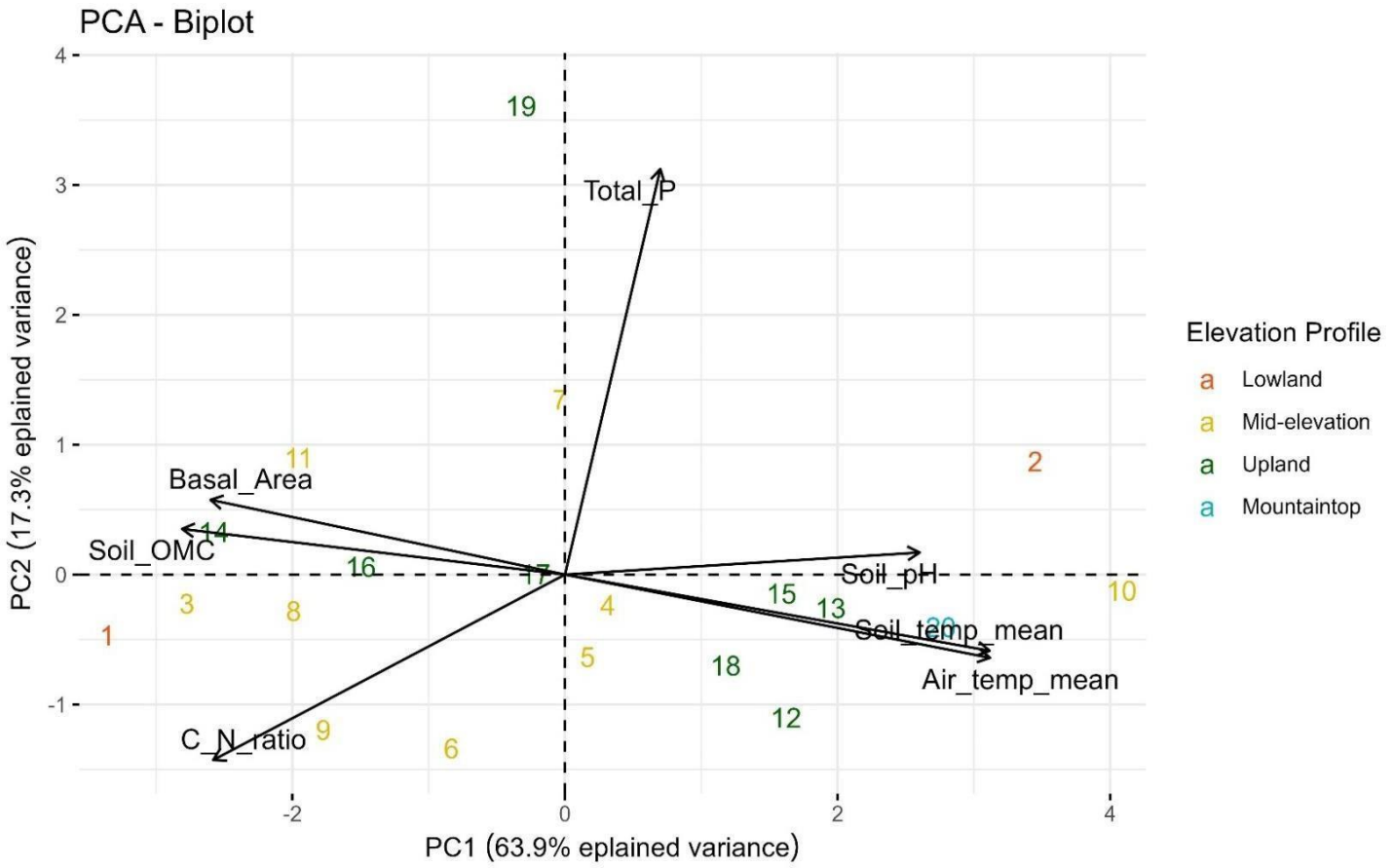

Figure 2.7. Principal component analysis for environmental variables showing data points that represent sites (*n*= 20) in the Australian Wet Tropics World Heritage Area. The first and second principal component that contribute more than 80% of total variation is shown here. The study site identifiers are shown here as numbers and the elevation profile coloured for 'lowland' as orange (*n*=2 sites), mid-elevation as yellow (*n*=9 sites), upland as green (*n*=8 sites) and one mountaintop site as blue. The loadings of environmental variables such as temperatures for Soil and above-ground Air, soil pH, C:N ratio, soil P, Organic Matter Content (OMC), and Basal Area are shown as arrows along the co-ordinate axes.

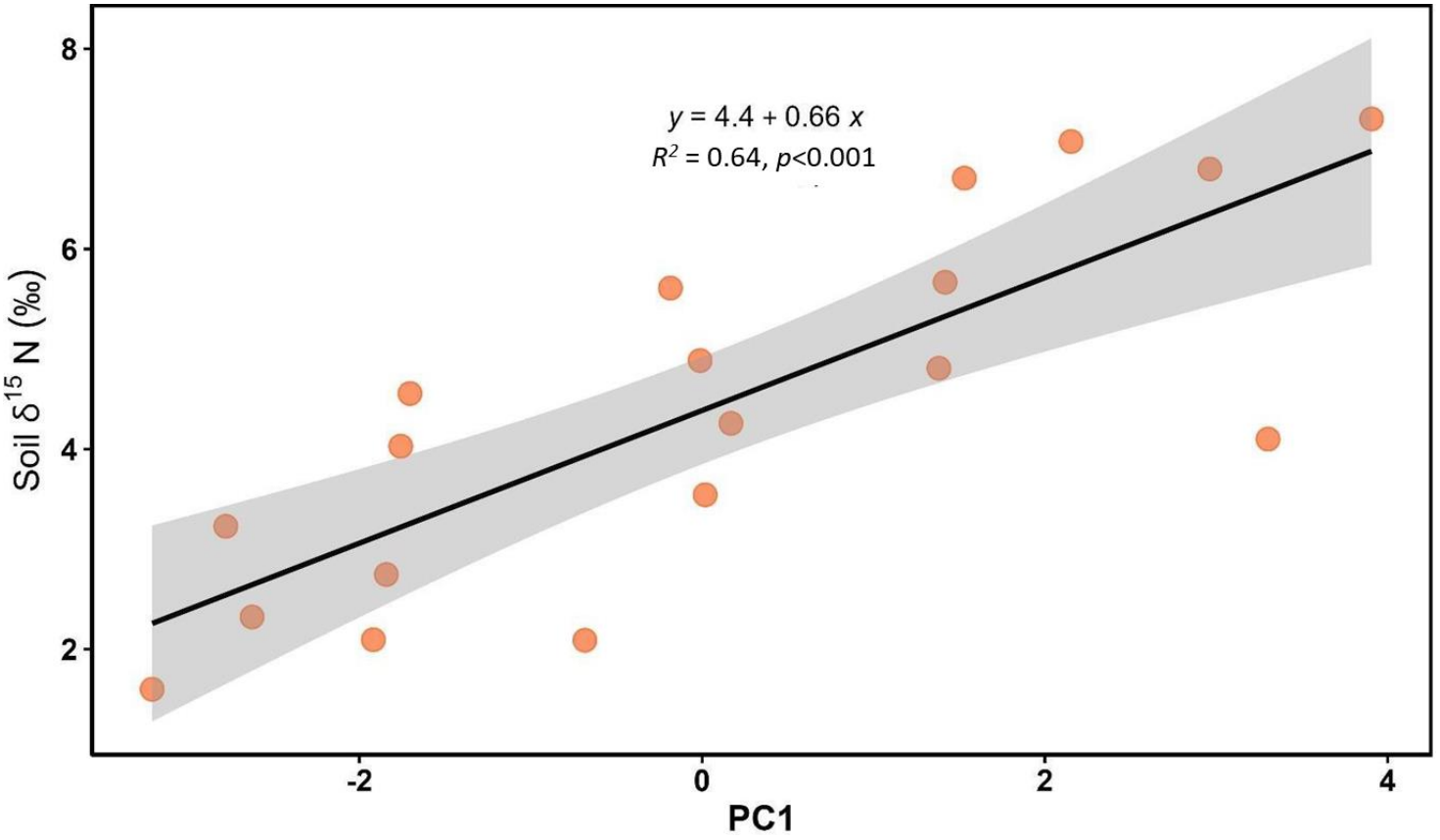

Figure 2.8. Soil $\delta^{15}N$ isotope composition plotted against PC1 scores from study sites in the Australian Wet Tropics. Regression line with 95% confidence is shown as a grey band.

Supplementary Table 2.1A. Summary of the Principal Component Analysis showing the percentage variation of different components of the Eigen values.

	PC1	PC2	PC3	PC4	PC5	PC6	PC7
Variance	2.10	1.09	0.74	0.61	0.51	0.31	0.03
Percent of variance	63.9	17.3	8.0	5.4	3.7	1.4	0.1
Cumulative % of variance	63.9	81.2	89.2	94.7	98.5	99.9	100

Supplementary Table 2.1B. Summary of the Principal Component Analysis showing correlations of environmental variables with the first four components.

	PC1	PC2	PC3	PC4
Soil Temperature	0.454704359	-0.046222772	0.19988256	0.478260683
Air Temperature	0.455389115	-0.070945063	0.21649604	0.443621258
Soil pH	0.375134123	0.726321962	0.22275404	-0.179910551
Soil OMC	-0.409835310	-0.161006818	0.17409510	0.571846074
C:N ratio	-0.365157687	0.100354082	0.86251410	-0.137782459
Basal Area	-0.379252603	0.655200767	-0.29868285	0.442838729
Total Soil P	0.001197873	0.002116109	-0.01029275	0.001007163

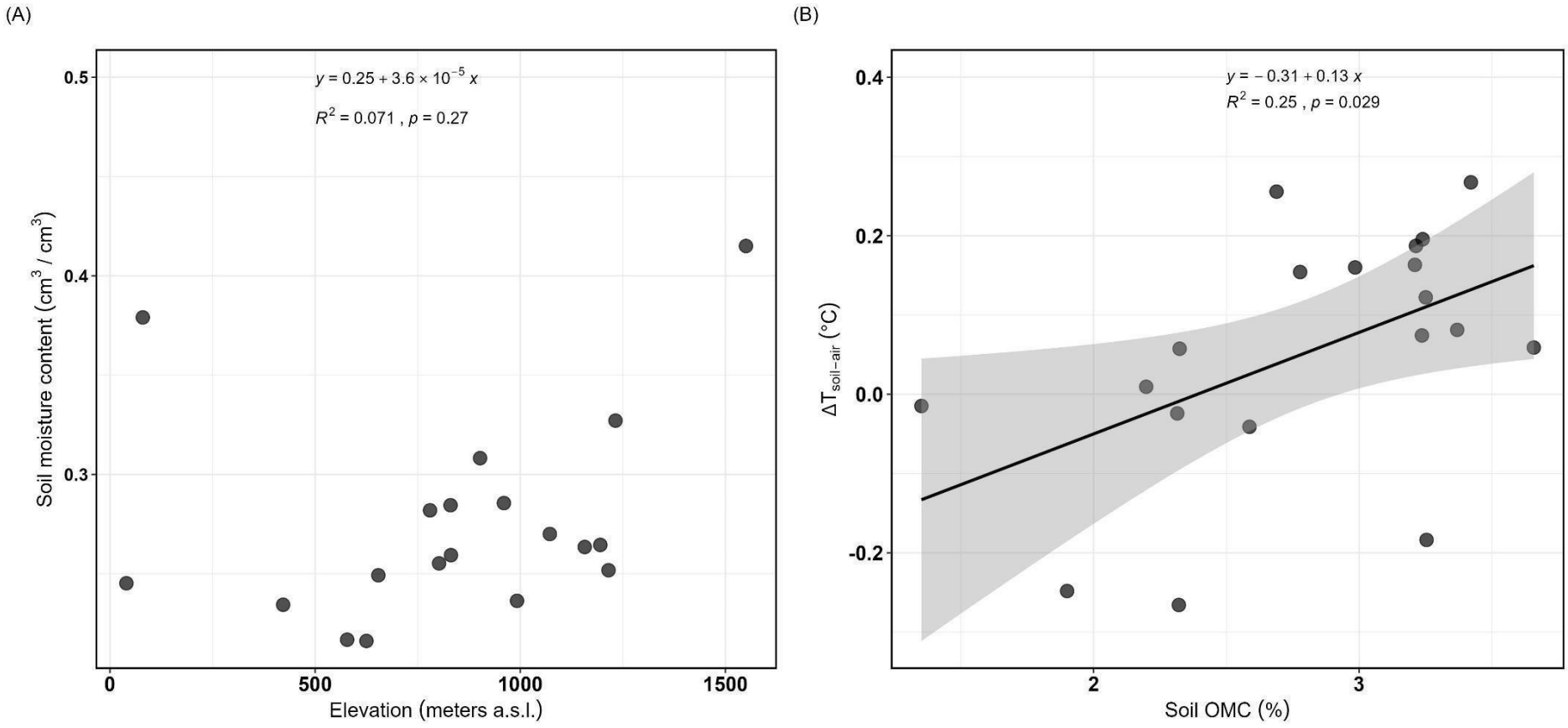

Supplementary Figure 2.1. A plot of mean annual values of soil volumetric moisture content from various study sites from across elevation in the Australian Wet Tropics (*n*=20) **(A)**; Relationship between the Soil-to-Air temperature difference and soil organic matter content observed in this study **(B).**

Chapter 3: Temperature, nutrient availability, and species traits interact to shape elevation responses of Australian tropical trees

This chapter has been published in the journal *Frontiers in Forests and Global change*.

Singh Ramesh A, Cheesman AW, Flores-Moreno H, Preece ND, Crayn DM and Cernusak LA (2023). *Temperature, nutrient availability, and species traits interact to shape elevation responses of Australian tropical trees*. Front. For. Glob. Change 6:1089167. DOI: 10.3389/ffgc.2023.1089167 (published January 2023)

Saplings of the lowland, *Flindersia ifflana* in nutrient poor soils being monitored for its growth under experimental conditions **(Left)**; Leaves of *Flindersia* being processed in field for trait measurements **(top-right);** Seedlings of mountaintop restricted species, *Flindersia oppositifolia* being germinated for experiments **(bottom-right).**

frontiers | Frontiers in Forests and Global Change

TYPE Original Research
PUBLISHED 19 January 2023
DOI 10.3389/ffgc.2023.1089167

OPEN ACCESS

EDITED BY
Lucy Penn Kerhoulas,
Cal Poly Humboldt, United States

REVIEWED BY
Kelsey Bryant,
University of Idaho, United States
John T. Van Stan,
Cleveland State University, United States

*CORRESPONDENCE
Arun Singh Ramesh
arun.singhramesh@my.jcu.edu.au

SPECIALTY SECTION
This article was submitted to Forest Ecophysiology, a section of the journal Frontiers in Forests and Global Change

RECEIVED 04 November 2022
ACCEPTED 04 January 2023
PUBLISHED 19 January 2023

CITATION
Singh Ramesh A, Cheesman AW, Flores-Moreno H, Preece ND, Crayn DM and Cernusak LA (2023) Temperature, nutrient availability, and species traits interact to shape elevation responses of Australian tropical trees.
Front. For. Glob. Change 6:1089167.
doi: 10.3389/ffgc.2023.1089167

Temperature, nutrient availability, and species traits interact to shape elevation responses of Australian tropical trees

Arun Singh Ramesh[1,2]*, Alexander W. Cheesman[1,3], Habacuc Flores-Moreno[2,4], Noel D. Preece[1], Darren M. Crayn[1,5] and Lucas A. Cernusak[1]

[1]Centre for Tropical Environment and Sustainability Science, College of Science and Engineering, James Cook University, Smithfield, QLD, Australia, [2]Terrestrial Ecosystem Research Network, The University of Queensland, St Lucia, QLD, Australia, [3]College of Life and Environmental Sciences, University of Exeter, Exeter, United Kingdom, [4]Commonwealth Scientific and Industrial Research Organisation, Brisbane, QLD, Australia, [5]Australian Tropical Herbarium, James Cook University, Smithfield, QLD, Australia

Elevation gradients provide natural laboratories for investigating tropical tree ecophysiology in the context of climate warming. Previously observed trends with increasing elevation include decreasing stem diameter growth rates (GR), increasing leaf mass per area (LMA), higher root-to-shoot ratios (R:S), increasing leaf $\delta^{13}C$, and decreasing leaf $\delta^{15}N$. These patterns could be driven by decreases in temperature, lower soil nutrient availability, changes in species composition, or a combination thereof. We investigated whether these patterns hold within the genus *Flindersia* (Rutaceae) along an elevation gradient (0–1,600 m) in the Australian Wet Tropics. *Flindersia* species are relatively abundant and are important contributors to biomass in these forests. Next, we conducted a glasshouse experiment to better understand the effects of temperature, soil nutrient availability, and species on growth, biomass allocation, and leaf isotopic composition. In the field, GR and $\delta^{15}N$ decreased, whereas LMA and $\delta^{13}C$ increased with elevation, consistent with observations on other continents. Soil C:N ratio also increased and soil $\delta^{15}N$ decreased with increasing elevation, consistent with decreasing nutrient availability. In the glasshouse, relative growth rates (RGR) of the two lowland *Flindersia* species responded more strongly to temperature than did those of the two upland species. Interestingly, leaf $\delta^{13}C$ displayed an opposite relationship with temperature in the glasshouse compared with that observed in the field, indicating the importance of covarying drivers in the field. Leaf $\delta^{15}N$ increased in nutrient-rich compared to nutrient-poor soil in the glasshouse, like the trend in the field. There was a significant interaction for $\delta^{15}N$ between temperature and species; upland species showed a steeper increase in leaf $\delta^{15}N$ with temperature than lowland species. This could indicate more flexibility in nitrogen acquisition in lowland compared to upland species with warming. The distinguishing feature of a mountaintop restricted *Flindersia* species in the glasshouse was a very high R:S ratio in nutrient-poor soil at low temperatures, conditions approximating

the mountaintop environment. Our results suggest that species traits interact with temperature and nutrient availability to drive observed elevation patterns. Capturing this complexity in models will be challenging but is important for making realistic predictions of tropical tree responses to global warming.

KEYWORDS

elevation gradient, *Flindersia*, growth temperature, leaf $\delta^{13}C$, leaf $\delta^{15}N$, relative growth rate, root-to-shoot ratio, soil nutrient availability

1. Introduction

Elevation gradients, and their associated changes in temperature, provide natural laboratories for studying how tropical trees might respond to global warming (Malhi et al., 2010; Tito et al., 2020). Increasing elevation, and by extension lower temperatures, have been associated with both species-specific and community-based trends; these include decreasing growth rates (Rapp et al., 2012), increasing root-to-shoot ratios (R:S) (Fahey et al., 2016), increasing leaf mass per area (LMA) (Rapp et al., 2012; Van De Weg et al., 2012; Fahey et al., 2016), increasing foliar $\delta^{13}C$, and decreasing foliar $\delta^{15}N$ (Sparks and Ehleringer, 1997; Li et al., 2009). Foliar $\delta^{13}C$ and $\delta^{15}N$ have been used as indicators of intrinsic water-use efficiency (Cernusak et al., 2013), and ecosystem nitrogen cycling (Martinelli et al., 1999), respectively. However, although some of these trends with increasing elevation appear to be general in the literature (Vitousek et al., 1990; Bauters et al., 2017; Mumbanza et al., 2021), the mechanisms driving the observations are not fully resolved. Disentangling the direct and indirect role that temperature plays in determining these trends in plant functional traits is vital to understanding elevation gradients as proxies for predicting the response of forests to future climate scenarios.

In addition to decreasing temperatures, increasing elevation is associated with variation in other climatic factors, such as precipitation, vapor pressure deficit, and solar radiation (Malhi et al., 2010). Similarly, the availability of soil nutrients, such as N and P, can also change as a function of elevation, both because of changes in temperature-driven mineralization rates, and inherent litter decomposability (Salinas et al., 2011). Together, these environmental factors are all recognized as major drivers of tropical tree growth and selective filters for plant functional traits (Rapp et al., 2012; Cheesman et al., 2018; Bauman et al., 2022a). Trends in functional traits observed across elevation may therefore result from, to varying degrees, changes in temperature, vapor pressure deficit, soil nutrients, species turnover, and the interaction of these factors (Read et al., 2014; Fahey et al., 2016).

Declining temperatures and nutrient availability with increasing elevation can influence resource allocation in tropical trees (Unger et al., 2012). For example, N allocation toward photosynthetic tissues may be reduced (Xiao et al., 2018; Ziegler et al., 2020), and climatic and soil conditions may favor biomass allocation toward roots (Kobe et al., 2010; Poorter et al., 2012). This may lead to the selection of species at high elevations with functional adaptations for slower growth, such as an intrinsically high R:S, and with leaf traits oriented toward the slow end of the leaf economic spectrum, including a larger leaf mass per unit leaf area (LMA), lower mass based N concentration, and a more robust leaf structure associated with longer leaf lifespans (Wright et al., 2005; Valladares and Niinemets, 2008; Poorter et al., 2012). Low temperatures and nutrient availability may also lead to the production of leaves, leaf-litter, and thereby soil organic material with limited N availability and a highly recalcitrant carbon content. This self-reinforcing trend may lead to observed traits being directly impacted by nutrient availability and decoupled (in the short term) from the direct impacts of changing temperature.

The relationship between water availability and foliar $\delta^{13}C$ is generally well-established (Diefendorf et al., 2010), with foliar $\delta^{13}C$ becoming more negative as precipitation and soil water availability increase. Yet, somewhat surprisingly, leaf $\delta^{13}C$ often becomes higher with elevation in spite of general increases in water availability (Sparks and Ehleringer, 1997); this appears to be related to increasing LMA and decreasing atmospheric pressure (Körner, 2007; Chen et al., 2017). Higher LMA can increase the leaf internal resistance to CO_2 diffusion, thereby reducing chloroplastic CO_2 concentrations during photosynthesis (Cernusak et al., 2013), resulting in an increase in the foliar $\delta^{13}C$ (Vitousek et al., 1990; Li et al., 2009). Increased LMA can also lead to increased leaf N and P concentrations per unit leaf area, which can confer increased leaf photosynthetic capacity, further decreasing discrimination against ^{13}C (Bauman et al., 2022a). Nevertheless, decreases in foliar $\delta^{13}C$ with increasing elevation have been reported in some cases (Sah and Brumme, 2003), and could be related to lower leaf-to-air vapour pressure deficits (VPD) with increasing elevation, resulting in an increased ratio of intercellular to ambient CO_2 concentrations (c_i/c_a) through opening of stomata (Cernusak et al., 2013; Chen et al., 2017).

Foliar $\delta^{15}N$ has been observed to decrease with increasing elevation in tropical rainforest trees (Bauters et al., 2017). This is thought to be the result of more open N cycling at warm, low elevations, and with tighter N cycling at higher elevations as a result of slower N mineralization rates caused by low temperatures and less decomposable litter (Martinelli et al., 1999; Baumgartner et al., 2021). More open N cycling feeds N loss pathways from the ecosystem that tend to leave the residual N pool relatively enriched in ^{15}N (Martinelli et al., 1999; Craine et al., 2015). Some studies have also reported a positive trend or no change in foliar $\delta^{15}N$ with elevation, attributing this to increased water stress in some mountainous regions, or due to the nature of site-specific biogeochemical processes; such as ammonium immobilization for example (Vitousek et al., 1989; Yi and Yang, 2006). Likewise, differences in plant functional types are known to contribute toward variation in foliar $\delta^{15}N$ due to differences in nitrogen acquisition strategies and microbial associations, such as symbiotic associations with N fixing bacteria and mycorrhizal fungi (Cernusak et al., 2009; Liu et al., 2010). However, within species from a single genus found in moist tropical rainforests, we would not expect to find these latter complications. Thus, $\delta^{15}N$ signatures

can still be generally useful as indicators of nitrogen cycling at the ecosystem scale and across environmental gradients, if care is taken to minimize variation associated with different plant functional types and ecological strategies (Amundson et al., 2003).

Understanding how temperature directly and indirectly shapes observed patterns in species distribution and plant functional traits across elevation will allow a mechanistic understanding of how changing temperatures are likely to impact natural systems. In this study, we first examined patterns of tree stem diameter growth and leaf functional traits (LMA, $\delta^{13}C$ and $\delta^{15}N$) in a dominant tropical rainforest tree genus, *Flindersia*, distributed along an elevation gradient in the Australian Wet Tropics World Heritage Area (Bradford et al., 2014a). We then conducted a glasshouse experiment to examine the relative impacts of temperature, soil nutrient availability, and species in driving these observations. We hypothesized that trends across elevation would reflect a combination of both direct temperature effects, indirect temperature effects mediated by nutrient availability, and species' traits associated with habitat preference (lowland versus upland). To gain insight, we used the glasshouse experiment to test for effects of temperature and nutrient availability, and their interactions with species and habitat preference, on growth rates, biomass allocation, LMA, $\delta^{13}C$ and $\delta^{15}N$.

2. Materials and methods

2.1. Species selection and study area

Flindersia R.Br., of the family Rutaceae, comprises *ca* 17 species of trees and shrubs distributed across Malesia, Australia, and New Caledonia, with 15 species known to occur in the tropics and sub-tropics of Australia (Scott et al., 2000; Bayly et al., 2013). Nine species in the Australian Wet Tropics are commonly observed among the dominant taxa and contribute to biomass in rainforest plots in these forests (Bradford et al., 2014a), ranging from near sea level to the summits of the highest peaks (Zich et al., 2020). *Flindersia*, in general, are known to reliably produce seeds, which are enclosed in fruits that are easy to spot in the canopy, and are therefore more accessible compared to seeds of some other co-occurring taxa (Zich et al., 2020). We explored herbarium records and species distribution observations from the Atlas of Living Australia (ALA) (Belbin, 2011) and used these observations to identify four focal *Flindersia* species for this study: *F. ifflana* F. Muell., *F. bourjotiana* F. Muell., *F. brayleyana* F. Muell., and *F. oppositifolia* (F. Muell.) T.G. Hartley & L.W. Jessup. *Flindersia oppositifolia* is a tropical mountaintop species with a very restricted distribution and a narrow climate niche, whereas the other species are more widely distributed along the elevation gradient and have a broad climate niche. Among these, *F. brayleyana* displays a predominantly upland distribution, whereas *F. bourjotiana* and *F. ifflana* have predominantly lowland distributions (**Supplementary Table 1**).

We filtered the ALA observations for each species using the spatial thinning package 'spThin' (Aiello-Lammens et al., 2015) in R, set at a scale of 0.5 km for the mountaintop restricted species and 5km resolution for the widespread taxa at 10 repetitions for each species, which returned a total of 95 spatially-thinned occurrences within the Australian Wet Tropics. We then extracted a suite of gridded environmental variables from WorldClim for the occurrence locations, including mean annual temperature (BIO1) (**Figure 1A**) and mean annual precipitation (BIO12) (**Figure 1B**; Fick and Hijmans, 2017).

2.2. Stem diameter growth and plant functional trait measurements across elevation

Individual stem diameter growth rates (GR) were calculated for mature rainforest *Flindersia* species distributed across elevation in the Australian Wet Tropics and captured in long-term forest census plots (n = 13 sites). For each individual within a site, we calculated the linear increase in diameter for stems greater than 10 cm diameter at breast height (n = 2 to 20 individuals per site) between 1971 and 2013 (Bradford et al., 2014b). For *F. oppositifolia*, restricted to mountaintops, we calculated GR (n = 33 individuals) for the period from 2010 to 2019 using a rainforest plot established by Torello Raventos (2014), which we re-censused in 2019. Field campaigns to collect plant functional traits (LMA, foliar $\delta^{13}C$ and $\delta^{15}N$) of exposed canopy branches of focal *Flindersia* species (a minimum of 2 individuals per site) were conducted in four locations (**Supplementary Table 1**) across a range in elevation, using standard trait measurement protocols (Cornelissen et al., 2003). Data from a previous trait campaign (Bauman et al., 2022a) were also added to this analysis (n = 16 individuals across five sites for the focal species).

2.3. Soil nutrient and isotope analyses across elevation

Surface soil samples were collected from 20 rainforest plots spanning an elevation range from 40 to 1,550 m in the Australian Wet Tropics. Of these, 16 plots had dimensions 20 m × 20 m, whereas the mountaintop plot had dimension 50 m × 20 m, and the two lowland sites were each 100 m × 100 m. The sites were selected to include those for which soils were derived from granitic parent material, except for the two lowest elevation plots, for which soils were derived from granitic and metamorphic colluvium. Five cores per site (at the 4 corners of the plot and one at the center) were sampled using an auger (~10 cm deep) after removing leaf litter. Samples were bulked and homogenized at the plot level. Samples were then oven-dried at ~105°C for 72 h and ground to a fine powder using a Benchtop Ring Mill (Rocklabs, Mineral Stats INC., Colorado) at the Advanced Analytical Centre (AAC), James Cook University (JCU), Cairns. Soil pH in H_2O and in 0.01M $CaCl_2$ was measured on oven-dried samples using an ISFET pH pen (Model 24006 DeltaTrak). Subsamples were used to determine C and N concentrations and isotopic ratios ($\delta^{13}C$ and $\delta^{15}N$) as described below for leaf tissue. Total soil P was analyzed using a microwave assisted acid digestion of oven dried samples followed by ionization detection using the Inductively Coupled Plasma-Atomic Emission Spectrometer (ICP-AES) at the AAC, JCU, Townsville.

2.4. Glasshouse experimental growth conditions

We collected seeds from the four focal species, with each species collected at a single site (**Supplementary Table 1**). The

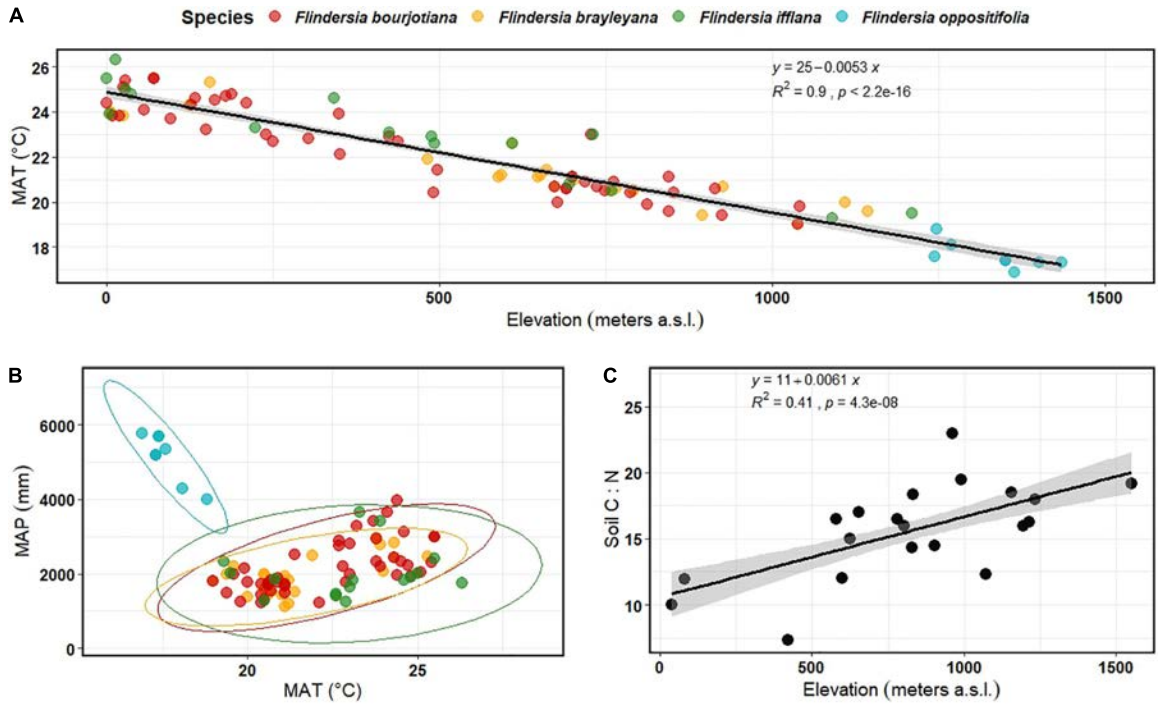

FIGURE 1
(A) Variation in mean annual temperature (MAT) across elevation in the Australian Wet Tropics, based on the *Flindersia* species occurrence records obtained after spatial thinning at 0.5 km resolution and interpolated using WorldClim v.2 bioclimatic variables (MAT, BIO1) (n = 95); **(B)** Scatter plot of mean annual precipitation (MAP, BIO12) as a function of mean annual temperature (MAT, BIO1), with ellipses representing species' climate niche across the occurrence range of the four focal *Flindersia* species within the Australian Wet Tropics (n = 95); **(C)** Variation in soil C:N ratio across an elevation gradient in the Australian Wet Tropics measured during this study (n = 20).

four collection sites were distributed across most of the elevation range found in the Australian Wet Tropics (Lowland species, *F. ifflana* ∼ 300 m and *F. bourjotiana* ∼ 600 m, and Upland species *F. brayleyana* ∼ 990 m and *F. oppositifolia* ∼ 1,550 m). The seeds were allowed to germinate under ambient shade-house conditions at the Environmental Research Complex (ERC), (∼30 m a.s.l.) JCU, Cairns, Australia. Healthy saplings were transplanted (approximately 3 months after sowing seeds) into either 13.5 L pots (Garden City Pots, Model: P300ST00) containing nutrient-rich soil (NR), comprising a 1:1 mixture by volume of premium garden potting mix and compost (Northside Landscape Supplies Pty. Ltd., Trinity Beach); or 8.5 L pots (Garden City Pots, Model: P250STTL) containing nutrient-poor soil (NP). The nutrient-poor soil comprised a locally collected dermasol, low in organic matter and supplemented with perlite and washed river sand to improve drainage (**Supplementary Table 2**). The two soil mixtures, nutrient-rich and nutrient-poor, had similar $\delta^{15}N$ at the start of the experiment, based on measurements of subsamples; these values were 5.4 and 5.3‰, respectively.

The experimental pots were transferred into a climate-controlled glasshouse facility. The facility is divided into three temperature-controlled chambers, each with a shade screen (SOLARO, Ludvig Svensson Inc. Kinna, Sweden) that reduces incident irradiance to approximately 50% of the incoming irradiance. Further details of the experimental facility can be found in Forbes et al. (2020). Three growth temperature treatments were implemented by setting chambers to track the external temperature profile with a chamber-specific offset, specifically a) 0°C offset, b) −7°C offset, and c) + 5°C offset. These chamber temperature conditions mimic the lowland provenance, mountaintop provenance, and a lowland warming scenario, respectively. The climatic conditions were controlled via the Building Management System (BMS) with temperature and relative humidity (RH) in each chamber measured (QFM2160 Temperature and Humidity Probe, Siemens) and recorded at 5 min intervals in the BMS. We further characterized the temperature regimes with a Temperature Soil Moisture Sensor [TMS-4, TOMST s.r.o, Prague, (Wild et al., 2019)] in each experimental chamber to record the temperature in the immediate environment of the saplings. A summary of chamber conditions over the course of the experiment is given in **Table 1**. We calculated the VPD of each chamber from the temperature and relative humidity measurements (Campbell and Norman, 1998).

A minimum of three healthy saplings per soil treatment per species were monitored for growth in each chamber to give a total of 24 saplings (3 Saplings × 2 Soil treatments × 4 Species) per chamber. All pots were hand-watered to field capacity daily throughout the experiment. To avoid any chamber bias across the experimental treatments, the treatments were rotated among the chambers monthly.

2.5. Glasshouse experimental biomass measurements

Before the start of the glasshouse experimental treatments, initial plant biomass was estimated for individuals using a species-specific allometric relationship derived from root-collar diameter, stem height, and the total dry biomass of three destructively harvested

TABLE 1 Environmental conditions in the glasshouse during the experiment for the three glasshouse chambers.

	Cold				Ambient				Elevated			
Time	Temperature (°C)		RH (%)	VPD (kPa)	Temperature (°C)		RH (%)	VPD (kPa)	Temperature (°C)		RH (%)	VPD (kPa)
	BMS	TOMST			BMS	TOMST			BMS	TOMST		
Day	19 ± 3.2	17 ± 3.5	76 ± 5.8	0.53 ± 0.24	26 ± 3.6	25 ± 3.5	83 ± 8.5	0.61 ± 0.37	31 ± 4.1	30 ± 4.6	71 ± 11	1.39 ± 0.69
Night	14 ± 1.9	12 ± 1.9	84 ± 3.5	0.26 ± 0.08	20 ± 3.1	19 ± 3.1	91 ± 6.3	0.22 ± 0.18	25 ± 3.1	24 ± 3.1	79 ± 9	0.68 ± 0.36
Average	16.5 ± 2.5	14.5 ± 2.7	80 ± 4.6	0.40 ± 0.16	23 ± 3.35	22 ± 3.3	87 ± 7.4	0.41 ± 0.27	28 ± 3.6	27 ± 3.8	75 ± 10	1.03 ± 0.52

Air temperature was recorded using the building management system (BMS) software and additionally with a temperature moisture sensor (TMS-4, TOMST, Czech Republic), recorded at intervals of 5 min. Relative humidity (RH) and vapor pressure deficit (VPD) were recorded with the BMS. All values given in means ± 1SD. Daytime and night-time have been separated, with daytime being hours between 0700 and 1700 local time.

saplings. Final biomass was measured from destructive harvests of three plants per species by treatment combination, except for *F. bourjotiana* in the nutrient-rich, elevated temperature treatment, where only two plants survived. Thus, a total of 71 plants were harvested for final biomass.

The dry mass of leaves, stems and roots were measured separately and used to calculate Above Ground Biomass (AGB, sum of leaf and stem dry mass) and Below Ground Biomass (BGB, total root dry mass). The AGB and BGB were used to calculate the root-to-shoot ratio (R:S). From each plant, three to four leaves were collected for determination of LMA, $\delta^{13}C$ and $\delta^{15}N$, as described below. Relative growth rates (RGR, mg g^{-1} day^{-1}) were calculated using equation 1 (Hoffmann and Poorter, 2002):

$$RGR = \frac{\ln\left(M_f\right) - \ln(M_i)}{\Delta t} \quad (1)$$

where, M_f is the final biomass, M_i is the estimated initial biomass, and Δt is the length of the experiment in days.

2.6. Leaf-level functional traits

For both field-collected, and glasshouse grown leaves, leaf area was calculated from scanned fresh leaves (3 to 5 leaves per individual) using Image-J software, which in conjunction with oven-dried leaf mass was used to calculate LMA (g m^{-2}). Further, oven-dried leaves were ground to a fine powder using a Bench Top Ring Mill. Foliar $\delta^{13}C$ and $\delta^{15}N$ isotope ratios were determined using a Costech Elemental Analyzer, fitted with a zero-blank auto-sampler and coupled via a ConFloIV interface to a Thermo Finnigan Delta-V PLUS isotope ratio mass spectrometer (Bremen, Germany). Stable isotope results are reported as per mil (‰) deviations from the VPDB and AIR reference standard scales for $\delta^{13}C$ and $\delta^{15}N$, respectively. Precisions (± 1 standard deviation) on internal standards were better than ± 0.1‰ and ± 0.2‰ for C and N, respectively.

2.7. Statistical analysis

2.7.1. Field observations

All statistical analyses were conducted within the 'R studio' environment, using R version 4.1.2 (R Core Team, 2021). We computed ordinary least-squares linear regressions for each of the response variables to understand how field observed traits (i.e., GR, LMA, $\delta^{13}C$ and $\delta^{15}N$) varied with elevation (**Supplementary Table 3**). We conducted these analyses at the genus level; that is, individual species identities were not accounted for in the models. For the field measurements, each species was sampled at one or few locations, and so accounting for individual species did not improve the models. All dependent variables were checked for normality assumptions using the Shapiro–Wilk's test for normality and we used square root transformation on GR to meet normality assumptions. Predictor variables were standardized prior to analyses. The 95% Confidence Intervals and *P*-values were computed using the Wald approximation.

2.7.2. Glasshouse experiment

We computed ordinary least-squares linear regressions for each of the response variables: RGR, R:S, LMA and foliar $\delta^{13}C$ and $\delta^{15}N$ against Temperature, Soil nutrient status (i.e., nutrient-rich versus nutrient-poor), Species and the interactions between Species and Temperature and Soil nutrient status. Model selection was carried out using the 'performance' package in R (Lüdecke et al., 2021), and the model that yielded the lowest AIC was then chosen for each of the response variables. Temperature was taken as a continuous variable from the long-term air temperature averages for each growth chamber (**Table 1**). Type III ANOVA was performed on the chosen models, followed by *post hoc* comparisons of means using the 'emmeans' package in R (Lenth et al., 2018). We built a custom linear contrast for comparison of species according to their habitat preference (lowland versus upland), for response variables where Species interacted with Temperature. We did this to better understand whether species responses were structured by their elevation preference. For this comparison *F. ifflana* and *F. bourjotiana* were considered as lowland, and *F. brayleyana* and *F. oppositifolia* as upland. We checked for normality using visual histograms on all dependent variables, and then a Shapiro-Wilk's test for normality was performed followed by testing the homogeneity of variances ($P > 0.05$). We log-transformed the response variables RGR and used square root transformation for LMA to meet normality assumptions.

3. Results

3.1. Field observations: Temperature and soil nutrient availability with elevation

Recorded observations of the four focal *Flindersia* species in the Australian Wet Tropics, in conjunction with gridded climate data for each observation location, indicated a linear decline in Mean Annual

Temperature (MAT) with elevation in the distribution ranges, with a slope of –5.3°C km^{-1} (Figure 1A). The three widespread species shared similar climate niche space (based on its MAT and Mean Annual Precipitation (MAP)), while the mountaintop-restricted species displayed the lowest MAT and highest MAP (Figure 1B; Supplementary Table 1). Further, for the three widespread species, elevational distributions were largely consistent with the elevations of seed collection for the glasshouse experiment, except for *F. brayleyana*, which was collected at ∼990 m, in the upper part of its range (Supplementary Table 1). Thus, the locations of seed collection also contributed to our consideration of habitat preferences for *F. ifflana* and *F. bourjotiana* to be lowland, and for *F. brayleyana* and *F. oppositifolia* to be upland.

Soil C:N ratio increased with elevation (R^2 = 0.41, P < 0.01) (Figure 1C) and soil δ^{15}N decreased with elevation (R^2 = 0.57, P < 0.001) (Supplementary Figure 3), suggesting that nitrogen availability declines with increasing elevation. The difference in soil δ^{15}N from the lowest site (40 m) to the highest site (1,550 m) was ∼5.7‰ with a slope of –3.5‰ km^{-1} of elevation gain (Supplementary Figure 3). Soil δ^{13}C did not change significantly with elevation (Supplementary Figure 3).

3.2. Field observations: Stem diameter growth rates, LMA, foliar δ^{13}C and δ^{15}N

Across an elevation gradient of 1,600 m in the Australian Wet Tropics, *Flindersia* species demonstrated a significant decline in stem diameter growth rates (R^2 = 0.18, P < 0.01). These declined by *ca* 0.3 cm year^{-1} km^{-1} of elevation gain (Figure 2A).

The decline in GR among *Flindersia* species with elevation was accompanied by increasing LMA with increasing elevation (R^2 = 0.22, P < 0.05) (Figure 2B). The LMA increased by *ca* 25 g m^{-2} km^{-1} of elevation gain. When averaged for each species within a site, the highest LMA was recorded for *F. oppositifolia* (187 ± 27 g m^{-2}) at Mount Bellenden Ker (1,550 m elevation) and the lowest for *F. ifflana* (156 ± 1 g m^{-2}) at Kuranda National Park (∼300 m elevation). When averaged for each site, the highest LMA was recorded at Mount Bellenden Ker, and the lowest LMA (∼142 ± 3 g m^{-2}) was recorded at Kaaru Creek (∼500 m elevation).

Foliar δ^{13}C also increased significantly with elevation by *ca* 2.6‰ km^{-1} (R^2 = 0.50, P < 0.01) (Figure 2C). The average foliar δ^{13}C across the entire dataset was –29.0 ± 1.5‰ (n = 30). The least negative δ^{13}C was observed for the mountaintop species, *F. oppositifolia* (–27.5‰ at 1,550 m) and most negative for *F. brayleyana* (–31.25‰ at 720 m).

Foliar δ^{15}N significantly declined with increasing elevation (R^2 = 0.78, P < 0.001) by *ca* 8.5‰ km^{-1} of elevation gain (Figure 2D). Average foliar δ^{15}N across the entire dataset was –0.05 ± 3.9‰ (n = 30). There was a large reduction of nearly 10‰ observed from the lowland site (4.8‰ at ∼300 m elevation) to the mountaintop site (–5.2 ‰ at 1,550 m elevation).

3.3. Glasshouse experiment: Relative growth rate, root-to-shoot ratio, and LMA

Soil nutrient status had a significant effect on RGR, such that RGR was higher for plants in nutrient-rich compared to nutrient-poor soil (Figure 3 and Table 2). The two species that responded most strongly to an increase in nutrient availability in terms of RGR were *F. ifflana*, the most lowland of the species, and *F. oppositifolia*, the mountaintop restricted species (Figure 3). There was also an interaction effect between Species and the extent of increase in RGR with increasing temperature. The lowland species showed steeper increases in RGR with increasing temperature than the upland species (Figure 3). This was confirmed by the *post hoc*, linear contrast where the slope of temperature response was larger in the lowland than in the upland species [$t_{(59)}$ = 3.8, p < 0.001]. In general, the lowland species displayed an increasing RGR across the full temperature range, whereas the upland species did not.

Root-to-shoot ratios (R:S) showed significant effects among Species and with Soil nutrient status (Table 2). The R:S was higher in nutrient-poor than in nutrient-rich soil, and there was a significant Species by Soil interaction (Table 2). This species-soil interaction was driven by the differential species response in the nutrient-poor Soil treatment. A pairwise, *post hoc* comparison among Species in the nutrient-poor Soil treatment, confirmed that the mountaintop-restricted species, *F. oppositifolia*, had a significantly higher R:S ratio compared to all other species [*F. ifflana*, $t_{(59)}$ = –3.6, p < 0.001; *F. bourjotiana*, $t_{(59)}$ = –4.85, p < 0.001; and *F. brayleyana*, $t_{(59)}$ = –4.18, p < 0.001]. A pairwise, *post hoc* comparison among Species in the nutrient-rich Soil treatment indicated no significant differences among species. The highest R:S ratio for any Species by treatment combination occurred for *F. oppositifolia* in nutrient-poor Soil in the cold Temperature treatment (Figure 3).

There were no significant effects of Temperature, Soil nutrient status or Species on LMA in the glasshouse (Table 2 and Figure 3).

3.4. Glasshouse experiment: Foliar stable isotope composition

For foliar δ^{13}C in the glasshouse, there were significant main effects of Temperature, Soil nutrient status, and Species (Figure 4 and Table 2). Foliar δ^{13}C generally increased (became less negative) in plants grown in nutrient-rich Soil and increased with increasing Temperature. Average foliar δ^{13}C across the glasshouse dataset was –29.7 ± 1.4‰. There was an increase in δ^{13}C of 1.3‰ associated with nutrient-rich compared to nutrient-poor Soil, and the rate of increase in δ^{13}C was 0.1‰ per°C (Supplementary Table 4). A pairwise, *post hoc* comparison among Species showed that *F. brayleyana* had a more negative δ^{13}C than all other species [*F. ifflana*, $t_{(65)}$ = 3.68, p < 0.01; *F. bourjotiana*, $t_{(65)}$ = 3.02, p < 0.05; and *F. oppositifolia*, $t_{(65)}$ = –3.46, p < 0.01]. Consistent with this, *F. brayleyana* in the field had also shown the most negative δ^{13}C among the four species (Figure 2).

Foliar δ^{15}N displayed a consistent variation with Soil nutrient status, which was the most important predictor in the model (Table 2). Plants in nutrient-rich Soil in the glasshouse displayed a higher δ^{15}N than those in nutrient-poor Soil; the increase in foliar δ^{15}N associated with nutrient-rich compared to nutrient-poor Soil according to the model was 2.0‰ (Supplementary Table 4). There was also a significant interaction between Species and Temperature (Table 2 and Figure 4). The *post hoc*, linear contrast between upland and lowland species showed that foliar δ^{15}N increased with temperature at a steeper rate in the upland species, *F. brayleyana* and *F. oppositifolia*, compared to the lowland species, *F. ifflana* and

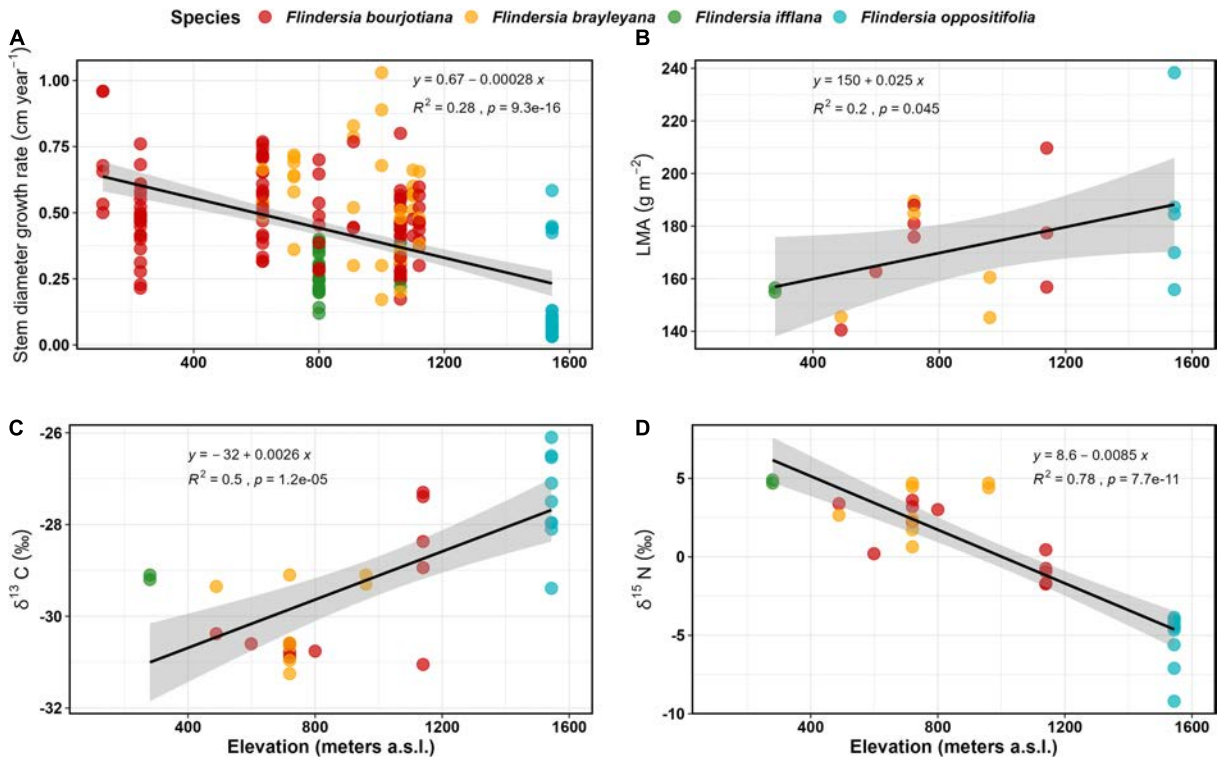

FIGURE 2
Field observed trends for **(A)** Stem diameter growth rates (cm year^{-1}) (data and model predictions are square root transformed) (n = 195); **(B)** Leaf mass per unit Area (g m^{-2}) (n = 20); **(C)** Leaf δ^{13} C (‰) (n = 30); and **(D)** Leaf δ^{15} N (‰) (n = 30) of the four focal *Flindersia* species studied across an elevation gradient in the Australian Wet Tropics.

F. bourjotiana [$t_{(62)}$ = −2.87, p < 0.01]. The difference in slope between upland and lowland species was 0.13‰ per°C.

4. Discussion

We investigated trends in tree growth and leaf functional traits along an elevation gradient in the Australian Wet Tropics using a single, regionally important genus to gain insight into the responses of closely related species with differing elevational distributions. Observations in tropical rainforests on other continents have shown that tree growth rates and foliar δ^{15}N typically decline with elevation (Bauters et al., 2017; Malhi et al., 2017), whereas LMA and foliar δ^{13}C typically increase with elevation (Vitousek et al., 1990; Mumbanza et al., 2021). We confirmed from our field-based observations that similar trends also occur in *Flindersia* species in Australian tropical rainforests. These trends with elevation could be a result from at least three important drivers: decreasing temperatures, decreasing soil nutrient availability, and changes in species composition (Malhi et al., 2010; Rapp, 2010). Using a factorial glasshouse experiment, we attempted to disentangle these potential drivers to better understand their relative roles in controlling plant form and function. We detected direct effects of temperature and nutrient availability on some of the examined traits, and our results also suggested that some variation could be attributed to species adaptations to their preferred elevational ranges. Our experiment provided new insights in instances where the observed field trends could not be reproduced in the glasshouse by varying temperature and soil nutrient availability in isolation.

4.1. Growth rates, biomass allocation strategies and LMA

The observed decline in stem diameter growth rates among *Flindersia* species with increasing elevation was accompanied by a decline in MAT, i.e., ∼–5.3°C km^{-1} (**Figure 1A**), along with increasing C:N ratio in soils, indicative of declining nitrogen availability (**Figure 1C**). Previous studies have reported similar declines in growth rates with MAT among closely related *Weinmannia* species, in the Peruvian Andes (Rapp, 2010) and the southwest Andes (Tito et al., 2018). The effect of declining temperature with elevation drives slower metabolic rates, while slower nitrogen mineralization rates likely further contribute toward growth reductions (He et al., 2016; Gong et al., 2020). Our glasshouse experimental results also supported the idea that slower growth rates with increasing elevation could be partly explained by changes in species composition. Although species' mean RGR across the experimental treatments did not reflect the species' site of origin on the elevation gradient (i.e., RGR increasing with decreasing elevation of origin), we did find that the RGR of the upland species did not respond as strongly to temperature as in the lowland species. Interestingly, the mountaintop species, *F. oppositifolia*, displayed similar growth rates compared to the lowland collected species under lowland temperatures and in nutrient-rich soil (**Figure 3**). This bodes well for this mountaintop-restricted species, at least from an *ex situ* conservation perspective, in terms of its potential for growth in plantings at lower elevations (Primack et al., 2021). It may also indicate that warming temperatures *per se*, which are predicted to eliminate its current climate niche (Costion et al., 2015), may

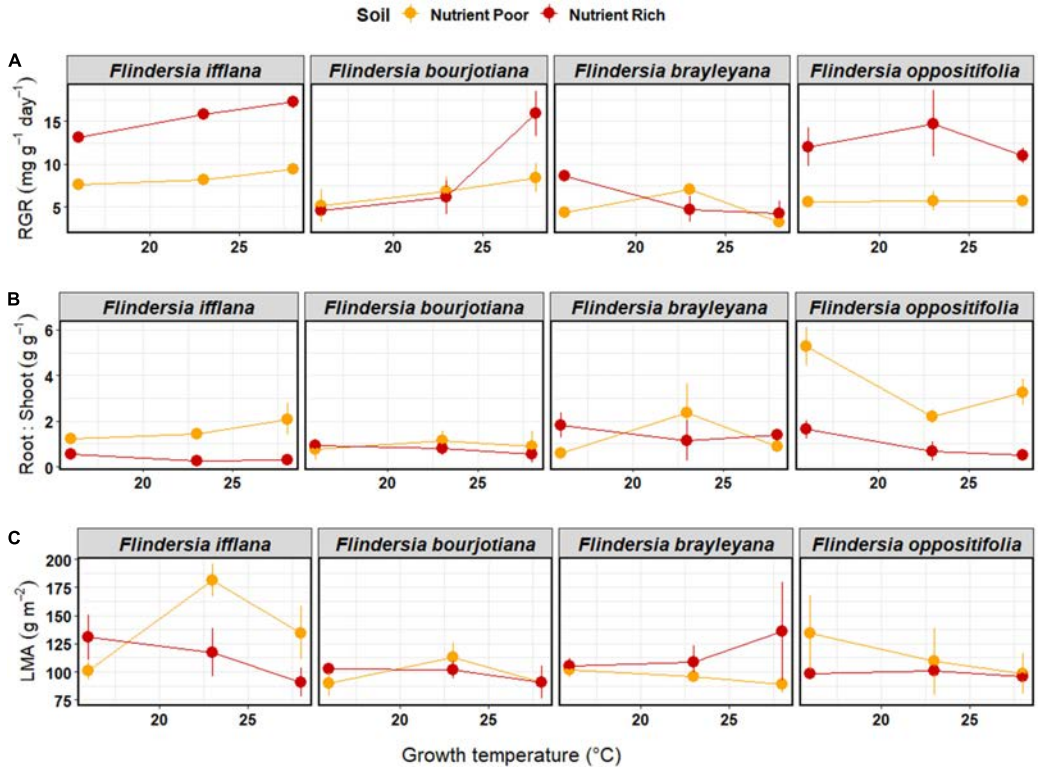

FIGURE 3
Means (±1SE) of **(A)** relative growth rate (mg g^{-1} day^{-1}), **(B)** root-to-shoot ratio (g g^{-1}), and **(C)** leaf mass per unit area (g m^{-2}) among temperature and soil nutrient treatments (nutrient-rich soil = red, nutrient-poor soil = orange) in the glasshouse experiment. Each dot represents a mean of three individual saplings. Species are arranged left to right according to their observed elevation ranges, with leftmost being lowland and rightmost being mountaintop.

not negatively impact growth *in situ,* with optimal growth of this species occurring at temperatures higher than currently experienced. However, other factors associated with warming, such as increasing atmospheric water stress (Bauman et al., 2022b), and effects on seed bank dynamics (Liyanage et al., 2022), along with biotic interactions, may negatively impact survival of such mountaintop endemic plants (Cheesman and Winter, 2013).

In our glasshouse experiment, we observed that Soil nutrient status and Species had significant impacts on R:S ratios, but that the chamber temperature did not. This was exemplified by the observation that the mountaintop species in our experiment had a very high R:S under nutrient-poor, cold conditions, as has been reported with other montane taxa in their native growth provenance across the tropics (Wu et al., 2013; Fahey et al., 2016). Biomass allocation strategies under resource poor conditions have been explained by the optimal partitioning theory, which predicts that plants generally increase allocation of biomass toward the organs that acquire the most limiting resources (Kobe et al., 2010; Poorter et al., 2012), the roots in this case. Plants generally prefer a more conservative approach by investing more in roots under cold temperatures and lower nutrient availability and more in above ground parts with warmer temperatures and higher nutrient availability (Girardin et al., 2014). In general, Australian rainforest plants have adapted to nutrient-poor soils (Congdon and Herbohn, 2009; Gleason et al., 2010). However, the relatively higher allocation of biomass to roots in mountaintop plants may also indicate an adaptive functional strategy toward shallow soils and toward physical support from strong winds, in addition to nutrient foraging (Körner, 2007; Girardin et al., 2010; Wu et al., 2013). These observations suggest that an important trait that allows *F. oppositifolia* to compete successfully in the mountaintop environment is a greater capacity to allocate biomass to roots in cold, nutrient-poor conditions, which was not observed in the lowland species in the glasshouse under similar growth conditions.

Our observation of an increase in LMA with elevation compares well with field-based studies in the tropics (Neyret et al., 2016; Martin et al., 2020). The importance of LMA as an indicator of plant growth strategies is well established in the literature (Westoby et al., 2002; Poorter et al., 2009). LMA is the product of leaf thickness and density (Roderick et al., 1999), and studies have reported that plants generally display thicker and/or denser leaves in more stressful environments (Poorter et al., 2009). Higher LMA generally corresponds to the slow end in the fast-slow continuum of the leaf economic spectrum, indicative of a more conservative rather than acquisitive strategy (Wright et al., 2004). It has been suggested that higher LMA at lower temperatures might come about because of reduced leaf expansion rates (Westoby et al., 2002; Poorter et al., 2009; Van De Weg et al., 2012). Other factors potentially contributing to observed variation in LMA across elevation could be differences in incident light across sites given differences in cloud cover (Martin et al., 2020). Although, we did not quantify variation in irradiance where leaves were collected along the elevation gradient, all leaves in the study were 'fully exposed' sunlit leaves, but we must acknowledge this could have been an additional factor contributing to the observed variability in LMA.

10.3389/ffgc.2023.1089167

TABLE 2 Summary table of the type III ANOVA results from linear regressions for each of the response variables against growth temperature, soil nutrient status, species and interactions with species from the glasshouse experiment.

Predictors	log (RGR)				R:S				1/sqrt (LMA)				$\delta^{13}C$				$\delta^{15}N$			
	Sum of squares	F statistic	DF	*p*	Sum of squares	F statistic	DF	*p*	Sum of squares	F statistic	DF	*p*	Sum of squares	F statistic	DF	*p*	Sum of squares	F statistic	DF	*p*
(Intercept)	2.23	17.69	1	**<0.001**	0.87	1.02	1	0.319	0.153	1,045.0	1	**<0.001**	2,782.8	1,950.4	1	**<0.001**	4.48	5.30	1	**0.025**
Temperature	0.17	1.38	1	0.244	0.02	0.28	1	0.595	–	–	–	–	15.23	10.67	1	**0.002**	1.04	1.23	1	0.271
Species	1.88	4.96	3	**0.004**	18.45	7.088	3	**<0.001**	0.001	2.10	3	0.108	25.30	5.92	3	**0.001**	5.49	2.16	3	0.10
Soil	1.61	12.74	1	**0.001**	6.72	7.75	1	**0.007**	–	–	–	–	14.16	9.93	1	**0.002**	73.55	87.02	1	**<0.001**
Temperature × Species	2.64	6.95	3	**<0.001**	7.19	2.67	3	**0.050**	–	–	—	–	–	–	–	–	10.50	4.14	3	**0.010**
Soil × Species	1.38	3.65	3	**0.017**	21.22	8.15	3	**<0.001**	–	–	–	–	–	–	–	–	–	–	–	–
Residuals	7.42	NA	59	NA	51.19	NA	59	NA	51.19	NA	67	NA	92.73	NA	65	NA	52.40	NA	62	NA

The *p*-values in bold indicate significant effects. Where interaction effects or a predictor itself were not significant and their removal resulted in a lower AIC, a simpler model has been shown. The removal of an interaction or a predictor has been indicated with '–'.

We expected LMA, being a key growth trait reflecting acclimation to stress and/or resource poor conditions (Poorter et al., 2009), should have responded in our experimental treatments to temperature and/or soil nutrient availability. Surprisingly, we did not observe changes in LMA in our glasshouse experiment as we would have expected based on the observed field trend. This could possibly be explained by ontogenetic differences, insofar as mature trees were sampled in the field compared to saplings in the glasshouse experiment. Ontogeny has been previously highlighted as important in comparing trait measurements between experimental and field studies, especially for tropical plants (Poorter et al., 2012; Scalon et al., 2022).

4.2. Foliar $\delta^{13}C$ and elevation

The influence of climate and soil properties in the field was reflected in the foliar isotopic composition with increasing elevation. Foliar isotope ratios are useful proxies to understand plant photosynthetic water use and nutrient dynamics in tropical ecosystems (Cernusak et al., 2007a; Craine et al., 2015). We observed an overall trend of increasing foliar $\delta^{13}C$ (**Figure 2C**) with increasing elevation (ca ~2.6‰ km^{-1}) among the *Flindersia* trees that we sampled in the Australian Wet Tropics. This can be compared to global studies on C_3 plants in humid forests, where on average ~1.3‰ km^{-1} increase in foliar $\delta^{13}C$ has been reported with elevation (Li et al., 2009). Likewise, a study reported a change from –29.5‰ in lower elevation sites to as high as –24.8‰ in montane sites of Hawaii for a single species, *Metrosideros polymorpha* Gaudich (Cordell et al., 1998). Such large intraspecific variation has been attributed to increase in species' water-use efficiency with increasing elevation and its inherent adaptive plasticity to variable environmental conditions (Cordell et al., 1998; Peri et al., 2012). Studies have also reported variation in foliar $\delta^{13}C$ with other environmental attributes such as precipitation, soil nutrients, solar radiation, and VPD (Vitousek et al., 1990; Chen et al., 2017; Zou et al., 2019; Bauman et al., 2022a). Variation in foliar $\delta^{13}C$ with elevation can also result from the influence of leaf morphology (leaf thickness or LMA, for example), which leads to longer diffusion pathways for CO_2 into the leaf and decreases the internal-to-ambient CO_2 concentration ratio (c_i/c_a) and hence causes enrichment of foliar $\delta^{13}C$ in montane flora (Körner et al., 1986; Prentice et al., 2014). Another contributing factor could be increased viscosity of water with lower temperature, which causes larger frictional resistance to water transport and hence a partial closure of stomata thereby decreasing c_i/c_a and increasing foliar $\delta^{13}C$ (Prentice et al., 2014).

Two aspects of our observations of foliar $\delta^{13}C$ in the glasshouse went in opposite directions to the trends in the field. We did observe changes in foliar $\delta^{13}C$ in response to temperature, but the direction of this response was opposite to that in the field. Foliar $\delta^{13}C$ became less negative with increasing experimental temperature, whereas in the field it was more negative at lower (warmer) than at higher (cooler) elevations. Such a trend, as observed in the glasshouse, of increasing $\delta^{13}C$ with increasing temperature has been previously reported from arid or semi-arid sites (Chen et al., 2017), and could be explained by increased VPD at warmer temperatures, which causes stomatal closure (Grossiord et al., 2020). Such conditions lead to a lower c_i/c_a resulting in a higher $\delta^{13}C$ with increasing VPD (Cernusak et al., 2013). In our glasshouse study, VPD increased with increasing temperature, and so when plotted against VPD, foliar $\delta^{13}C$

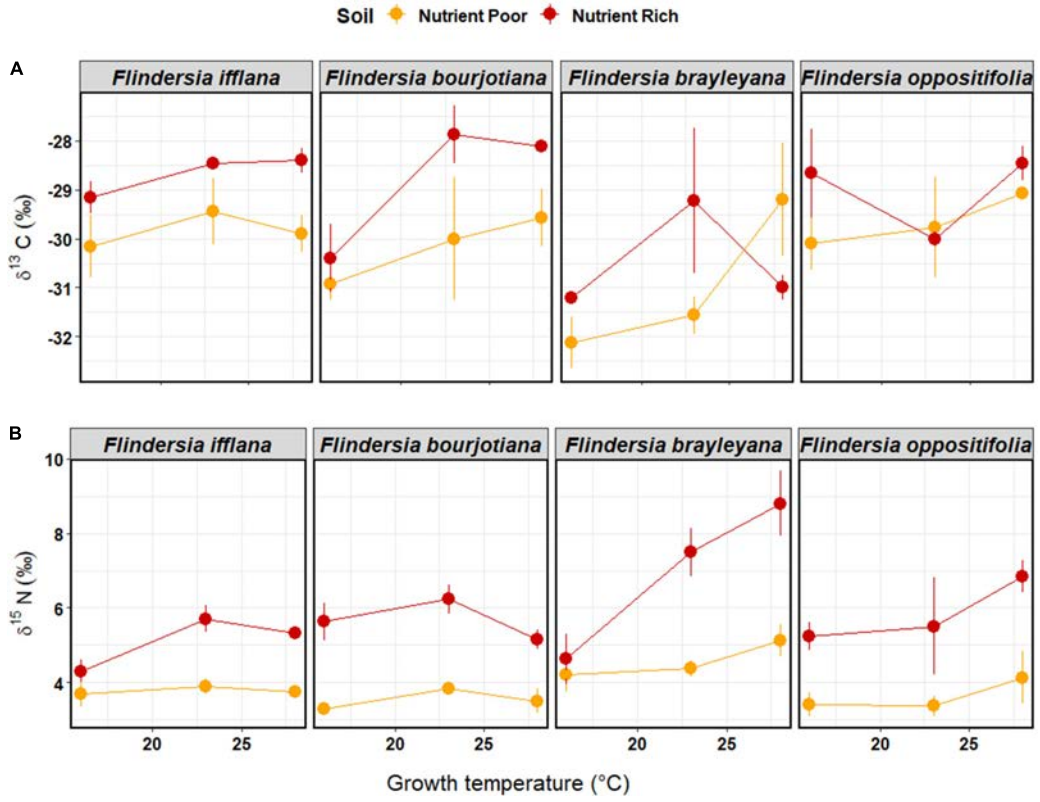

FIGURE 4
Means (±1SE) of **(A)** leaf $\delta^{13}C$ (‰) and **(B)** leaf $\delta^{15}N$ (‰) among temperature and soil nutrient treatments (nutrient-rich soil = red, nutrient-poor soil = orange) in the glasshouse experiment. Each dot represents a mean of three individual saplings. Species are arranged left to right according to their observed elevation ranges, with leftmost being lowland and rightmost being mountaintop.

increased with increasing VPD (**Supplementary Figure 6**), as would be expected, all else being equal. Interestingly, for the field collections in the Australian Wet Tropics, the annual mean VPD also decreases with decreasing temperature as elevation increases (Bauman et al., 2022b; **Supplementary Figure 2**). This suggests that the role of VPD in driving field trends in foliar $\delta^{13}C$ is insufficient to overcome drivers pushing in the other direction as elevation increases to enrich foliar $\delta^{13}C$.

The second aspect of our glasshouse results for foliar $\delta^{13}C$ that did not agree with the field trends was the response to nutrient availability. Plants grown in nutrient-rich soil had higher $\delta^{13}C$ than those grown in nutrient-poor soil (**Figure 4**). This was expected, based on previous studies (Cernusak et al., 2007b; Palma et al., 2020), and the known physiological response of lower c_i/c_a in leaves with a higher photosynthetic capacity resulting from higher nitrogen concentrations (Cernusak et al., 2013). However, in the field, we demonstrated that nutrient availability likely decreases with increasing elevation, as indicated by the increase in soil C:N ratio (**Figure 1C**). Thus, if we consider this in isolation, it indicates an opposite response to that observed in the glasshouse: foliar $\delta^{13}C$ in the field became higher with increasing elevation as soil nitrogen availability likely decreased, rather than increased.

We suggest that there are two driving factors in the field that can explain foliar $\delta^{13}C$ responses to elevation, and which are apparently sufficient to overcome effects of temperature on VPD and nutrient availability that push in the opposite direction. The first is changes in leaf structure that occurred in the field with increasing elevation, but which were absent in the glasshouse. The increase in LMA with increasing elevation in the field would likely be indicative of a greater tortuosity for diffusion of CO_2 inside the leaf, increasing the intercellular air space diffusion resistance, and thicker cell walls, increasing the mesophyll diffusion resistance, both ultimately lowering chloroplastic CO_2 concentrations and therefore discrimination against ^{13}C. The effect of more robust leaf structure was identified by Vitousek et al. (1990) as the most potent driver of foliar $\delta^{13}C$ trends with elevation in *Metrosideros polymorpha* Gaudich. in Hawaii. The second driving factor in the field that did not occur in the glasshouse is the decrease in atmospheric pressure that accompanies an increase in elevation. Effects of this on ^{13}C discrimination are less mechanistically understood, but it is known that a decrease in oxygen partial pressure in the chloroplast can increase the efficiency of carboxylation (Farquhar and Wong, 1984), which may further decrease discrimination against ^{13}C. Thus, our glasshouse results suggest that the drawdown of chloroplastic CO_2 in the field is likely to be related to the low atmospheric pressure at higher elevations and changes in leaf structure that increase the diffusion resistance through the internal airspace and mesophyll (Vitousek et al., 1990; Wang et al., 2017), neither of which occurred in the glasshouse with a change in temperature. Our glasshouse results also show that a change in water viscosity that occurs with temperature was not a strong enough driver of variation in foliar $\delta^{13}C$ to overcome the effect of the increases in VPD that coincided with increasing temperature (**Supplementary Figure 6**).

Given the known relationship between mean annual precipitation (MAP) and foliar $\delta^{13}C$ (Cernusak et al., 2013; Cornwell et al., 2018), it is reasonable to ask whether a difference in soil water availability between the field and the glasshouse might have impacted our results. In the glasshouse, the experimental pots were watered to field capacity by hand each day, and we therefore feel confident that they did not experience substantive soil water deficits. With respect to the field collections, the Australian Wet Tropics in general is characterized by MAP approaching and exceeding 2,000 mm (Turton et al., 1999), a range in which foliar $\delta^{13}C$ in tropical rainforests is largely insensitive to MAP (Leffler and Enquist, 2002; Diefendorf et al., 2010). In a recent analysis, it was shown that mean climatological water deficit was not a significant predictor of tree growth rates across forests in the Australian Wet Tropics similar to those that we sampled (Bauman et al., 2022a). Furthermore, sap flow measurements at lowland, mid-elevation, and high elevation sites in the Australian Wet Tropics indicated that transpiration at the tree level is largely unresponsive to seasonal variations in soil moisture (McJannet et al., 2007; Binks et al., 2022). At the Daintree Rainforest Observatory, a lowland site, a multi-year throughfall exclusion experiment resulted in no response of foliar $\delta^{13}C$ in the treated plot compared to the control plot (Pivovaroff et al., 2021). Finally, mean foliar $\delta^{13}C$ values in our study for the three species with broader elevation ranges were very similar in the glasshouse compared to the field (*F. ifflana*, –29.3‰ vs. –29.2‰; *F. bourjotiana*, –29.6‰ vs. –29.6‰; *F. brayleyana*, –30.7‰ vs. –30.5‰), as can also be seen in **Figures 2**, **4**. The mountaintop species, *F. oppositifolia*, had a mean value in the glasshouse of –29.3‰ compared to –27.5‰ in the field. This enrichment of approximately 2‰ for *F. oppositifolia* grown in the field at 1,550 m elevation compared to the plants grown near sea level in the glasshouse cannot have resulted from a limitation of soil water availability on the mountaintop; observed MAP on the top of Mount Bellenden Ker near where the trees were sampled exceeds 7,000 mm (McJannet et al., 2007). The WorldClim gridded climate product provided an estimate of 5,650 mm (**Supplementary Table 1**), but this reflects a known bias in coarser scale products for this site due to the complex topography (Turton et al., 1999). These considerations combined argue strongly against soil water deficit as an important driver of the foliar $\delta^{13}C$ data that we present in this paper.

4.3. Foliar $\delta^{15}N$ and elevation

For foliar $\delta^{15}N$ we found a marked decrease with increasing elevation (~ –8.5‰ km^{-1} elevation), which is a much larger change compared to most studies in the tropics (Liu et al., 2007; Liu and Wang, 2010; Bauters et al., 2017; Wang et al., 2019). For instance, a study from Mt Gongga, in the southwest region of China, reported on average ~ –1.3‰ difference from 1,100 to 4,900 m elevation (Li et al., 2009); and –1.4‰ to 14.2‰ across an elevation gradient from 900 to ~4,000 m in the Ethiopian Rift valley (Liu et al., 2007). The closest to our observation comes from one study involving *Pinus spp.* in Nepal that reported nearly –8‰ difference over 800 m elevation (Sah and Brumme, 2003). These trends are known to be related in part to a decline in $\delta^{15}N$ of soil nitrogen with elevation (Wang et al., 2019). We did find some evidence of such a relationship between foliar $\delta^{15}N$ and that of the soil nitrogen in our study (**Supplementary Figure 5**). The enrichment of $\delta^{15}N$ at warmer, lowland sites is thought to result from a more open nitrogen cycle, where nitrogen loss pathways discriminate against the heavier isotope, ^{15}N, leaving the residual nitrogen pool ^{15}N enriched (Martinelli et al., 1999; Ma et al., 2012; Peri et al., 2012; Wang et al., 2019). The marked decline in foliar $\delta^{15}N$ that we observed in the Australian Wet Tropics suggests that a slowing and tightening of the nitrogen cycle with increasing elevation is likely a key driver of decreasing tree growth rates.

Furthermore, under glasshouse conditions we did observe differences in foliar $\delta^{15}N$ consistent with field-based trends, although the observed variation was generally not as large as seen in field. The differences in foliar $\delta^{15}N$ in the field versus the glasshouse might be related to soil development processes. For example, the trends in the glasshouse reflect a snapshot of the species' growth within the experimental period reflecting foliar signatures based on available soil N. On the other hand, those observed in the field partly reflect the ecosystem nitrogen pool that would have developed from nutrient cycling processes integrated over millennia (Craine et al., 2015). In our glasshouse study, variation in foliar $\delta^{15}N$ induced by soil nutrient status was still pronounced, with higher foliar $\delta^{15}N$ in nutrient-rich (~5.9‰) compared to nutrient-poor (~3.8‰) soils, averaged for all species. We suggest that this increase in foliar $\delta^{15}N$ in the nutrient-rich pots can be explained by greater opportunity for N loss from the pots by $\delta^{15}N$ fractionating pathways than in the case where nutrient availability is low and available N is effectively captured by the soil-plant system. In support of this, we also observed that foliar $\delta^{15}N$ varied as a function of root mass (**Supplementary Figure 7**), indicating the influence of larger root systems in capturing available nitrogen, thereby limiting loss pathways from the soil-plant system that would otherwise leave the residual $\delta^{15}N$ in the system ^{15}N enriched (Baumgartner et al., 2021).

We observed a significant interaction between Species and Temperature for foliar $\delta^{15}N$ in the glasshouse study (**Table 2**). This indicated that as growth temperature increased, foliar $\delta^{15}N$ tended to increase in the upland species, but not in the lowland species (**Figure 4**). We suggest that the species difference in foliar $\delta^{15}N$ indicates a better ability of the lowland species to absorb increasingly available nitrogen as increasing temperatures drove faster nitrogen mineralization rates in the experimental pots. The lowland species, in turn, were able to take advantage of this by increasing their relative growth rates under these conditions (as see in **Figure 3**). The upland species, on the other hand, have likely evolved to function in conditions of relatively low nitrogen availability, and lacked the capacity to ramp up their nitrogen uptake to the same extent in response to the warmer growth temperatures. This would have allowed greater nitrogen losses from the soil-plant systems, which then caused increases in foliar $\delta^{15}N$. Thus, our results indicate that there are likely important belowground traits related to nutrient absorption capacity that distinguish *Flindersia* species with differing habitat preferences along the elevation gradient. It is also important to note the role of soil microbes in controlling the $\delta^{15}N$ of the soil-plant system, and in modulating soil nitrogen transformations that can lead to nitrogen isotope fractionations (Houlton et al., 2006; Pajares and Bohannan, 2016; Hestrin et al., 2019); although we recognize the importance of these processes, we did not quantify them in the present study.

4.4. Concluding remarks

Climate change is driving warmer temperatures in the tropics, and it has been suggested that these could potentially have negative

effects on tropical tree growth, with implications for biomass productivity and ecosystem functioning (Hatfield and Prueger, 2015; Malhi et al., 2015). It is important to recognize that responses of tropical trees to global warming involve a myriad of interacting factors. Our study demonstrated that altering temperature in isolation of other factors that covary in nature can lead to counterintuitive results, for example in the case of foliar $\delta^{13}C$. In natural ecosystems, temperature itself may only indirectly drive impacts of warming. For example, mortality in mature rainforest trees of the Australian Wet Tropics has been increasing in recent decades, but the trend in increase in tree mortality can be better attributed to increasing air VPD, which has accompanied the increase in air temperature (Bauman et al., 2022b). We also observed in this study that elevation patterns in tree function are linked to changes in nutrient availability, and even to the change in atmospheric pressure that coincides with a change in elevation.

Adaptations of *Flindersia* species to their different preferred habitats along the elevation gradient were evident in their responses to temperature in the glasshouse. We found that upland species did not show increasing growth rates with increasing temperatures, whereas lowland species did, indicating their ability to acclimate to warmer conditions. In addition, we observed that a distinguishing feature of a mountaintop-restricted species was a proportionally larger allocation toward roots under nutrient-poor, cold conditions. This feature is known to help plants with physical support from higher wind speeds on tropical mountaintops, and likely contributes to nutrient foraging when soil nutrients are scarce (Körner, 2003). As the climate warms, impacts on nutrient cycling at the ecosystem scale may lag direct effects of temperature on tree metabolism; understanding how such changes will interact with species traits is a formidable, but an important, challenge.

Data availability statement

The raw data supporting the conclusions of this article will be made available by the authors, without undue reservation.

Author contributions

ASR and LAC conceived the manuscript with inputs from AWC and HF-M. ASR conducted field data collection and designed the experiment under the supervision of LAC and AWC. DMC helped develop species selection. NDP facilitated seed collection. ASR conducted the data analysis with inputs from HF-M and LAC. ASR wrote the first draft with LAC. All authors edited and approved the final draft for publication.

Funding

The Ian Potter Foundation (Funding number 20190013), the Skyrail Rainforest Foundation, and the Wet Tropics Management Authority.

Acknowledgments

We acknowledge the traditional owners of the land where this research was conducted, the Kuku-yalanji, Durbalngan, and Djabuganjdji people, and thank the Department of Environment and Science, Queensland National Parks for granting a permit to collect seeds from various rainforest provenances in the Australian Wet Tropics. We thank Jen Whan for assisting with the isotope analyses, Stuart Worboys, Penny van Oosterzee, and Ana Palma for assisting with field seed collections, and Damian Settle for assisting with experimental plant harvests. We thank the reviewers for their comments that helped improve this manuscript. We also acknowledge the Ian Potter Foundation, the Skyrail Rainforest Research Foundation, and the Wet Tropics Management Authority for funding this research. ASR thanks James Cook University for providing an International Postgraduate Research Scholarship.

Conflict of interest

The authors declare that the research was conducted in the absence of any commercial or financial relationships that could be construed as a potential conflict of interest.

Publisher's note

All claims expressed in this article are solely those of the authors and do not necessarily represent those of their affiliated organizations, or those of the publisher, the editors and the reviewers. Any product that may be evaluated in this article, or claim that may be made by its manufacturer, is not guaranteed or endorsed by the publisher.

Supplementary material

The Supplementary Material for this article can be found online at: https://www.frontiersin.org/articles/10.3389/ffgc.2023.1089167/full#supplementary-material

References

Aiello-Lammens, M. E., Boria, R. A., Radosavljevic, A., Vilela, B., and Anderson, R. P. (2015). spThin: An R package for spatial thinning of species occurrence records for use in ecological niche models. *Ecography* 38, 541–545. doi: 10.1111/ecog.01132

Amundson, R., Austin, A. T., Schuur, E. A., Yoo, K., Matzek, V., Kendall, C., et al. (2003). Global patterns of the isotopic composition of soil and plant nitrogen. *Glob. Biogeochem. Cycles* 17, 1–5. doi: 10.1029/2002GB001903

Bauman, D., Fortunel, C., Cernusak, L. A., Bentley, L. P., Mcmahon, S. M., and Rifai, S. W. (2022a). Tropical tree growth sensitivity to climate is driven by species intrinsic growth rate and leaf traits. *Glob. Change Biol.* 28, 1414–1432. doi: 10.1111/gcb.15982

Bauman, D., Fortunel, C., Delhaye, G., Malhi, Y., Cernusak, L. A., Bentley, L. P., et al. (2022b). Tropical tree mortality has increased with rising atmospheric water stress. *Nature* 608, 528–533. doi: 10.1038/s41586-022-04737-7

Baumgartner, S., Bauters, M., Barthel, M., Drake, T. W., Ntaboba, L. C., Bazirake, B. M., et al. (2021). Stable isotope signatures of soil nitrogen on an environmental–geomorphic gradient within the Congo Basin. *SOIL* 7, 83–94. doi: 10.5194/soil-7-83-2021

Bauters, M., Verbeeck, H., Demol, M., Bruneel, S., Taveirne, C., Van Der Heyden, D., et al. (2017). Parallel functional and stoichiometric trait shifts in South American and African forest communities with elevation. *Biogeosciences* 14, 5313–5321. doi: 10.5194/bg-14-5313-2017

Bayly, M. J., Holmes, G. D., Forster, P. I., Cantrill, D. J., and Ladiges, P. Y. (2013). Major clades of Australasian Rutoideae (Rutaceae) based on rbcL and atpB sequences. *PLoS One* 8:e72493. doi: 10.1371/journal.pone.0072493

Belbin, L. (2011). "The atlas of living Australia's spatial portal," in *Proceedings of the environmental information management conference*, (Santa Barbara, CA: University of California), 28–29.

Binks, O., Cernusak, L. A., Liddell, M., Bradford, M., Coughlin, I., Carle, H., et al. (2022). Forest system hydraulic conductance: Partitioning tree and soil components. *New Phytol.* 233, 1667–1681. doi: 10.1111/nph.17895

Bradford, M. G., Metcalfe, D. J., Ford, A., Liddell, M. J., and Mckeown, A. (2014a). Floristics, stand structure and aboveground biomass of a 25-ha rainforest plot in the wet tropics of Australia. *J. Trop. For. Sci.* 26, 543–553.

Bradford, M. G., Murphy, H. T., Ford, A. J., Hogan, D. L., and Metcalfe, D. J. (2014b). Long-term stem inventory data from tropical rain forest plots in Australia. *Ecology* 95, 2362–2362. doi: 10.1890/14-0458R.1

Campbell, G. S., and Norman, J. M. (1998). *An introduction to environmental biophysics*. New York, NY: Springer-Verlag. doi: 10.1007/978-1-4612-1626-1

Cernusak, L. A., Aranda, J., Marshall, J. D., and Winter, K. (2007a). Large variation in whole-plant water-use efficiency among tropical tree species. *New Phytol.* 173, 294–305. doi: 10.1111/j.1469-8137.2006.01913.x

Cernusak, L. A., Winter, K., Aranda, J., Turner, B. L., and Marshall, J. D. (2007b). Transpiration efficiency of a tropical pioneer tree (*Ficus insipida*) in relation to soil fertility. *J. Exp. Bot.* 58, 3549–3566. doi: 10.1093/jxb/erm201

Cernusak, L. A., Ubierna, N., Winter, K., Holtum, J. A. M., Marshall, J. D., and Farquhar, G. D. (2013). Environmental and physiological determinants of carbon isotope discrimination in terrestrial plants. *New Phytol.* 200, 950–965. doi: 10.1111/nph.12423

Cernusak, L. A., Winter, K., and Turner, B. L. (2009). Plant $\delta^{15}N$ correlates with the transpiration efficiency of nitrogen acquisition in tropical trees. *Plant Physiol.* 151, 1667–1676. doi: 10.1104/pp.109.145870

Cheesman, A. W., Preece, N. D., Oosterzee, P., Erskine, P. D., and Cernusak, L. A. (2018). The role of topography and plant functional traits in determining tropical reforestation success. *J. Appl. Ecol.* 55, 1029–1039. doi: 10.1111/1365-2664.12980

Cheesman, A. W., and Winter, K. (2013). Growth response and acclimation of CO_2 exchange characteristics to elevated temperatures in tropical tree seedlings. *J. Exp. Bot.* 64, 3817–3828. doi: 10.1093/jxb/ert211

Chen, Z., Wang, G., and Jia, Y. (2017). Foliar $\delta^{13}C$ Showed No Altitudinal Trend in an Arid Region and Atmospheric Pressure Exerted a Negative Effect on Plant $\delta^{13}C$. *Front. Plant Sci.* 8:1070. doi: 10.3389/fpls.2017.01070

Congdon, R. A., and Herbohn, J. L. (2009). Ecosystem dynamics of disturbed and undisturbed sites in north Queensland wet tropical rain forest. I. Floristic composition, climate and soil chemistry. *J. Trop. Ecol.* 9, 349–363. doi: 10.1017/S0266467400007409

Cordell, S., Goldstein, G., Mueller-Dombois, D., Webb, D., and Vitousek, P. M. (1998). Physiological and morphological variation in *Metrosideros polymorpha*, a dominant Hawaiian tree species, along an altitudinal gradient: The role of phenotypic plasticity. *Oecologia* 113, 188–196. doi: 10.1007/s004420050367

Cornelissen, J. H. C., Lavorel, S., Garnier, E., Díaz, S., Buchmann, N., Gurvich, D. E., et al. (2003). A handbook of protocols for standardised and easy measurement of plant functional traits worldwide. *Aust. J. Bot.* 51, 335–380. doi: 10.1071/BT02124

Cornwell, W. K., Wright, I. J., Turner, J., Maire, V., Barbour, M. M., Cernusak, L. A., et al. (2018). Climate and soils together regulate photosynthetic carbon isotope discrimination within C_3 plants worldwide. *Glob. Ecol. Biogeogr.* 27, 1056–1067. doi: 10.1111/geb.12764

Costion, C. M., Simpson, L., Pert, P. L., Carlsen, M. M., John Kress, W., and Crayn, D. (2015). Will tropical mountaintop plant species survive climate change? Identifying key knowledge gaps using species distribution modelling in Australia. *Biol. Conserv.* 191, 322–330. doi: 10.1016/j.biocon.2015.07.022

Craine, J. M., Brookshire, E. N. J., Cramer, M. D., Hasselquist, N. J., Koba, K., Marin-Spiotta, E., et al. (2015). Ecological interpretations of nitrogen isotope ratios of terrestrial plants and soils. *Plant Soil* 396, 1–26. doi: 10.1007/s11104-015-2542-1

Diefendorf, A. F., Mueller, K. E., Wing, S. L., Koch, P. L., and Freeman, K. H. (2010). Global patterns in leaf ^{13}C discrimination and implications for studies of past and future climate. *Proc. Natl. Acad. Sci. U.S.A.* 107, 5738–5743. doi: 10.1073/pnas.0910513107

Fahey, T. J., Sherman, R. E., and Tanner, E. V. J. (2016). Tropical montane cloud forest: Environmental drivers of vegetation structure and ecosystem function. *J. Trop. Ecol.* 32, 355–367. doi: 10.1017/S0266467415000176

Farquhar, G., and Wong, S. (1984). An empirical model of stomatal conductance. *Funct. Plant Biol.* 11, 191–210. doi: 10.1071/PP9840191

Fick, S. E., and Hijmans, R. J. (2017). WorldClim 2: New 1-km spatial resolution climate surfaces for global land areas. *Int. J. Climatol.* 37, 4302–4315. doi: 10.1002/joc.5086

Forbes, S. J., Cernusak, L. A., Northfield, T. D., Gleadow, R. M., Lambert, S., and Cheesman, A. W. (2020). Elevated temperature and carbon dioxide alter resource allocation to growth, storage and defence in cassava (*Manihot esculenta* Crantz). *Environ. Exp. Bot.* 173:103997. doi: 10.1016/j.envexpbot.2020.103997

Girardin, C. A. J., Espejob, J. E. S., Doughty, C. E., Huasco, W. H., Metcalfe, D. B., and Durand-Baca, L. (2014). Productivity and carbon allocation in a tropical montane cloud forest in the Peruvian Andes. *Plant Ecol. Divers.* 7, 107–123. doi: 10.1080/17550874.2013.820222

Girardin, C. A. J., Malhi, Y., Aragao, L. E. O. C., Mamani, M., Huasco, W. H., Durand, L., et al. (2010). Net primary productivity allocation and cycling of carbon along a tropical forest elevational transect in the Peruvian Andes. *Glob. Change Biol.* 16, 3176–3192. doi: 10.1111/j.1365-2486.2010.02235.x

Gleason, S. M., Read, J., Ares, A., and Metcalfe, D. J. (2010). Species-soil associations, disturbance, and nutrient cycling in an Australian tropical rainforest. *Oecologia* 162, 1047–1058. doi: 10.1007/s00442-009-1527-2

Gong, H., Li, Y., Yu, T., Zhang, S., Gao, J., Zhang, S., et al. (2020). Soil and climate effects on leaf nitrogen and phosphorus stoichiometry along elevational gradients. *Glob. Ecol. Conserv.* 23:e01138. doi: 10.1016/j.gecco.2020.e01138

Grossiord, C., Buckley, T. N., Cernusak, L. A., Novick, K. A., Poulter, B., Siegwolf, R. T. W., et al. (2020). Plant responses to rising vapor pressure deficit. *New Phytol.* 226, 1550–1566. doi: 10.1111/nph.16485

Hatfield, J. L., and Prueger, J. H. (2015). Temperature extremes: Effect on plant growth and development. *Weather Clim. Extrem.* 10, 4–10. doi: 10.1016/j.wace.2015.08.001

He, X., Hou, E., Liu, Y., and Wen, D. (2016). Altitudinal patterns and controls of plant and soil nutrient concentrations and stoichiometry in subtropical China. *Sci. Rep.* 6:24261. doi: 10.1038/srep24261

Hestrin, R., Hammer, E. C., Mueller, C. W., and Lehmann, J. (2019). Synergies between mycorrhizal fungi and soil microbial communities increase plant nitrogen acquisition. *Commun. Biol.* 2:233. doi: 10.1038/s42003-019-0481-8

Hoffmann, W. A., and Poorter, H. (2002). Avoiding bias in calculations of relative growth rate. *Ann. Bot.* 90, 37–42. doi: 10.1093/aob/mcf140

Houlton, B. Z., Sigman, D. M., and Hedin, L. O. (2006). Isotopic evidence for large gaseous nitrogen losses from tropical rainforests. *Proc. Natl. Acad. Sci. U.S.A.* 103, 8745–8750. doi: 10.1073/pnas.0510185103

Kobe, R. K., Iyer, M., and Walters, M. B. (2010). Optimal partitioning theory revisited: Nonstructural carbohydrates dominate root mass responses to nitrogen. *Ecology* 91, 166–179. doi: 10.1890/09-0027.1

Körner, C. (2003). "Plant ecology at high elevations," in *Alpine plant life*, (Berlin: Springer), 1–7. doi: 10.1007/978-3-642-18970-8_1

Körner, C. (2007). The use of 'altitude' in ecological research. *Trends Ecol. Evol.* 22, 569–574. doi: 10.1016/j.tree.2007.09.006

Körner, C., Bannister, P., and Mark, A. (1986). Altitudinal variation in stomatal conductance, nitrogen content and leaf anatomy in different plant life forms in New Zealand. *Oecologia* 69, 577–588. doi: 10.1007/BF00410366

Leffler, A. J., and Enquist, B. J. (2002). Carbon isotope composition of tree leaves from Guanacaste, Costa Rica: Comparison across tropical forests and tree life history. *J. Trop. Ecol.* 18, 151–159. doi: 10.1017/S0266467402002109

Lenth, R., Singmann, H., Love, J., Buerkner, P., and Herve, M. (2018). *Emmeans: Estimated marginal means, aka least-squares means. R package version 1, 3.*

Li, J., Wang, G., Liu, X., Han, J., Liu, M., and Liu, X. (2009). Variations in carbon isotope ratios of C_3 plants and distribution of C_4 plants along an altitudinal transect on the eastern slope of Mount Gongga. *Sci. China Ser. D Earth Sci.* 52, 1714–1723. doi: 10.1007/s11430-009-0170-4

Liu, X., Wang, G., Li, J., and Wang, Q. (2010). Nitrogen isotope composition characteristics of modern plants and their variations along an altitudinal gradient in Dongling Mountain in Beijing. *Sci. China Ser. D Earth Sci.* 53, 128–140. doi: 10.1007/s11430-009-0175-z

Liu, X., Zhao, L., Gasaw, M., Gao, D., Qin, D., and Ren, J. (2007). Foliar $\delta^{13}C$ and $\delta^{15}N$ values of C_3 plants in the Ethiopia Rift Valley and their environmental controls. *Chin. Sci. Bull.* 52, 1265–1273. doi: 10.1007/s11434-007-0165-5

Liu, X. Z., and Wang, G. (2010). Measurements of nitrogen isotope composition of plants and surface soils along the altitudinal transect of the eastern slope of Mount Gongga in southwest China. *Rapid Commun. Mass Spectrom.* 24, 3063–3071. doi: 10.1002/rcm.4735

Liyanage, G., Offord, C., Crayn, D., Guja, L., Worboys, S., and Sommerville, K. (2022). Understanding seed dormancy and germination aids conservation of rainforest species from tropical montane cloud forest: A case study confirming morphophysiological dormancy in the genus Tasmannia. *Aust. J. Bot.* 70, 399–408. doi: 10.1071/BT22011

Lüdecke, D., Ben-Shachar, M. S., Patil, I., Waggoner, P., and Makowski, D. (2021). performance: An R package for assessment, comparison and testing of statistical models. *J. Open Sour. Softw.* 6:3139. doi: 10.21105/joss.03139

Ma, J.-Y., Sun, W., Liu, X.-N., and Chen, F.-H. (2012). Variation in the stable carbon and nitrogen isotope composition of plants and soil along a precipitation gradient in Northern China. *PLoS One* 7:e51894. doi: 10.1371/journal.pone.0051894

Malhi, Y., Doughty, C. E., Goldsmith, G. R., Metcalfe, D. B., Girardin, C. A. J., and Marthews, T. R. (2015). The linkages between photosynthesis, productivity, growth and

biomass in lowland Amazonian forests. *Glob. Change Biol.* 21, 2283–2295. doi: 10.1111/gcb.12859

Malhi, Y., Girardin, C. A. J., Goldsmith, G. R., Doughty, C. E., Salinas, N., Metcalfe, D. B., et al. (2017). The variation of productivity and its allocation along a tropical elevation gradient: A whole carbon budget perspective. *New Phytol.* 214, 1019–1032. doi: 10.1111/nph.14189

Malhi, Y., Silman, M., Salinas, N., Bush, M., Meir, P., and Saatchi, S. (2010). Introduction: Elevation gradients in the tropics: Laboratories for ecosystem ecology and global change research. *Glob. Change Biol.* 16, 3171–3175. doi: 10.1111/j.1365-2486.2010.02323.x

Martin, R. E., Asner, G. P., Bentley, L. P., Shenkin, A., Salinas, N., Huaypar, K. Q., et al. (2020). Covariance of sun and shade leaf traits along a tropical forest elevation gradient. *Front. Plant Sci.* 10:1810. doi: 10.3389/fpls.2019.01810

Martinelli, L. A., Piccolo, M. C., Townsend, A. R., Vitousek, P. M., Cuevas, E., Mcdowell, W., et al. (1999). Nitrogen stable isotopic composition of leaves and soil: tropical versus temperate forests. *Biogeochemistry* 46, 45–65. doi: 10.1007/BF01007573

McJannet, D., Wallace, J., and Reddell, P. (2007). Precipitation interception in Australian tropical rainforests: II. Altitudinal gradients of cloud interception, stemflow, throughfall and interception. *Hydrol. Process.* 21, 1703–1718. doi: 10.1002/hyp.6346

Mumbanza, F. M., Bauters, M., Meunier, F., Boeckx, P., Cernusak, L. A., and De Deurwaerder, H. P. (2021). Lianas and trees exhibit divergent intrinsic water-use efficiency along elevational gradients in South American and African tropical forests. *Glob. Ecol. Biogeogr.* 30, 2259–2272. doi: 10.1111/geb.13382

Neyret, M., Bentley, L. P., Oliveras, I., Marimon, B. S., Marimon-Junior, B. H., and Almeida De Oliveira, E. (2016). Examining variation in the leaf mass per area of dominant species across two contrasting tropical gradients in light of community assembly. *Ecol. Evol.* 6, 5674–5689. doi: 10.1002/ece3.2281

Pajares, S., and Bohannan, B. J. M. (2016). Ecology of nitrogen fixing, nitrifying, and denitrifying microorganisms in tropical forest soils. *Front. Microbiol.* 7:1045. doi: 10.3389/fmicb.2016.01045

Palma, A. C., Winter, K., Aranda, J., Dalling, J. W., Cheesman, A. W., Turner, B. L., et al. (2020). Why are tropical conifers disadvantaged in fertile soils? Comparison of *Podocarpus guatemalensis* with an angiosperm pioneer, *Ficus insipida*. *Tree Physiol.* 40, 810–821. doi: 10.1093/treephys/tpaa027

Peri, P. L., Ladd, B., Pepper, D. A., Bonser, S. P., Laffan, S. W., and Amelung, W. (2012). Carbon (δ^{13}C) and nitrogen (δ^{15}N) stable isotope composition in plant and soil in Southern Patagonia's native forests. *Glob. Change Biol.* 18, 311–321. doi: 10.1111/j.1365-2486.2011.02494.x

Pivovaroff, A. L., Mcdowell, N. G., Rodrigues, T. B., Brodribb, T., Cernusak, L. A., Choat, B., et al. (2021). Stability of tropical forest tree carbon-water relations in a rainfall exclusion treatment through shifts in effective water uptake depth. *Glob. Change Biol.* 27, 6454–6466. doi: 10.1111/gcb.15869

Poorter, H., Niinemets, Ü, Poorter, L., Wright, I. J., and Villar, R. (2009). Causes and consequences of variation in leaf mass per area (LMA): A meta-analysis. *New Phytol.* 182, 565–588. doi: 10.1111/j.1469-8137.2009.02830.x

Poorter, H., Niklas, K. J., Reich, P. B., Oleksyn, J., Poot, P., and Mommer, L. (2012). Biomass allocation to leaves, stems and roots: Meta-analyses of interspecific variation and environmental control. *New Phytol.* 193, 30–50. doi: 10.1111/j.1469-8137.2011.03952.x

Prentice, I. C., Dong, N., Gleason, S. M., Maire, V., and Wright, I. J. (2014). Balancing the costs of carbon gain and water transport: Testing a new theoretical framework for plant functional ecology. *Ecol. Lett.* 17, 82–91. doi: 10.1111/ele.12211

Primack, R. B., Ellwood, E. R., Gallinat, A. S., and Miller-Rushing, A. J. (2021). The growing and vital role of botanical gardens in climate change research. *New Phytol.* 231, 917–932. doi: 10.1111/nph.17410

R Core Team (2021). *R: A language and environment for statistical computing*. Vienna: R Foundation for Statistical Computing.

Rapp, J., Silman, M., Clark, J., Girardin, C., Galiano, D., and Tito, R. (2012). Intra- and interspecific tree growth across a long altitudinal gradient in the Peruvian Andes. *Ecology* 93, 2061–2072. doi: 10.1890/11-1725.1

Rapp, J. M. (2010). *Climate control on plant performance across an Andean altitudinal gradient*. Winston-Salem, NC: Wake Forest University.

Read, Q. D., Moorhead, L. C., Swenson, N. G., Bailey, J. K., and Sanders, N. J. (2014). Convergent effects of elevation on functional leaf traits within and among species. *Funct. Ecol.* 28, 37–45. doi: 10.1111/1365-2435.12162

Roderick, M. L., Berry, S. L., Saunders, A. R., and Noble, I. R. (1999). On the relationship between the composition, morphology and function of leaves. *Funct. Ecol.* 13, 696–710. doi: 10.1046/j.1365-2435.1999.00369.x

Sah, S., and Brumme, R. (2003). Altitudinal gradients of natural abundance of stable isotopes of nitrogen and carbon in the needles and soil of a pine forest in Nepal. *J. For. Sci.* 49, 19–26. doi: 10.17221/4673-JFS

Salinas, N., Malhi, Y., Meir, P., Silman, M., Roman Cuesta, R., Huaman, J., et al. (2011). The sensitivity of tropical leaf litter decomposition to temperature: Results from a large-scale leaf translocation experiment along an elevation gradient in Peruvian forests. *New Phytol.* 189, 967–977. doi: 10.1111/j.1469-8137.2010.03521.x

Scalon, M. C., Bohn, A., Coelho, G. C., Meister, L., Alves, R. D. F., Secco, R. T., et al. (2022). Relationship between growth trajectories and functional traits for woody trees in a secondary tropical forest. *Front. For. Glob. Change* 5:754656. doi: 10.3389/ffgc.2022.754656

Scott, K. D., Mcintyre, C. L., and Playford, J. (2000). Molecular analyses suggest a need for a significant rearrangement of Rutaceae subfamilies and a minor reassessment of species relationships within *Flindersia*. *Plant System. Evol.* 223, 15–27. doi: 10.1007/BF00985324

Sparks, J. P., and Ehleringer, J. R. (1997). Leaf carbon isotope discrimination and nitrogen content for riparian trees along elevational transects. *Oecologia* 109, 362–367. doi: 10.1007/s004420050094

Tito, R., Vasconcelos, H. L., and Feeley, K. J. (2018). Global climate change increases risk of crop yield losses and food insecurity in the tropical Andes. *Glob. Change Biol.* 24, e592–e602. doi: 10.1111/gcb.13959

Tito, R., Vasconcelos, H. L., and Feeley, K. J. (2020). Mountain ecosystems as natural laboratories for climate change experiments. *Front. For. Glob. Change* 3:38. doi: 10.3389/ffgc.2020.00038

Torello Raventos, M. (2014). *Environmental controls on wood density in tropical forests*. Townsville: James Cook University.

Turton, S. M., Hutchinson, M. F., Accad, A., Hancock, P. E., and Webb, T. (1999). "Producing fine-scale rainfall climatology surfaces for Queensland's wet tropics region," in *Geodiversity: Readings in Australian geography at the close of the 20th century*. Special Publication Series. 6, eds J. A. Kesby, J. M. Stanley, R. F. McLean, and L. J. Olive (Canberra, ACT: School of Geography and Oceanography, University College), 415–428.

Unger, M., Homeier, J., and Leuschner, C. (2012). Effects of soil chemistry on tropical forest biomass and productivity at different elevations in the equatorial Andes. *Oecologia* 170, 263–274. doi: 10.1007/s00442-012-2295-y

Valladares, F., and Niinemets, Ü (2008). Shade tolerance, a key plant feature of complex nature and consequences. *Annu. Rev. Ecol. Evol. System.* 39, 237–257. doi: 10.1146/annurev.ecolsys.39.110707.173506

Van De Weg, M. J., Meir, P., Grace, J., and Ramos, G. D. (2012). Photosynthetic parameters, dark respiration and leaf traits in the canopy of a Peruvian tropical montane cloud forest. *Oecologia* 168, 23–34. doi: 10.1007/s00442-011-2068-z

Vitousek, P. M., Field, C. B., and Matson, P. A. (1990). Variation in foliar δ^{13}C in hawaiian metrosideros polymorpha: a case of internal resistance? *Oecologia* 84, 362–370. doi: 10.1007/BF00329760

Vitousek, P. M., Shearer, G., and Kohl, D. H. (1989). Foliar ^{15}N natural abundance in Hawaiian rainforest: Patterns and possible mechanisms. *Oecologia* 78, 383–388. doi: 10.1007/BF00379113

Wang, H., Prentice, I. C., Davis, T. W., Keenan, T. F., Wright, I. J., and Peng, C. (2017). Photosynthetic responses to altitude: An explanation based on optimality principles. *New Phytol.* 213, 976–982. doi: 10.1111/nph.14332

Wang, X., Jiang, Y., Ren, H., Yu, F.-H., and Li, M.-H. (2019). Leaf and soil δ^{15}N patterns along elevational gradients at both treelines and shrublines in three different climate zones. *Forests* 10:557. doi: 10.3390/f10070557

Westoby, M., Daniel, S., Angela, T., Moles, Peter, A., Vesk, A., et al. (2002). Plant ecological strategies: some leading dimensions of variation between species. *Ann. Rev. Ecol. System.* 33, 125–159. doi: 10.1146/annurev.ecolsys.33.010802.150452

Wild, J., Kopecký, M., Macek, M., Šanda, M., Jankovec, J., and Haase, T. (2019). Climate at ecologically relevant scales: A new temperature and soil moisture logger for long-term microclimate measurement. *Agricult. For. Meteorol.* 268, 40–47. doi: 10.1016/j.agrformet.2018.12.018

Wright, I. J., Reich, P. B., Cornelissen, J. H. C., Falster, D. S., Garnier, E., Hikosaka, K., et al. (2005). Assessing the generality of global leaf trait relationships. *New Phytol.* 166, 485–496. doi: 10.1111/j.1469-8137.2005.01349.x

Wright, I. J., Reich, P. B., Westoby, M., Ackerly, D. D., Baruch, Z., Bongers, F., et al. (2004). The worldwide leaf economics spectrum. *Nature* 428, 821–827. doi: 10.1038/nature02403

Wu, J., Hong, J., Wang, X., Sun, J., Lu, X., Fan, J., et al. (2013). Biomass partitioning and its relationship with the environmental factors at the alpine steppe in Northern Tibet. *PLoS One* 8:e81986. doi: 10.1371/journal.pone.0081986

Xiao, Y., Liu, S., Tong, F., Chen, B., and Kuang, Y. (2018). Dominant species in subtropical forests could decrease photosynthetic N allocation to carboxylation and bioenergetics and enhance leaf construction costs during forest succession. *Front. Plant Sci.* 9:117. doi: 10.3389/fpls.2018.00117

Yi, X. F., and Yang, Y. Q. (2006). Enrichment of stable carbon and nitrogen isotopes of plant populations and plateau pikas along altitudes. *J. Anim. Feed Sci.* 15, 661–667. doi: 10.22358/jafs/66937/2006

Zich, F., Hyland, B., Whiffin, T., and Kerrigan, R. (2020). *Australian tropical rainforest plants*, 8th Edn. Available at https://apps.lucidcentral.org/rainforest/ (accessed March 1, 2021).

Ziegler, C., Dusenge, M. E., Nyirambangutse, B., Zibera, E., Wallin, G., and Uddling, J. (2020). Contrasting dependencies of photosynthetic capacity on leaf nitrogen in early- and late-successional tropical montane tree species. *Front. Plant Sci.* 11:500479. doi: 10.3389/fpls.2020.500479

Zou, J., Yu, L., and Huang, Z. (2019). Variation of leaf carbon isotope in plants in different lithological habitats in a Karst Area. *Forests* 10:356. doi: 10.3390/f10040356

Supplementary Material

Temperature, nutrient availability, and species traits interact to shape elevation responses of Australian tropical trees

Supplementary Table 3.1. *Flindersia* species used in the study, seed collection locations and seedling germination success when grown under enclosed shade house growth conditions at the Environmental Research Complex (16°48'56.6"S 145°41'01.3"E), James Cook University, Cairns.

Species	Latitude	Longitude	MAT (°C)	MAP (mm)	Location	Date of Collection	Elevation (meters a.s.l)	Date of seed Sown	Number of seeds sown	Number of seeds germinated	Germination success (%)
Lowland habitat preference											
Flindersia ifflana	16.90414	145.6039	24	1758	Kuranda National Park	7-Dec-19	298	16-Dec-19	46	38	82
Flindersia bourjotiana	16.57887	145.31364	22	1982	Mt Lewis National Park	14-Dec-19	599	30-Dec-19	23	19	82
Upland habitat preference											
Flindersia brayleyana	17.43152	145.1546	21	1841	Thiaki Property, Atherton	9-Dec-19	990	18-Dec-19	46	23	50
Flindersia oppositifolia	16.80311	145.70682	17	5650	Mount Bellenden Ker	10-Nov-19	1548	14-Nov-19	202	142	70

Supplementary Table 3.2. Soil properties for the two soil treatments used in the glasshouse experiment.

	Soil Type	
	Nutrient Rich	**Nutrient Poor**
C (mg g^{-1})	39	3
N (mg g^{-1})	2	0.2
P (mg g^{-1})	0.64	0.11
K (µg g^{-1})	1328	1258
Na (µg g^{-1})	146	137
Ca (µg g^{-1})	765	738
Mg (µg g^{-1})	987	987
pH in H_2O	5.2	5.8
pH in $CaCl_2$	4.8	5.1
Soil OMC (%)	2.4	0.8

Supplementary Table 3.3. Summary of the linear regression model results for stem diameter growth rates, LMA, $\delta^{13}C$ and $\delta^{15}N$ as functions of elevation. Significant *p*-values are indicated in bold.

	sqrt (Stem diameter growth rates (cm year^{-1})			**LMA (g m^2)**			**δ ^{13}C (‰)**			**δ ^{15}N (‰)**		
Predictors	***Estimates***	***CI***	***p***	***Estimates***	***CI***	***p***	***Estimates***	***CI***	***p***	***Estimates***	***CI***	***p***
(Intercept)	0.66772	(0.61050, 0.73040)	**<0.001**	149.99408	(125.13110, 174.85702)	**<0.001**	-31.73875	(-32.842380, -30.63512)	**<0.001**	8.55436	(6.66992, 10.43880)	**<0.001**
Elevation	-0.00028	(-0.00034, -0.00021)	**<0.001**	0.02472	(0.00060, 0.04884)	**0.045**	0.00262	(0.00161, 0.00363)	**<0.001**	-0.00853	(-0.01026, -0.00680)	**<0.001**
Observations		195			20			30			30	
R^2 /R^2 adjusted		0.285 / 0.281			0.205 / 0.161			0.502 / 0.484			0.785 / 0.777	

Supplementary Table 3.4. Summary table of linear regressions for the glasshouse experiment for each of the response variables against growth temperature (T_{growth}), Soil nutrient status, Species and its interactions. The *p*-values in bold indicates significant effects. Where interaction effects were not significant and their removal resulted in a lower AIC, the simpler model has been shown here with '—' indicating removal of an interaction effect.

	log (RGR)			**R:S**			**1/sqrt (LMA)**			**δ ^{13}C**			**δ ^{15}N**		
Predictors	***Estimates***	***CI***	***p***	***Estimates***	***CI***	***p***	***Estimates***	***CI***	***p***	***Estimates***	***CI***	***p***	***Estimates***	***CI***	***p***
(Intercept)	1.68	(0.88, 2.47)	**<0.001**	1.05	(-1.04, 3.14)	0.319	0.09	(0.09, 0.10)	**<0.001**	-31.81	(-33.2, -30.37)	**<0.001**	2.33	(0.31, 4.36)	**0.025**
Tgrowth	0.02	(0.01, 0.05)	0.244	0.02	(-0.07, 0.11)	0.595				0.09	(0.04, 0.15)	**0.002**	0.05	(-0.04, 0.14)	0.271
Species [*Flindersia bourjotiana*]	-1.37	(2.53, -0.22)	**0.020**	0.03	(-2.98, 3.04)	0.984	0.01	(0.00, 0.02)	**0.023**	-0.25	(-1.05, 0.56)	0.546	1.27	(-1.62, 4.15)	0.383
Species [*Flindersia brayleyana*]	0.81	(-0.32, 1.94)	0.155	0.24	(-2.72, 3.19)	0.873	0.01	(0.00, 0.02)	0.084	-1.47	(-2.26, -0.67)	**<0.001**	-2.33	(-5.18, 0.52)	0.107
Species [*Flindersia oppositifolia*]	0.05	(-1.07, 1.18)	0.923	5.66	(2.71, 8.61)	**<0.001**	0.01	(-0.00, 0.02)	0.065	-0.09	(-0.88, 0.71)	0.824	-0.66	(-3.51, 2.18)	0.643
Soil [Nutrient Rich]	0.60	(0.26,0.93)	**0.001**	-1.22	(-2.10, -0.34)	**0.007**	—	—	—	0.89	(0.33, 1.46)	**0.002**	2.04	(1.60, 2.47)	**<0.001**
Tgrowth * Species [*Flindersia bourjotiana*]	0.05	(0.00, 0.10)	0.060	-0.03	(-0.16, 0.10)	0.639	—	—	—	—	—	—	-0.05	(-0.18, 0.08)	0.452
Tgrowth * Species [*Flindersia brayleyana*]	-0.06	(-0.11, -0.02)	**0.011**	-0.02	(-0.15, 0.10)	0.713	—	—	—	—	—	—	0.16	(0.04, 0.29)	**0.011**
Tgrowth * Species [*Flindersia oppositifolia*]	-0.02	(-0.07, 0.03)	0.401	-0.16	(-0.29, -0.04)	**0.012**	—	—	—	—	—	—	0.04	(-0.08, 0.17)	0.491
Species [*Flindersia bourjotiana*] * Soil [Nutrient Rich]	-0.46	(-0.94, 0.03)	0.064	1.08	(-0.19, 2.34)	0.094	—	—	—	—	—	—	—	—	—
Species [*Flindersia brayleyana*] * Soil [Nutrient Rich]	-0.48	(-0.96, -0.01)	**0.046**	1.38	(0.14, 2.62)	**0.030**	—	—	—	—	—	—	—	—	—
Species [*Flindersia oppositifolia*] * Soil [Nutrient Rich]	0.16	(-0.32, 0.63)	0.512	-1.40	(-2.65, -0.16)	**0.027**	—	—	—	—	—	—	—	—	—
Observations	71			71			71			71			71		
R^2 / R^2 adjusted	0.652 / 0.587			0.572 / 0.492			0.086 / 0.045			0.367 / 0.319			0.692 / 0.652		

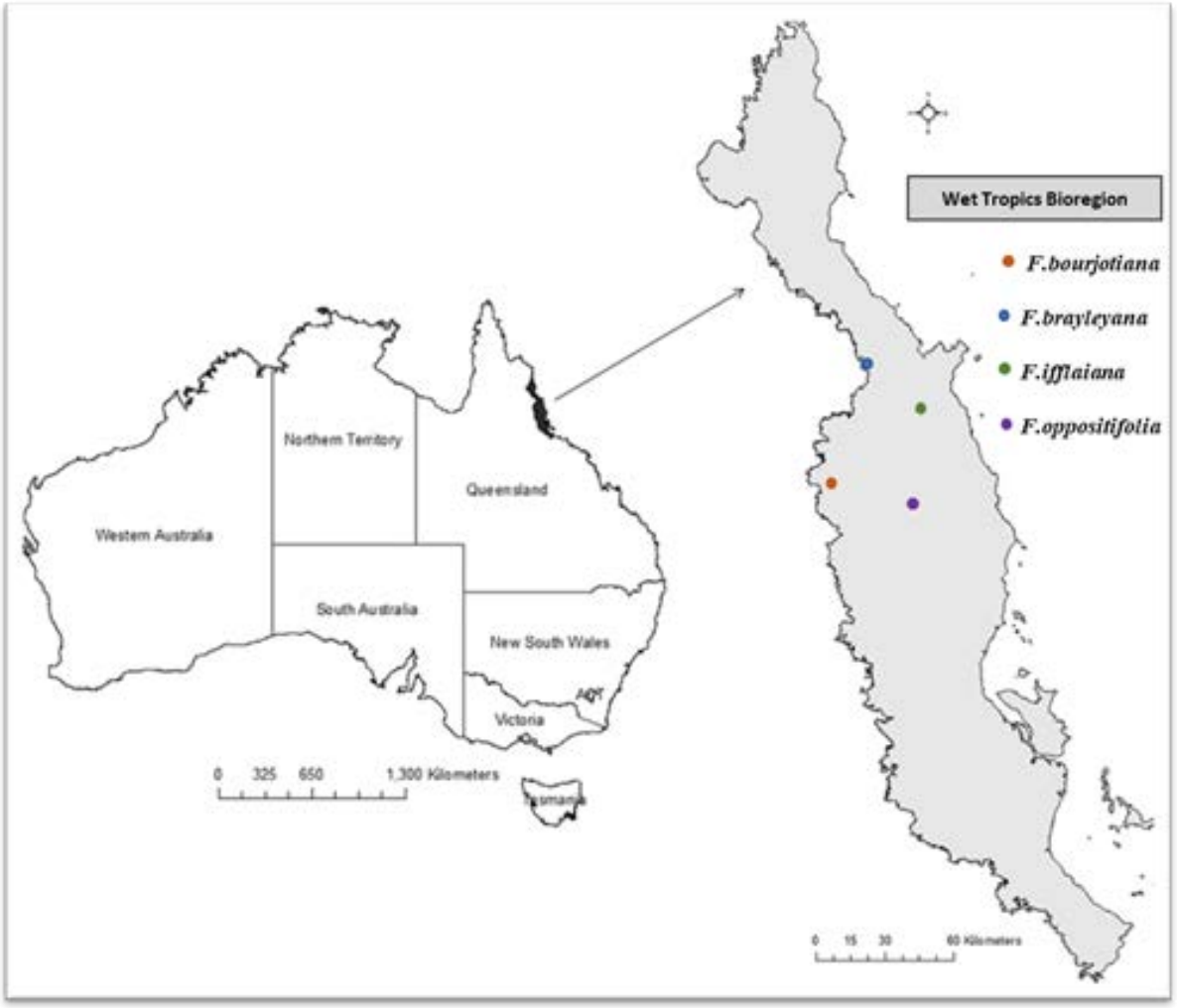

Supplementary Figure 3.1. A map of The Australian Wet Tropics Bioregion with the locations of four *Flindersia spp.* under study

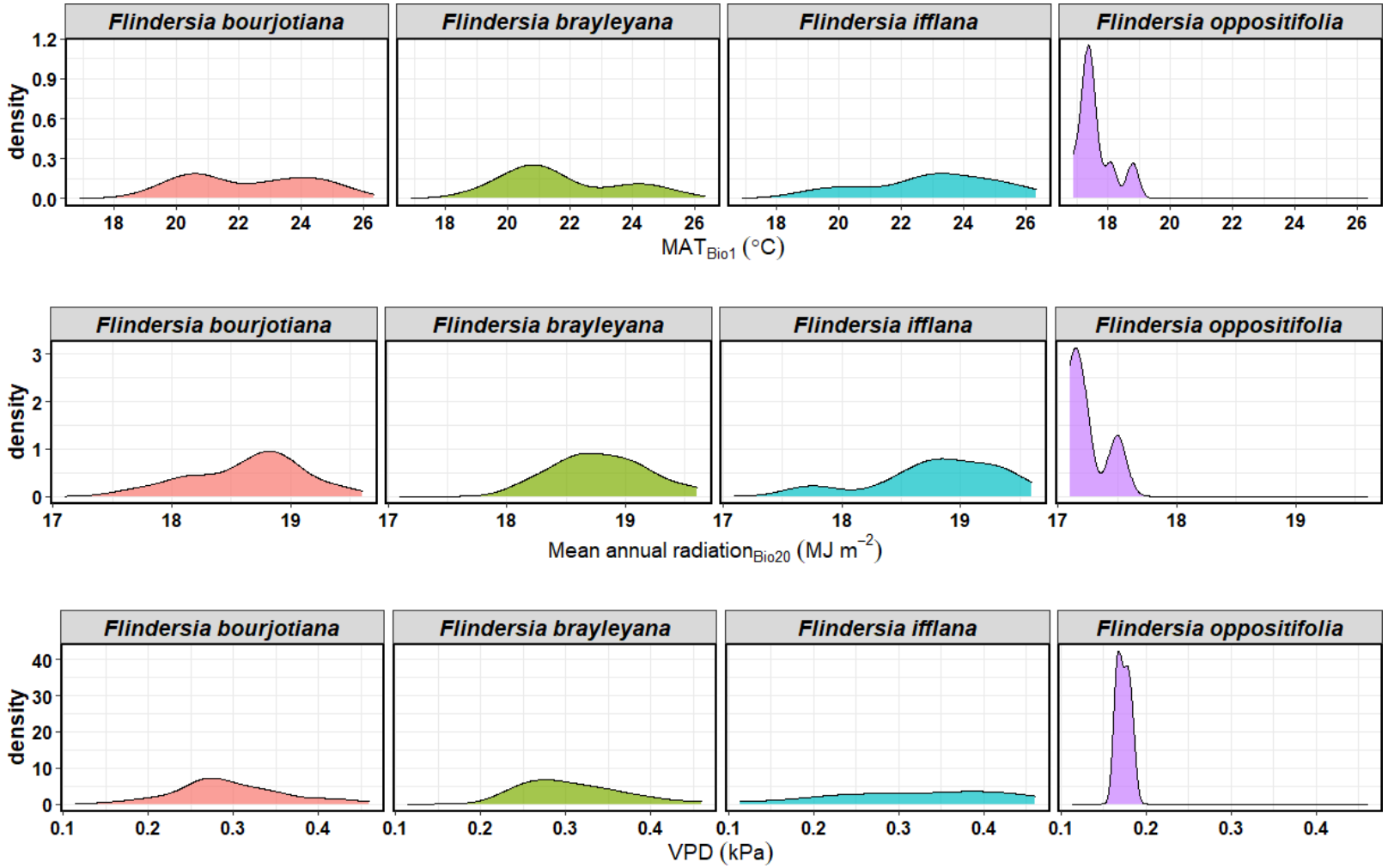

Supplementary Figure 3.2 (from top to bottom) - Density plots based on the *Flindersia spp.* occurrence records in relation to bioclimatic variables: BIO1 (MAT), mean annual radiation and VPD, obtained after spatial thinning at 0.5km resolution and interpolated using WorldClim v.2 bioclimatic variables.

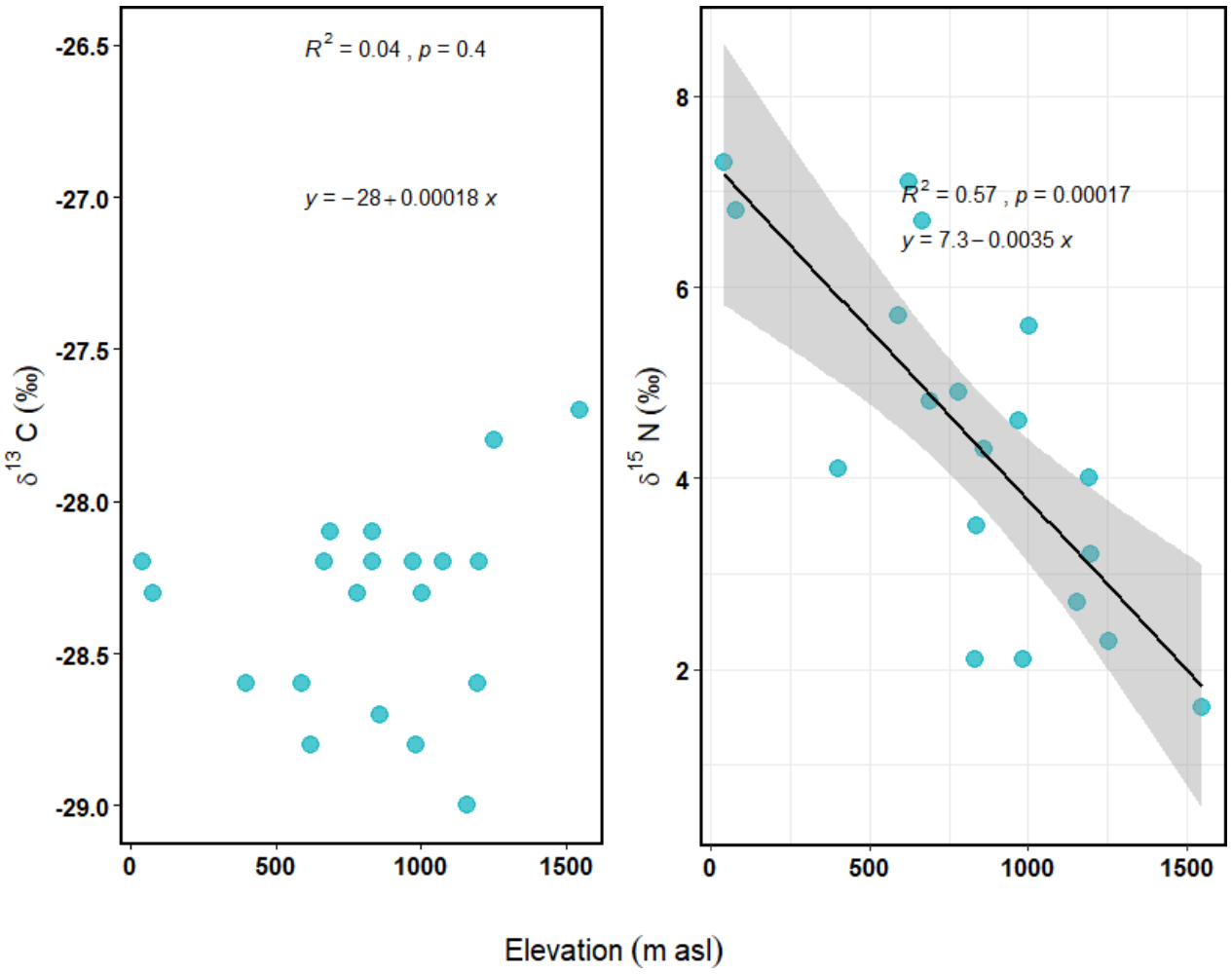

Supplementary Figure 3.3. Soil $\delta^{13}C$ and $\delta^{15}N$ for soils formed on granitic parent material across an elevation gradient in the Australian Wet Tropics.

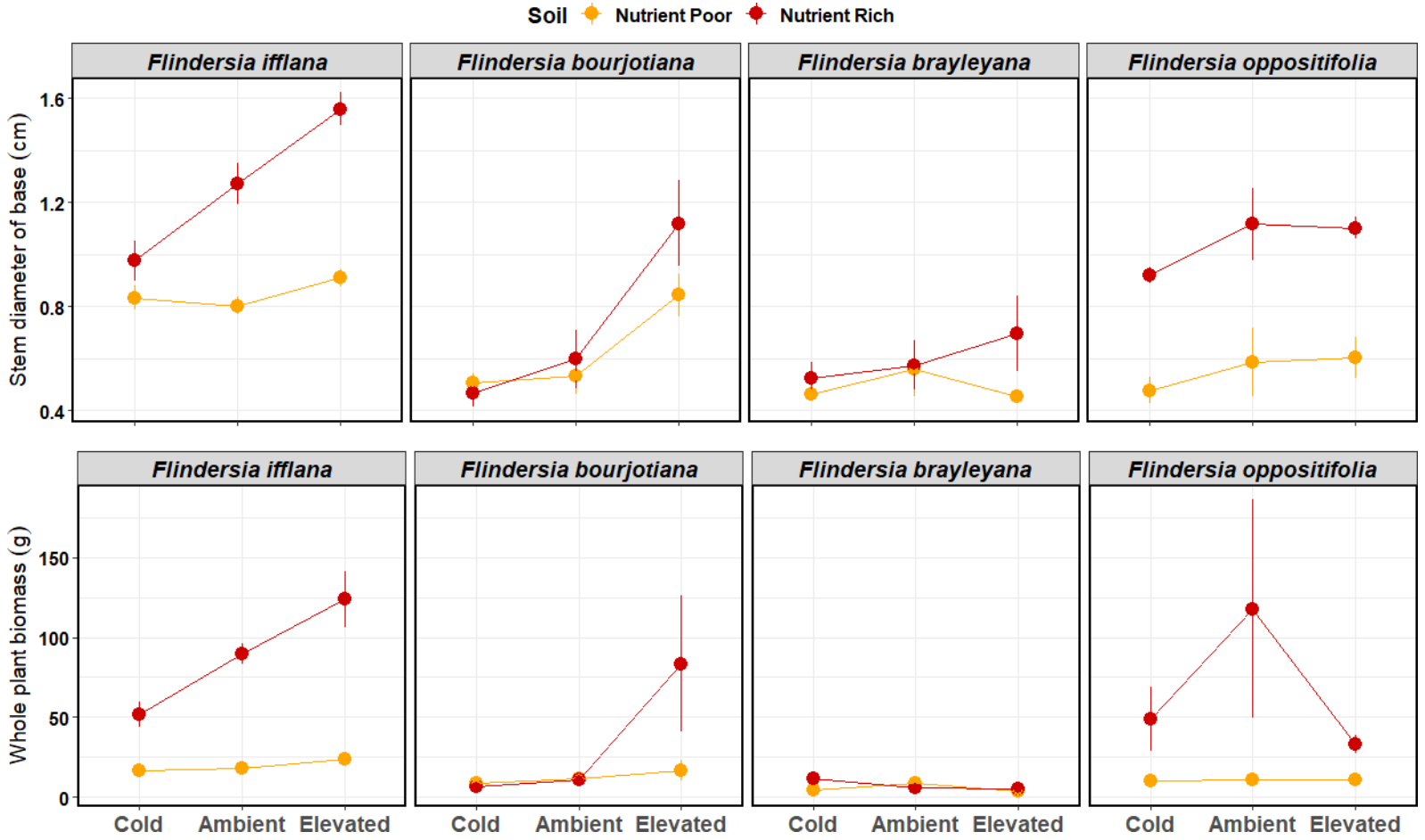

Supplementary Figure 3.4. Means (± SE) of stem diameter growth at the base of the stem (top row) and whole plant biomass (bottom row) among T_{growth} and Soil nutrient treatments (nutrient rich soil = red, nutrient poor soil = orange) from the glasshouse experiment. Species are shown left to right according to their elevational ranges, leftmost being lowland and rightmost being mountaintop.

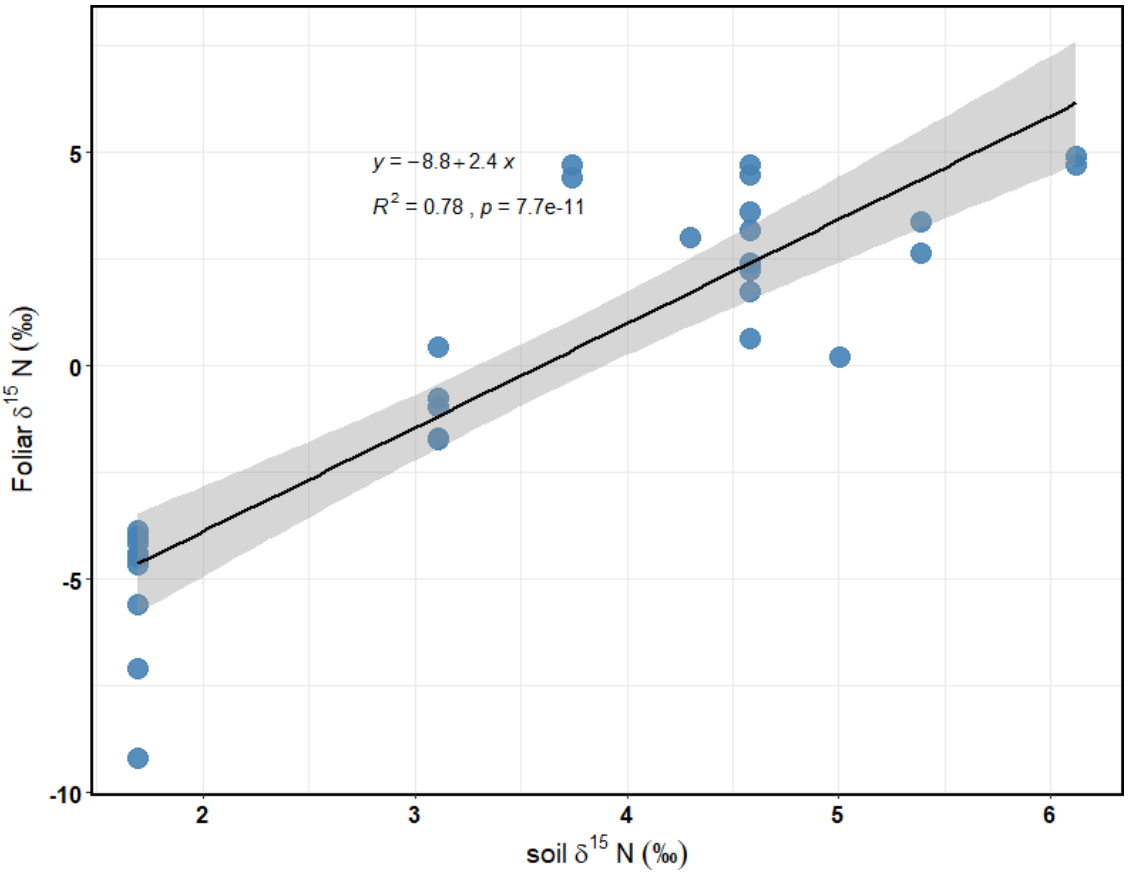

Supplementary Figure 3.5. Relationship between leaf and soil $\delta^{15}N$ for field collections of *Flindersia* species in the Australian Wet Tropics.

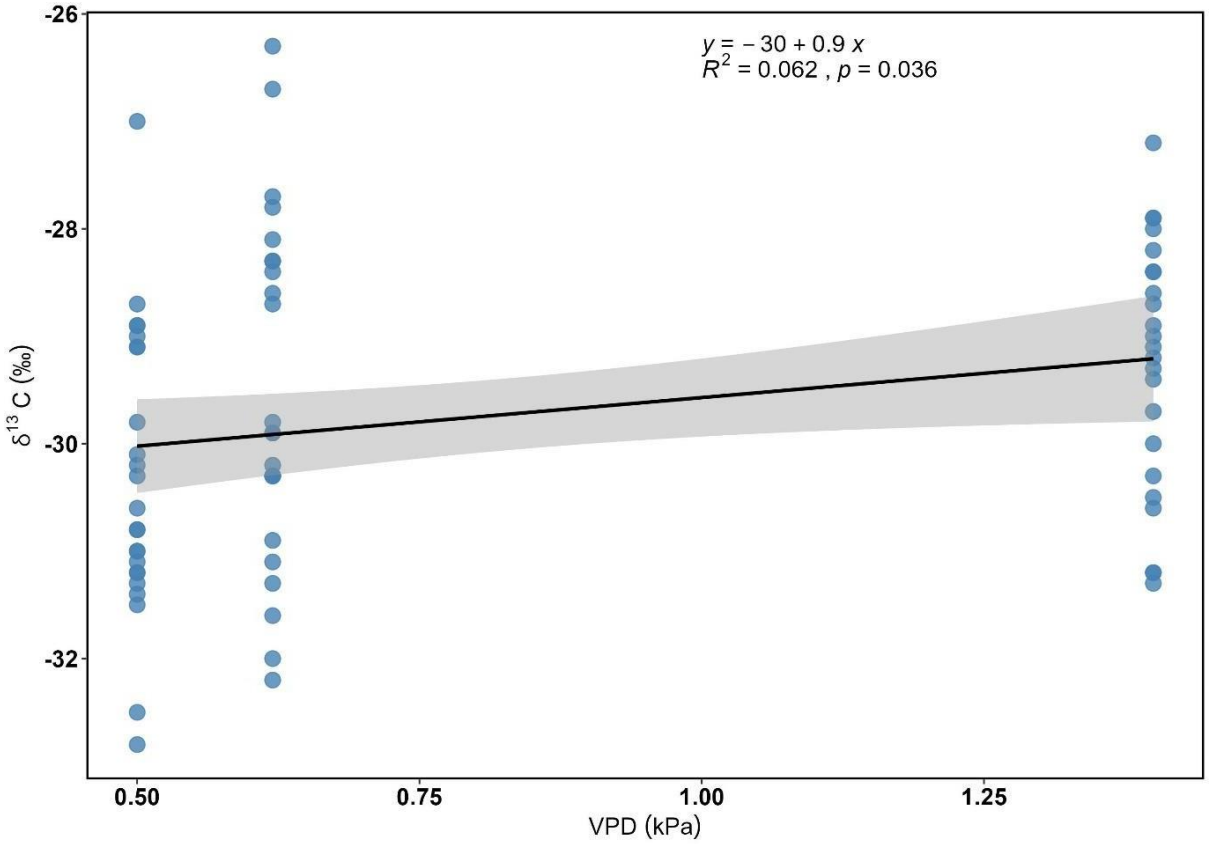

Supplementary Figure 3.6. Leaf $\delta^{13}C$ as a function of daytime vapour pressure deficit, calculated from experiment long observations of air temperature and relative humidity in the glasshouse experiment.

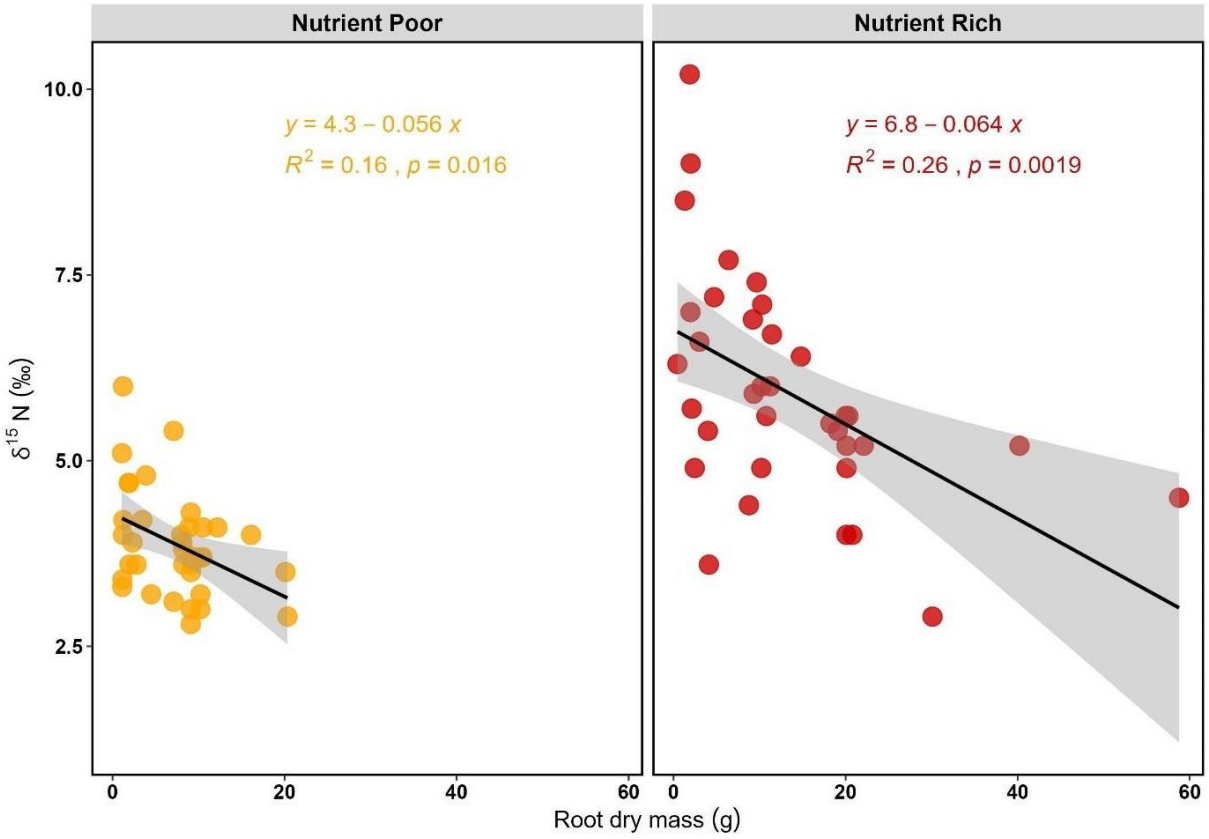

Supplementary Figure 3.7. Leaf $\delta^{15}N$ in relation to root dry mass for plants grown in the glasshouse experiment.

Chapter 4: Foliar chemistry in tropical rainforest trees is regulated by the temperature responses of leaf photosynthetic capacities

This chapter is currently under preparation for submission to the journal *Plant, Cell & Environment*.

Leaf gas exchange performed on experimental saplings (~3.5 months into the experiments) using a Li-COR 6400 XT in one of the experimental growth chambers.

Abstract

The relative allocation of resources in leaves to photosynthesis (e.g., chlorophyll and RuBisCO) and defense (e.g., phenolics) reflects an important axis in plant ecological strategies. Yet, the physiological constraints on these investments and potential for acclimation under climate warming scenarios in tropical rainforest trees are poorly understood. I evaluated the temperature response of leaf photosynthetic capacity (i.e., maximum rates of carboxylation of the enzyme RuBisCO (V_{cmax}) and maximum rates of electron transport (J_{max})), and the intercellular carbon dioxide transition point (C_i–T), i.e., the C_i at which photosynthesis transitions from V_{cmax} to J_{max} limited photosynthesis. I studied these processes in saplings of four tropical rainforest tree species sourced from contrasting thermal niches in the Australian Wet Tropics, under varying soil nutrients and growth temperatures (T_{growth}). I further evaluated the relationship of these parameters with leaf antioxidant capacity, soluble phenolics and chlorophyll concentrations under the experimental conditions. I observed a decline in the J_{max}/V_{cmax} ratio with increasing leaf temperatures (T_{leaf}) in short term temperature responses, and at a steeper rate for a mountaintop species and for plants grown under warmer T_{growth} conditions. Antioxidant capacity and phenolic concentrations were closely correlated, and I therefore focused subsequent analyses only on phenolics. Phenolic concentrations were positively correlated with J_{max}/V_{cmax} and increased with increasing C_i–T. Conversely, chlorophyll was positively correlated with V_{cmax} at 25°C and increased with leaf N_{area}. Leaf chlorophyll was higher in nutrient-rich soils and increased under warmer T_{growth} conditions in the lower elevation species but displayed limited plasticity in a mountaintop species. Phenolics strongly declined with warming and showed little-to-no dependence on soil nutrient availability. The correlation between J_{max}/V_{cmax} and C_i–T with phenolics suggests that an overinvestment in electron transport (J) under cooler T_{growth} was responsible for higher allocation to defense (phenolics) against oxidative stress from excess electrons. Finally, leaf chlorophyll variations among species suggested that the capacity of the mountaintop species to utilize increasingly available N is limited under warming. The study highlights the physiological controls on foliar chemistry, with implications for tropical rainforest tree growth and defense under climate warming.

4.1 Introduction

A key uncertainty under projected global climate change is the impacts higher temperatures will have on tropical tree growth, physiology, and chemistry (Cavaleri et al., 2015; Mercado et al., 2018). In tropical rainforests, temperature change is observed naturally across elevation gradients, as are changes in soil nutrient availability (Malhi, 2010). Such changes can have a direct impact on plant physiological processes and can determine the extent of species' distributions along elevation (Feeley et al., 2020; Tito et al., 2020). Therefore, species' elevational ranges may give an indication of their capacity to acclimate to different temperatures associated with global warming (Dusenge et al., 2021).

Almost all biological and chemical processes are sensitive to temperature (Slot and Winter, 2016). For plants in particular, the process of photosynthesis responds strongly to temperature (Hikosaka et al., 2005; Slot and Winter, 2016). Photosynthesis comprises two major sets of reactions, i.e., electron transport (the light reactions) and the carbon reduction cycle (Calvin–Benson cycle) (Sage and Kubien, 2007). According to the Farquhar et al. (1980) model of C_3 photosynthesis, the photosynthetic rates can be predicted as the majority of the rates of these two sets of reactions. A third state that occurs in the chloroplasts is the triose phosphate utilization (*TPU*), where photosynthesis does not respond to increasing CO_2 nor is inhibited by increasing oxygen concentrations (Sharkey, 2007). By fitting the biochemical model to photosynthetic responses to CO_2 concentration (A–C_i curves), estimates of the capacities of the three states can be extracted as J_{max} (maximum rate of electron transport at saturating light), V_{cmax} (maximum rate of carboxylation by the enzyme RuBisCO) and *TPU* (Sharkey et al., 2007). Whether investment in J_{max} and V_{cmax} has been successfully coordinated by the plant can be assessed by examining the intercellular carbon dioxide transition point (C_i–T) in the fitted photosynthesis model (Evans and von Caemmerer, 1996). If the C_i–T from V_{cmax} limitation to J_{max} limitation is close to the operating C_i, it would indicate coordination of investment in the two sets of reactions, such that resources have been optimally shared between them (Maire et al., 2012).

Temperature responses can also vary for different biological processes. The J_{max} and V_{cmax} each represent a series of reactions and the overall temperature responses are rather different for these two sets of reactions (Medlyn et al., 2002; Crous et al., 2022). For instance, J_{max} is sensitive to high temperatures because of its dependence of thylakoid membrane stability (Sharkey, 2005), and therefore photosynthetic rates may become more limited by

electron transport rates over carboxylation rates (Sage and Kubien, 2007). Likewise, the enzyme responsible for regulation of RuBisCO activity (activase) is sensitive to temperature, and both RuBisCO and electron transport rates have the potential to limit photosynthesis at higher temperatures (Crafts-Brandner & Salvucci, 2000). Alternately, studies have also found that stomatal conductance often constrains CO_2 supply towards carboxylation at high temperatures, and under such conditions reductions in leaf photosynthesis are due to limitations of RuBisCO (Sage and Kubien, 2007; Vårhammar et al, 2015). However, V_{cmax} in general has a steeper response to temperature compared to J_{max} because of the limitation of carbon assimilation by low temperatures, over the relative insensitivity of light harvesting to low temperatures; and the proportional difference in the temperature response can be seen in a shift in the J_{max}/V_{cmax} ratio with changing temperatures, i.e., decreases as temperature increases (Sage and Kubien, 2007).

Optimality theory suggests that plants should invest resources in J_{max} and V_{cmax} such that they are co-limiting to photosynthesis under the operating photosynthetic conditions (Prentice et al., 2014; Wang et al., 2017). Overinvestment in V_{cmax} would represent an unproductive use of leaf nitrogen, the nutrient most often limiting growth (Evans, 1989). Overinvestment in J_{max} would represent an excess supply of electrons, resulting in reactive oxygen species and photo-oxidative stress (Piluzza and Bullitta, 2011). Plants can cope with photo-oxidative stress by investing in antioxidant systems (Lima-Melo et al., 2019). One such important class of antioxidants is phenolics, which are known to have specific functional properties to deal with oxidative stress (Gururani et al., 2015; Piluzza and Bullitta, 2011).

Phenolics also play other roles, in addition to acting as antioxidants (Karabourniotis et al., 2014; Schneider et al., 2019). For example, they are important photoprotective agents against UV; they are digestibility reducers; they both slow decomposition of dead plant material and reduce herbivory rates of living tissues (Kubalt, 2016; Parsons, 2015; Schneider et al., 2019). If phenolics primarily play a role in defense against oxidative stress, I would expect their concentrations to increase under conditions where J_{max} is higher than V_{cmax} at the operating intercellular CO_2 concentration. If phenolics primarily play a role in defense against herbivores, one might expect investment according to the carbon-nutrient balance hypothesis (CNB) (Coley et al., 2002). The CNB hypothesis predicts that investment in carbon-based defensive compounds should increase under conditions of relatively low nitrogen supply by the soil and decrease as nitrogen supply increases (Coley et al., 2002). Phenolics represent a carbon-based defense against herbivores according to this hypothesis.

An important component of the light reactions of photosynthesis is the chlorophyll concentration in leaves (Evans and von Caemmerer, 1996). A chlorophyll pigment absorbs light energy, and when in an excited state, it initiates the electron transport chain. This results in production of ATP and $NADP^+$, energy transport molecules that are passed to the carbon reduction cycle (Farquhar et al., 1980). Successful acclimation to different growth temperatures and an ability to compete successfully at a range of elevations could be enhanced by plasticity in investment into J_{max} relative to V_{cmax}, and in chlorophyll relative to phenolics (Sumbele et al., 2012). Chlorophyll represents light harvesting capacity, and phenolics represent defense against excessive light harvesting. As temperature declines, with increasing elevation for example, and V_{cmax} declines more steeply than J_{max}, I would predict a lower investment in chlorophyll and higher investment in phenolics for optimal plant performance. The largest controller of leaf chlorophyll is the light environment, and this could also change with increasing elevation. Thus, I would expect species that are widely distributed across elevation gradients (thermal generalists) to show more plasticity in these leaf properties, i.e., allocation of chlorophyll versus phenolics, and a tropical mountaintop restricted species (thermal specialist) to show less plasticity.

In this study, I used seeds of *Flindersia* species collected from different elevations within the AWT (Supplementary Table 3.1) and grown in a glasshouse in three different temperature treatments and two soil nutrient availability treatments to test the following hypotheses:

1. The J_{max}/V_{cmax} ratio declines with increasing temperature, and the rate of decline is similar across species with different elevations of origin and growth treatment conditions;
2. Investment in phenolics is correlated with the J_{max}/V_{cmax} ratio at growth temperature and the *Ci* transition point at growth temperature, but not with leaf nitrogen concentration, indicating a primary role in defense against photo-oxidative stress, rather than investment according to the carbon-nutrient balance hypothesis;
3. Investment in chlorophyll increases with temperature as V_{cmax} at growth temperature increases, and it also increases with increasing leaf nitrogen concentration as V_{cmax} increases;
4. Flexibility in investment in light harvesting relative to defense against photo-oxidative stress, as mediated by chlorophyll and phenolic concentrations, will display a larger plasticity in thermal generalist species than in a thermal specialist

when plants are grown at different temperatures and soil nutrient availabilities.

4.2 Methods

4.2.1 Study species selection

As in Chapter 3, I chose the four *Flindersia* species based on their occurrence records, i.e., three thermal generalists of a broad thermal niche width, representing the lowland: *F. ifflana* F.Muell. (elevation range near sea level – 1100m, collected at ~ 300m a.s.l.), mid-elevation: *F. bourjotiana* F.Muell. (near sea level – 1200m, collected at ~600m a.s.l.), upland: *F. brayleyana* F.Muell. (near sea level – 1150m, collected at ~990m a.s.l.), and one thermal specialist of a narrow thermal niche width restricted to the tropical mountaintops: *F. oppositifolia* (F.Muell.) T.G.Hartley & L.W.Jessup (recorded above 1300m, collected at ~1550m a.s.l) (Supplementary Table 3.1; Supplementary Figure 3.2).

4.2.2 Experimental set-up and growth conditions

The experimental set-up was the same one used in Chapter 3. Seeds of *Flindersia* spp. representing three thermal generalists (elevation range of *ca* 300 to 990m a.s.l.) and a thermal specialist (*ca* 1550m a.s.l.) were sourced from different provenances within the AWT World Heritage Area (see Supplementary Table 3.1) and sown on a bed of nutrient-rich (NR) soil containing garden potting mix and compost (in a 1:1 ratio) during November – December 2019 (Supplementary Figure 4.1b). Seedlings were allowed to germinate for *ca* 3 months in shade house conditions at the Environmental Research Complex (ERC), James Cook University (JCU) (*ca* 30m a.s.l.) (Supplementary Figure 4.1c). Successfully germinated healthy saplings were then transplanted into 13.5 L pots (Garden City Pots, Model: P300ST00) containing the same NR soil and 8.5 L pots (Garden City Pots, Model: P250STTL) containing nutrient-poor soil (NP), a mixture of locally collected dermosol and washed river sand. Plant growth experiments were then conducted with these pots (n=72) in a glasshouse facility at the ERC. The two pot sizes were chosen to distinguish the nutrient rich versus the nutrient poor soils, which were sufficiently large enough (by volume) for sapling growth.

The glasshouse facility is divided into three temperature-controlled chambers with a SOLARO 5220 D O FB climate/shade screen (Ludvig Svensson Inc. Kinna, Sweden) that reduces total irradiance by approximately 50% and helps spread light more evenly within the chambers. The growth temperature (T_{growth}) treatments were, a) lowland Ambient temperature

chamber (with a 0°C offset); b) Cold temperature chamber (with *ca* –7°C offset) that mimics the mountaintop environment, and c) Elevated temperature chamber (with *ca* +5°C offset), a lowland future warming scenario. The temperature of the chambers was controlled using a Building Management System (BMS) to achieve the respective chamber temperature conditions through manipulation of a chilled water supply to the air handling units. Relative Humidity (RH) and the temperature were monitored (RHP-2R2B Temperature and Humidity Probe, Dwyer Instruments, Michigan City, IN, USA) and recorded every 5 minutes in the BMS (Apgaua et al., 2019).

I selected a minimum of 3 healthy saplings per Soil nutrient type per species under each growth temperature treatment to give a total of 24 saplings (3 saplings × 2 soil type × 4 species) for gas exchange and leaf chemistry measurements. All pots were hand watered daily to field capacity. The three temperature treatments were rotated among the chambers monthly to minimize any chamber microclimate bias.

4.2.3 Leaf gas exchange measurements

Leaf gas exchange measurements were conducted on healthy leaves from the selected pots in their respective growth conditions during 23rd June – 8th July 2020 (*ca* 3.5 months after the start of the experiment). Light saturated net photosynthesis was first measured at three CO_2 concentration set points (400, 1200 and 2000 ppm) across varying light intensities, i.e., Photosynthetically Active Radiation (PAR) from 0 – 2000 μmol m^{-2} s^{-1} using two portable photosynthesis systems (Li-COR 6400 XT, Li-COR Inc., Lincoln, NE, USA). The plants displayed saturating photosynthetic rates at approximately 1100 μmol m^{-2} s^{-1}. I then conducted light saturated net CO_2 assimilation (A–C_i) curves at saturating light (1200 μmol m^{-2} s^{-1}) across 13 CO_2 concentration set points (400 to 50 and up to 2000 ppm). The leaf temperature (T_{leaf}) was controlled to be representative of experimental-long chamber T_{growth}, (17°C- Cold, 23°C- Ambient and 28°C- Elevated), and RH in the leaf chamber was maintained from 60 to 85% during the measurements. Gas exchange in all pots was measured during daylight hours (8:00 AM to 3:00 PM). The C_3 photosynthesis model developed by Farquhar-von Caemmerer-Berry (FvCB) (Farquhar et al., 1980) was fitted to the A–C_i curves using the "*fitaci*" function. The model was first tested for its robustness by using the "*default*" fitting method and setting "*TPU*" as False. Since certain pots could not be fit using the default setting, I chose to refit the model using the fit method as "*bilinear*" and "TPU" as True in the "*plantecophys*" package (Duursma, 2015) in R studio (Team, 2021). Fitted model

coefficients, including V_{cmax} and J_{max} were extracted and further used to calculate J_{max}/V_{cmax} ratio. The other temperature response parameters for V_{cmax} and J_{max} were used as built-in the model (Duursma, 2015), whereas the CO_2 compensation point (Gamma Star) and Michaelis-Menton coefficient (Km) were extracted from each treatment by pot fit (Supplementary Table 4.2). The intercellular carbon dioxide transition point (C_i–T) point from V_{cmax} limitation to J_{max} limitation was also obtained from the fit of the FvCB model of C_3 photosynthesis (Duursma, 2015).

I conducted another set of leaf gas-exchange measurements between 24th August and 23rd September 2020 on healthy leaves using the saturating light levels as above at six leaf temperatures (15, 20, 25, 30, 35 and 40°C). To achieve the respective T_{leaf}, the chamber temperatures were manipulated using the BMS and the Li-COR block temperatures, and RH were maintained as above. Once the leaves achieved the target T_{leaf} they were allowed to acclimate for up to 15-20 mins and A–*Ci* curves were then generated across 13 CO_2 set points as above from pots across all treatments. On days that were hotter or cooler, certain leaves did not achieve either the lowest (15°C) or the highest (40°C) target T_{leaf} respectively, and hence the final dataset had measurements from fewer replicates than would have made up the full factorial. Thus, I collected a total of 361 A–C_i curves for estimation of V_{cmax} and J_{max} values used for final analysis.

4.2.4 Foliar chemistry

Soluble leaf phenolics, chlorophyll and nitrogen (N) concentration and leaf total antioxidant capacities were quantified from healthy fully expanded leaves (*ca* 3–5 leaves per pot) that were harvested towards the end of the growth experiment. Fresh leaves (n=3–5) from above were scanned using a flat-bed scanner (CanoScan LiDE 400, Canon Australia) and leaf area (cm^2) was calculated using Image-J software. Oven-dried (~50°C) mass of harvested leaves was then used to determine the Leaf dry Mass per unit leaf Area (LMA). Leaves from each pot were pooled, homogenized using a Benchtop Ring Mill (RockLabs Pvt Ltd, USA) and used for chemical analyses. Leaf N was quantified using a Costech Elemental Analyzer fitted with a zero-blank auto-sampler coupled via a ConFloIV to a ThermoFinnigan DeltaV^{PLUS} Continuous-Flow Isotope Ratio Mass Spectrometer (EA-IRMS) at the Advanced Analytical Centre (JCU). N concentrations were expressed in % dry weight.

Leaf total soluble phenolics were quantified using the Folin–Ciocalteu method (Cork and Krockenberger, 1991; Waterman, 1994) as modified for a microplate reader (Ritmejeryte

et al., 2019). Briefly, 20 mg of homogenized leaves were extracted three times in 1 mL of cold 50% acetone, followed by centrifuging at 26,000 g for 5 min and pooling the supernatants. Folin-Ciocalteau reagent and Na_2CO_3 were used to develop colour in a 20 mL aliquot of the pooled extract and absorbance was measured at 765 nm using FLUOstar Optima Microplate Reader (BMG LABTECH). Gallic Acid (GA) was used as a standard, and total phenolic concentrations were expressed as mg of GA equivalents per gram of leaf dry weight (mg GA g^{-1} DW).

Acetone extracts were also used to quantify leaf total antioxidant capacity as Ferric Reducing Ability of Plasma (FRAP), a measure of 'Antioxidant Power' developed by Benzie and Strain (1996) and modified for a microplate reader. Briefly, colour was developed using FRAP reagent containing 300mM acetate buffer: 10 mM 2, 4, 6-Tripyndyl-s-triazine (TPTZ) in 40 mM HCl: 20 mM $FeCl_3 \times H_2O$ (10:1:1) was made on the day of analysis and incubated at 37°C. 10 μL of extract (or standard) and 190 μL FRAP reagent were mixed and incubated in the dark for 30 min, following absorbance reading at 593 nm. Ascorbic acid (Vitamin-C) was used as the standard and the concentration of FRAP content was expressed as mg VC equivalents g^{-1} DW.

Leaf chlorophyll concentration was quantified from the leaf Chlorophyll Concentration Index (CCI) which was measured on each experimental sapling (the same fully expanded healthy experiment leaves that were used for nutrient analysis) using a hand-held Chlorophyll meter (model MC-100; Apogee Instruments, Inc. Logan, Utah). The meter measures the ratio of radiation transmittance at two different wavelengths (red and near infrared) and outputs chlorophyll concentration, which is calculated internally from the transmittance ratio measurement (as per manufacturer's instructions). The CCI obtained from the chlorophyll meter is highly correlated with in-vitro chlorophyll concentrations and has been tested with measurements from a wide range of plant species (Parry et al., 2014). I used a standard calibration curve for tropical trees: $-283.20 + 269.96\ (CCI)^{0.227}$ (Gonçalves et al., 2008) to calculate the leaf chlorophyll expressed in μmol m^{-2} of leaf.

4.2.5 Statistical analysis

All statistical analyses were conducted in R studio version 4.1.2 (Team, 2021). Before importing the data into R for statistical analyses, data wrangling and any mass-to-area based conversions of foliar chemistry from experiment results were performed in Microsoft Excel. To understand how the plant photosynthetic capacity responded to T_{leaf} I first explored the

V_{cmax}, J_{max} and the ratio of J_{max}/V_{cmax} plotted against T_{leaf}. The V_{cmax} and J_{max} displayed non-linear relationships with T_{leaf}, whereas the ratio of J_{max}/V_{cmax} displayed linear trends. Hence, I computed a linear mixed effects model for the J_{max}/V_{cmax} ratio against T_{leaf}, with T_{growth}, Species and Soil nutrient type and their interactions as fixed effects and individual pot (i.e., leaf) as a random intercept. Type III ANOVA was used on these models via the Satterthwaite's method for denominator degrees of freedom using the '*lmerTest*' package in R (Kuznetsova et al., 2017). This was done to represent the *F*-statistic in terms of their effect sizes that represents the amount of variance explained by each model's terms using the *F*-to-*partial*-Eta squared (η^2_p) conversion in the '*effectsize*' package in R (Ben-Shachar et al., 2021). This way the percentage of the partial variance is presented (after accounting for other predictors in the model). A post-hoc pairwise comparison of means was then conducted between Species using the Tukey method in the "*emmeans*" package (Lenth, 2021).

To understand how leaf phenolics, chlorophyll and the ratio of J_{max}/V_{cmax} responded to T_{growth}, I calculated general linear models on each of these response variables with independent variables of T_{growth}, Soil type, Species, and their interactions. Temperature was taken as a continuous variable from the long-term air temperature averages for each growth chamber (Chapter-3 Table 1). I then used a stepwise selection of the models with or without interactions based on the AIC values using the 'performance' package in R studio (Lüdecke et al., 2021). The models were of the general form:

$$Dependent\ variable \sim T_{growth} + Soil + Species + Soil \times Species + T_{growth} \times Species.$$

All response variables were checked for normality using visual histograms and a Shapiro-Wilk's normality test was performed on each of the response variables.

4.3 Results

4.3.1 Temperature response of leaf photosynthetic capacities

Leaf photosynthetic capacities, i.e., V_{cmax} and J_{max} increased with increasing leaf temperatures in a non-linear fashion (Supplementary Figure 4.2), whereas the ratio of J_{max}/V_{cmax} displayed a significant linear decline with T_{leaf} ($F_{(1, 288)} = 2114$, $p<0.001$) (Figure 4.1, Table 4.1). There was a strong interaction effect for the response of J_{max}/V_{cmax} with T_{leaf} x Species ($F_{(3, 288)} = 14.2$, $p<0.001$), T_{leaf} x T_{growth} ($F_{(2, 288)} = 9.07$, $p<0.001$) and T_{leaf} x Soil ($F_{(1, 288)} = 4.88$, $p<0.05$) (Figure 4.1, Table 4.1). The relative contribution of predictor variables based on the partial percent variance (η^2_p) was highest for the effect of T_{leaf} (η^2_p =0.88) followed by the interaction of T_{leaf} x Species (η^2_p =0.13) and T_{growth} (η^2_p =0.06) and all other

predictors had a very low η^2_p. A pairwise comparison of means of J_{max}/V_{cmax} averaged over levels of Soil and T_{growth} suggested significant difference between the upland, *F. brayleyana* and mountaintop, *F. oppositifolia* ($t_{(289)} = -4.64$, $p<0.001$) and mid-elevation, *F. bourjotiana* ($t_{(290)} = 5.89$, $p<0.001$); and between the lowland, *F.ifflana* and *F. bourjotiana* ($t_{(290)} = -4.23$, $p<0.001$) and *F.oppositifolia* ($t_{(288)} = -2.85$, $p<0.05$). The slope of the response of J_{max}/V_{cmax} to T_{leaf} was steeper for plants in the Cold T_{growth} chamber than in the Elevated T_{growth} chamber, with pairwise comparison of means showing significant difference in slopes between Cold-Elevated ($t_{(287)} = -1.37$, $p<0.0001$) and Ambient-Elevated ($t_{(289)} = 4.18$, $p<0.05$). For Species, the regression slopes of J_{max}/V_{cmax} against T_{leaf} were in the following order: *F. brayleyana* (upland, 2.24)> *F. oppositifolia* (mountaintop restricted, 2.03)> *F. bourjotiana* (mid-elevation, 1.9)> *F. ifflana* (lowland, 1.85). The ratio of J_{max}/V_{cmax} was the highest for the Species *F. brayleyana* (4.09) under Ambient T_{growth} (T_{leaf} at 15°C), and the least for *F. ifflana* (0.51) under Cold T_{growth} (T_{leaf} at ~40°C) (Table 4.1; Figure 4.1).

4.3.2 Relationship between leaf total phenolics with J_{max}/V_{cmax} and C_i transition point

Leaf phenolic concentrations were strongly positively correlated with the leaf total antioxidant capacity as determined by the FRAP assay (R^2 =0.92, $p<0.001$) (Figure 4.2c). Leaf phenolic concentrations displayed a strong linear increase with the ratio of J_{max}/V_{cmax} (R^2 =0.40, $p<0.001$) (Figure 4.2a) and the transition point of intercellular CO_2 concentrations ($C_i - T$) (R^2 =0.15, $p<0.01$) measured at the chamber T_{growth} (Figure 4.2b). There was no relationship between leaf phenolics and leaf nitrogen concentrations (Figure 4.2d).

4.3.3 Relationship of chlorophyll with $V_{cmax-25}$, J_{max-25} and leaf N

The leaf chlorophyll concentration across the data set was positively related to the maximum carboxylation capacity at 25°C ($V_{cmax-25}$) (R^2 =0.28, $p<0.001$) (Figure 4.3a) and the maximum rates of electron transport at 25°C (J_{max-25}) (R^2 =0.25, $p<0.001$) and leaf N on a leaf area basis (N_{area}) (R^2 =0.11, $p<0.001$) (Figure 4.3d).

4.3.4 Responses of leaf chlorophyll, phenolics, and J_{max}/V_{cmax} to T_{growth} and Soil type

The leaf chlorophyll concentration was higher in nutrient-rich soils across all Species and T_{growth} chambers and increased with increasing nutrient availability from Cold to Elevated for lower elevation species but declined from Ambient to Elevated for upland and

mountaintop restricted species under NR soil (Figure 4.4a). There was a significant independent effect for the response of Soil ($F_{(1, 59)} = 22.6$, $p<0.001$) and T_{growth} ($F_{(1, 59)} = 3.9$, $p<0.05$) and an interaction effect for Species x Soil ($F_{(1, 59)} = 5.9$, $p<0.05$). The pairwise comparisons of means in leaf chlorophyll when averaged over the levels of Soil displayed significant differences only for the upland *F. brayleyana* with mountaintop restricted *F. oppositifolia* ($t_{(59)} = 2.6$, $p<0.05$). Across the entire dataset, the highest (485μmol m^{-2}) and lowest (164 μmol m^{-2}) leaf chlorophyll was observed for *F. brayleyana* under NR – Ambient and NP – Cold respectively (Figure 4.4a, Table 4.3).

For leaf phenolics there was a strong significant decline for all Species with T_{growth} under both Soil types (Figure 4.4b). There was a significant independent effect of T_{growth} ($F_{(1, 59)} = 6.7$, $p<0.05$) and an interaction effect for Species x T_{growth} ($F_{(3, 59)} = 11.8$, $p<0.001$) and Species x Soil ($F_{(3, 59)} = 6.7$, $p<0.001$) (Table 4.2). The pairwise comparisons of means in leaf phenolics when averaged over the levels of Soil displayed significant differences between the lowland *F. ifflana* with upland *F. brayleyana* ($t_{(59)} = 5.6$, $p<0.001$), and between the mid-elevation species *F. bourjotiana* and *F. brayleyana* ($t_{(59)} = 4.4$, $p<0.001$) and finally between *F. brayleyana* and *F. oppositifolia* ($t_{(59)} = -3.07$, $p<0.05$). Across the experimental dataset the highest leaf phenolic concentration was observed for the mountaintop species, *F. oppositifolia* (146 ± 8 mg GA g^{-1} DW) under NR – Cold and the upland species, *F. brayleyana* (146 ± 21 mg GA g^{-1} DW) under NP – Cold, and the least was observed for *F. brayleana* (34 ± 8 mg GA g^{-1} DW) (Table 4.3). The largest decline (nearly -115%) in foliar phenolics was observed for *F. brayleyana* growing in NR soils from between Cold – Elevated growth treatments.

The ratio of J_{max}/V_{cmax} measured at growth temperature displayed a strong linear decline for all Species across the chamber T_{growth} conditions (Figure 4.4c). There was a strong independent effect for the response to T_{growth} ($F_{(1, 62)} = 124.45$, $p<0.001$) and Species ($F_{(1, 62)} = 4.18$, $p<0.01$) but no significant interaction effects were observed between the predictor variables.

The total leaf N_{mass} was higher in nutrient-rich soil across all Species by T_{growth} combinations (Figure 4.4d). There was a significant interaction effect for Soil x Species ($F_{(3, 63)} = 5.9$, $p<0.01$). The highest N_{mass} was observed for *F. brayleyana* (2.2%) under NR–Ambient conditions and the lowest for *F. bourjotiana* (0.6%) under NP – Elevated T_{growth} condition

4.4 Discussion

This study was aimed at understanding how species distributed along an elevation gradient respond to the effects of temperature and soil nutrient availability in terms of their leaf photosynthetic capacities (i.e., J_{max}/V_{cmax}) and leaf chemistry (such as chlorophyll, phenolics and N). I studied this among saplings of tropical rainforest tree species of the genus *Flindersia*, germinated from seeds sourced from various provenances along an elevation gradient in the AWT World Heritage Area. I evaluated species' acclimation potential by studying how instantaneous leaf temperature (T_{leaf}) response of J_{max}/V_{cmax} (obtained from the FvCB model) differs among species grown under varying soil nutrients and growth temperature conditions (T_{growth}). I then explored how species would invest their resources in defense compounds such as soluble phenolics under nutrient limited and thermally varying conditions by studying the relationship with J_{max}/V_{cmax} and the intercellular carbon dioxide transition point (C_i–T) obtained from the FvCB model. Next, I evaluated the relationship in energy harvesting pigments such as leaf chlorophyll concentration with maximum carboxylation capacity and maximum electron transport rates at 25° C ($V_{cmax\text{-}25}$ and $J_{max\text{-}25}$) and leaf area-based nitrogen concentration (N_{area}). Finally, I evaluated the flexibility among species in the allocation of chlorophyll, phenolics and leaf nitrogen across varying T_{growth} and soil nutrient availability. I also evaluated the long-term chamber T_{growth} response of J_{max}/V_{cmax} for all species by soil combinations.

4.4.1 Leaf temperature response of photosynthetic capacity in the short-term

The J_{max}/V_{cmax} declined with increasing T_{leaf} in the short-term, and the slopes declined with increasing chamber growth conditions from Cold to Elevated. Higher J_{max}/V_{cmax} in cooler T_{growth} conditions has been reported in previous studies and is attributed to differences in the temperature response of J_{max} and V_{cmax} (Crous et al., 2018; Scafaro et al., 2017), i.e., carboxylation rates tend to increase at a faster rate compared to electron transport rate as temperature increases. The significant declines in J_{max}/V_{cmax} response to temperature across growth chambers observed in this study are, however, in contrast with some previous studies that report no significant decline in response with warming (Crous et al., 2018; Dusenge et al., 2021). This could be a mechanism to offset the increase in the limitation of carboxylation capacity at higher temperatures (i.e., due to reduced stomatal conductance) (Dusenge et al.,

2021). Studies have also suggested that warming induced reductions in J_{max}/V_{cmax} could be related to a decline in leaf N allocation towards RuBisCO and the RuBP regeneration process (Hikosaka et al., 2006; Scafaro et al., 2017). However, I did not observe any significant trend in the temperature response of J_{max}/V_{cmax} with leaf N and no significant differences with soil nutrient availability were observed (Table 4.1), indicating the effects of warming induced reductions in enzyme–substrate activity may be stronger than the effect of nutrient availability (Fürstenau Togashi et al., 2018). Furthermore, the slopes in J_{max}/V_{cmax} against T_{leaf}, for the upland *F. brayleyana* and mountaintop *F. oppositifolia* (Table 4.1), were steeper compared to the lower elevation species, indicating that the response of J_{max}/V_{cmax} is generally higher for plants sourced from cooler growth provenance (Aspinwall et al., 2017; Crous et al., 2018). Also, I observed that among the thermal generalists, the upland species had a higher J_{max}/V_{cmax} at lowest T_{leaf}, 15°C, and displayed a steeper decline with increasing T_{leaf} compared to the lower elevation ones. It could be that the seeds sourced from a particular growth provenance may display stronger response to temperatures than from other sites (Crous et al., 2018; Dusenge et al., 2021). In this study the thermal generalist, *F. brayleyana* seeds were sourced from an upland provenance whose soils are generally rich in P (derived from basalt). Further studies may be necessary comparing the temperature response of leaf photosynthetic capacity from widespread plants growing in different rainforest provenances (Crous et al., 2018).

4.4.2 Relationship between phenolics and photosynthetic capacity

I observed a linear increase in the leaf phenolic concentrations with increasing J_{max}/V_{cmax} and the C_i –T across the growth temperature treatments. Under cold chamber T_{growth}, both leaf phenolic concentrations and the gas exchange parameters J_{max}/V_{cmax} and the C_i–T were higher. My interpretation is that low temperature caused an imbalance between J_{max} and V_{cmax}, such that electrons were in excess supply. Evidence of this can be found in the C_i –T. The C_i –T represents the transition point from limitation by RuBisCO to limitation by RuBP regeneration and is an indication of efficient use of both capacities, such that if the point is close to the operating C_i, it would indicate shared use of resources (Farqhuar et al., 1980). A C_i–T higher than the operating C_i would therefore mean higher J_{max} over V_{cmax} and excess electrons from the electron transport chain. In such a scenario, plants generally will have to combat the excess electrons from the electron transport chain by triggering signaling pathways to efficiently eliminate them from the system. This could be achieved by increasing

the production of phenolic compounds (Piluzza and Bullitta, 2011; Karabourniotis et al., 2014). Limited studies to-date have empirically evaluated the effects of photosynthetic capacities on phenolics (Sumbele et al., 2012), but none have reported this in the AWT.

I did not observe a relationship of phenolics with leaf N_{mass}, which contradicts the carbon-nutrient balance hypothesis (Coley et al., 2002). The CNB theory predicts that the investment in carbon-based defensive compounds should increase under conditions of relatively low nitrogen supply by the soil and phenolics primarily play a role in defense against herbivores. Therefore, this study undermines the CNB hypothesis, as have some studies in the literature (Hamilton et al., 2001). For instance, studies have suggested a more mechanistic approach was needed to better understand the investment in plant defense compounds. One such approach was the protein competition model of enzyme-substrate activity, where allocation of foliar phenolics is determined by the total protein demand and the activity of the enzyme phenylalanine ammonia-lyase, which is required for both, protein synthesis and the phenolic production (Jones and Hartley, 1999). Since N is important for protein synthesis, under nutrient (N) limited conditions, one would expect investment of resources on proteins required for growth and carbon fixation over production of phenolics. Thus, our study adds to the justification of the primary role of phenolics as a response to abiotic stressors, such as photo-oxidative stress (Lima-Melo et al., 2019), and only secondarily to herbivory (Close and McArthur, 2002). I also observed a significant correlation between the total leaf phenolics, and the leaf antioxidant capacity as denoted by the antioxidant power (FRAP) from experimental leaf samples (Figure 4.2c) as supporting evidence for their role in counteracting photo-oxidative stress.

4.4.3 Leaf chlorophyll relation with carboxylation capacity and leaf nitrogen

I observed that leaf chlorophyll was positively related to the maximum carboxylation capacity ($V_{cmax-25}$) and maximum electron transport rates at 25°C (J_{max-25}) and increased with leaf nitrogen on an area basis (N_{area}). The role of chlorophyll in electron transport and the co-ordination between the carboxylation capacity is well established in literature, where chlorophyll acts as the light-harvesting pigment in photosynthesis, absorbing the energy required for the carboxylation of CO_2 into organic molecules (Croft et al., 2017; Qian et al., 2021). Studies have found differences in chlorophyll concentrations in relation to leaf N and reported variation among species (Evans, 1989; Qian et al., 2021). With increasing leaf N availability, plants can effectively partition it between photosynthetic and non-photosynthetic

components (Hikosaka et al., 2006; Scafaro et al., 2017), and almost half of the available leaf N is allocated towards the photosynthetic apparatus (Evans, 1989; Hikosaka, 2004). I did see a marginal effect of species on foliar chlorophyll concentration (Table 4.2), but the difference in the soil nutrient availability was much larger than the effect of Species in the study (Figure 4.3a). That the chlorophyll concentration responded in such a way in relation to soil N availability indicates that the soil treatment was sufficient to shift the leaf chemical composition, which makes it even more striking that soil had no effect on leaf phenolic concentrations.

The carboxylation enzyme RuBisCO and the electron transport components are also generally expensive in terms of their investments via leaf nitrogen (Evans, 1989). It is reported that ~25% of leaf N is allocated towards RuBisCO and another 25% towards substrate activity (Evans, 1989), and the remaining fraction is probably involved in structural components of leaves. Although I did not quantify the RuBisCO content in experimental leaves in this study, I observed no significant relation between the $V_{cmax\text{-}25}$ and N_{area} (not shown here). This may be due to the leaf area (or LMA) being somewhat noisier across growth chambers in this study (Singh Ramesh et al., 2023).

4.4.4 Temperature and soil nutrient effects on foliar chlorophyll, phenolics and J_{max}/V_{cmax}

The observations of a strong relation of chlorophyll with leaf N from above were consistent across species (Figure 4.4a & d). Almost all species displayed a significant increase in chlorophyll concentrations under nutrient-rich soils and the trend of leaf N across species and soil nutrient types was similar (Figure 4.4a & d). Soil nutrient availability has a major influence on leaf nutrient content (Gong et al., 2020), and leaf N and P are important for driving foliar photosynthetic machinery (Bahar et al., 2017; Sharwood et al., 2017). Moreover, the three thermal generalists (lower elevation and upland species) were able to increase their N allocation to invest more in chlorophyll with increasing temperatures, whereas the thermal specialist mountaintop restricted species failed to take advantage of increased N availability under warmer growth conditions. This suggests a limited capacity in tropical montane species to utilize and allocate nutrients under climate warming (Vårhammar et al., 2015; Dusenge et al., 2021).

On the other hand, growth temperatures showed a direct and strong negative relationship with respect to leaf phenolics concentrations, which was higher for all species under cold temperatures, with little-to-no effect of soil nutrients. These trends are somewhat

comparable to previous studies on warming effects on phenolic concentrations (Holopainen et al., 2018). However, an increase in phenolic concentrations has also been reported under warmer temperatures (Moreira et al., 2020), and should be carefully considered, because although phenolics concentration in this study do show a negative relation with temperature, specific phenolic compounds like phenolic acids and polyphenols have been reported to increase as a response to heat stress (Wu et al., 2016; Shamloo et al., 2017; Holopainen et al., 2018), supporting the idea that phenolics production is probably more influenced by growth temperatures and is not affected by nutrient availability (Close and McArthur, 2002).

I found that the mountaintop species displayed a tendency to increase phenolics under NR soils, but the other species did not show a significant relation. This may be because of differences in the type of phenolic compounds (e.g., high or low molecular weight phenolics) which were not quantified in this study. This increase under the NR soil type further violates the carbon nutrient balance hypothesis where an increase in phenolics is supposed to be related to lower soil N (Coley et al., 2002). Therefore, the role of phenolics in plant defense against herbivory may only be an added advantage (Bryant et al., 1983; Coley et al., 1985; Coley and Barone, 1996; Moore et al., 2004). Although it is evident from the observations made in my study the role of phenolics in photo-oxidative stress, it does not mean that they can be directly applied to other systems or other species in the tropics. Further studies comparing other co-occurring and widely distributed species may be necessary to see if they follow a similar trend of phenolics with soil nutrient availability.

Studies have pointed out that allocation to foliar phenolics may be regulated by leaf photosynthetic capacities (Sumbele et al., 2012). Although there is no clarity on the exact mechanism behind biochemical investments in relation to foliar phenolic allocation, the current experimental observations show a decline in J_{max}/V_{cmax} ratio with T_{growth} that followed a similar pattern as the decline in phenolics with T_{growth} (Figure 4.4c), validating that the reductions in photosynthetic capacities with warmer temperatures may have influenced differences in allocation to foliar phenolics. The decline in J_{max}/V_{cmax} ratio with T_{growth} could be related to the temperature dependencies of J_{max} and V_{cmax}, which is generally different given the activation energies for J_{max} (at *ca* 50 kJ mol $^{-1}$) and for V_{cmax} (at *ca* 65 kJ mol $^{-1}$) (Medlyn et al., 2002). This would mean that V_{cmax} slows more than J_{max} with increasing elevation in the tropics, and therefore J_{max}/V_{cmax} ratio is higher when measured under cold temperatures. Therefore, photosynthesis becomes progressively more limited by the dark reactions under cold temperatures and can result in an oversupply of electrons from electron

transport leading to production of reactive oxygen species (Lima-Melo et al., 2019). Hence, the decline in phenolic production under the warmer chamber growth temperatures is tightly regulated by the decline in J_{max}/V_{cmax} ratio in this study, indicating that there may be a co-ordination between electron supply relative to demand and growth temperature (Walker et al., 2014).

4.5 Conclusion

Climate change has the potential to alter foliar chemistry, including biochemical compounds that are crucial for both plant growth and defense and central to species' ecological strategies (Karabourniotis et al., 2014; Holopainen et al., 2018; Salazar et al., 2018). This study has shown that the temperature response of leaf photosynthetic capacities among closely related species is strongly affected by warming, over the effects of soil nutrient availability. The difference in allocation of leaf phenolics among species is strongly correlated with leaf photosynthetic capacities. This was seen as an overinvestment of electron transport as indicated by its relationship with the intercellular carbon dioxide transition point. Leaf chlorophyll is mostly driven by leaf N in relation to increased soil nutrient availability. The investment in these components is dependent on species' capacity to utilize available N, that was seen as limited plasticity in allocation for the mountaintop restricted species under experimental warming.

This application of the FvCB model of C_3 plant photosynthesis to better understand the regulation of foliar chemistry is the first of its kind for tree species in the Australian Wet Tropics. Because the response of J_{max}/V_{cmax} ratio to temperature is general to all C_3 plants, the predictions from some of these findings could have fundamental implications for biogeochemical cycling over elevation gradients in tropical rainforests and could play an important role in structuring the herbivore and decomposer communities, with follow-on effects for other trophic levels (Sumbele et al., 2012; Borowiak et al., 2015).

Table 4.1. Summary of a linear mixed effects model of the short-term response of the ratio maximum rate of electron transport to maximum carboxylation rate of RuBisCO (J_{max}/V_{cmax}) for species (n=4) grown in experimental glasshouse conditions under varying Soil type (n=2) and growth temperatures (T_{growth}, n=3). The model was constructed with the response variable as a function of leaf temperatures (T_{leaf}), Soil and T_{growth} as fixed effects with the interactions of T_{leaf} with each of the predictor variables. Individual Pot (leaf) was treated as a random intercept in the model. Significant predictors and p-values are shown in bold.

	J_{max}/V_{cmax}		
Predictors	***Estimates***	***CI***	***p***
(Intercept)	4.01	(3.73, 4.30	**<0.001**
T_{leaf}	-0.07	(-0.08, -0.06)	**<0.001**
Soil [Nutrient Rich]	0.19	(-0.02, 0.39)	0.075
Species [*Flindersia bourjotiana*]	-0.48	(-0.77, 0.39)	**0.001**
Species [*Flindersia brayleyana*]	0.63	(0.33, 0.93)	**<0.001**
Species [*Flindersia oppositifolia*]	-0.16	(-0.43, 0.37)	0.267
T_{growth} **[Ambient]**	-0.39	(-0.64, -0.14)	**0.002**
T_{growth} [Elevated]	0.12	(-0.01, 0.37)	0.361
T_{leaf} *** Soil [Nutrient Rich]**	-0.01	(-0.01, <0.01)	**0.028**
T_{leaf} *** Species [*Flindersia bourjotiana*]**	**0.02**	**(-0.01, 0.03)**	**<0.001**
T_{leaf} * Species [*Flindersia brayleyana*]	-0.01	(-0.02, -0.00)	0.063
T_{leaf} *** Species [*Flindersia oppositifolia*]**	0.01	(0.00, 0.02)	**0.005**
T_{leaf} * T_{growth} [Ambient]	0.01	(-0.00, 0.01)	0.185
T_{leaf} ***** T_{growth} **[Elevated]**	-0.01	(-0.02, -0.00)	**0.005**
Random Effects			
σ^2	0.06		
τ00 Pot	0.04		
ICC	0.39		
N Pot	65		
Observations	356		
Marginal R^2 / Conditional R^2	0.809 / 0.883		

Table 4.2. Summary of linear regressions of total leaf phenolics, chlorophyll, the ratio maximum rate of electron transport to maximum carboxylation rate of RuBisCO (*Jmax*/*Vcmax*) and Nitrogen concentration against *Tgrowth,* Species, and Soil and with the interactions of the predictor variables. Significant *p*-values are shown in bold.

	Phenolics (mg GA g^{-1}DW)			**Chlorophyll (μmol m^{-2})**			***Jmax*/*Vcmax***			**Nitrogen (%)**		
Predictors	***Estimates***	***CI***	***p***	***Estimates***	***CI***	***p***	***Estimates***	***CI***	***p***	***Estimates***	***CI***	***p***
(Intercept)	153.50	(119.35, 187.64)	**<0.001**	116.56	(-7.54, 240.65)	0.065	4.77	(4.28, 5.27)	**<0.001**	1.06	(0.87, 1.25)	**<0.001**
Tgrowth	-1.69	(-3.00, -0.39)	**0.012**	4.71	(-0.04, 9.46)	0.052	-0.11	(-0.13, -0.09)	**<0.001**			
Species [*Flindersia bourjotiana*]	5.32	(-44.01, 54.66)	0.830	14.05	(-165.24, 193.34)	0.876	-0.78	(-1.48, -0.08)	**0.031**	-0.21	(-0.48, 0.06)	0.122
Species [*Flindersia brayleyana*]	106.63	(58.35, 154.92)	**<0.001**	-151.92	(-327.41, 23.57)	0.088	0.24	(-0.46, 0.93)	0.500	-0.07	(-0.34, 0.20)	0.622
Species [*Flindersia oppositifolia*]	32.61	(-15.67, 80.90)	0.182	164.96	(-10.53, 340.45)	0.065	0.34	(-0.36, 1.03)	0.335	0.41	(0.14, 0.68)	**0.003**
Soil [Nutrient Rich]	-11.41	(-27.41, 4.60)	0.159	138.43	(80.25, 196.60)	**<0.001**	–	–		0.30	(0.03, 0.57)	**0.030**
T_{growth} * Species [*Flindersia bourjotiana*]	-1.03	(-2.92, 0.87)	0.282	-0.08	(-6.96, 6.79)	0.980	0.03	(-0.00, 0.05)	0.078	–	–	–
T_{growth} * Species [*Flindersia brayleyana*]	-5.18	(-7.03, -3.33)	**<0.001**	4.10	(-2.62, 10.81)	0.227	-0.00	(-0.03, 0.03)	0.866	–	–	–
T_{growth} * Species [*Flindersia oppositifolia*]	-2.34	(-4.19, -0.49)	**0.014**	-4.87	(-11.58, 1.84)	0.152	-0.01	(-0.03, 0.02)	0.670	–	–	–
Species [*Flindersia bourjotiana*] * Soil [Nutrient Rich]	-8.66	(-31.68, 14.36)	0.455	20.66	(-63.01, 104.33)	0.623	–	–	–	-0.01	(-0.39, 0.38)	0.971
Species [*Flindersia brayleyana*] * Soil [Nutrient Rich]	-4.97	(-27.61, 17.66)	0.662	71.06	(-11.21, 153.33)	0.089	–	–	–	0.44	(0.06, 0.83)	**0.023**
Species [*Flindersia oppositifolia*] * Soil [Nutrient Rich]	36.58	(13.94, 59.22)	**0.002**	-98.12	(-180.39, -15.85)	**0.020**	–	–	–	-0.36	(-0.74, 0.03)	0.067
Observations	71			71			70			71		
R^2 / R^2 adjusted	0.787 / 0.747			0.682 / 0.623			0.891 / 0.879			0.512 / 0.458		

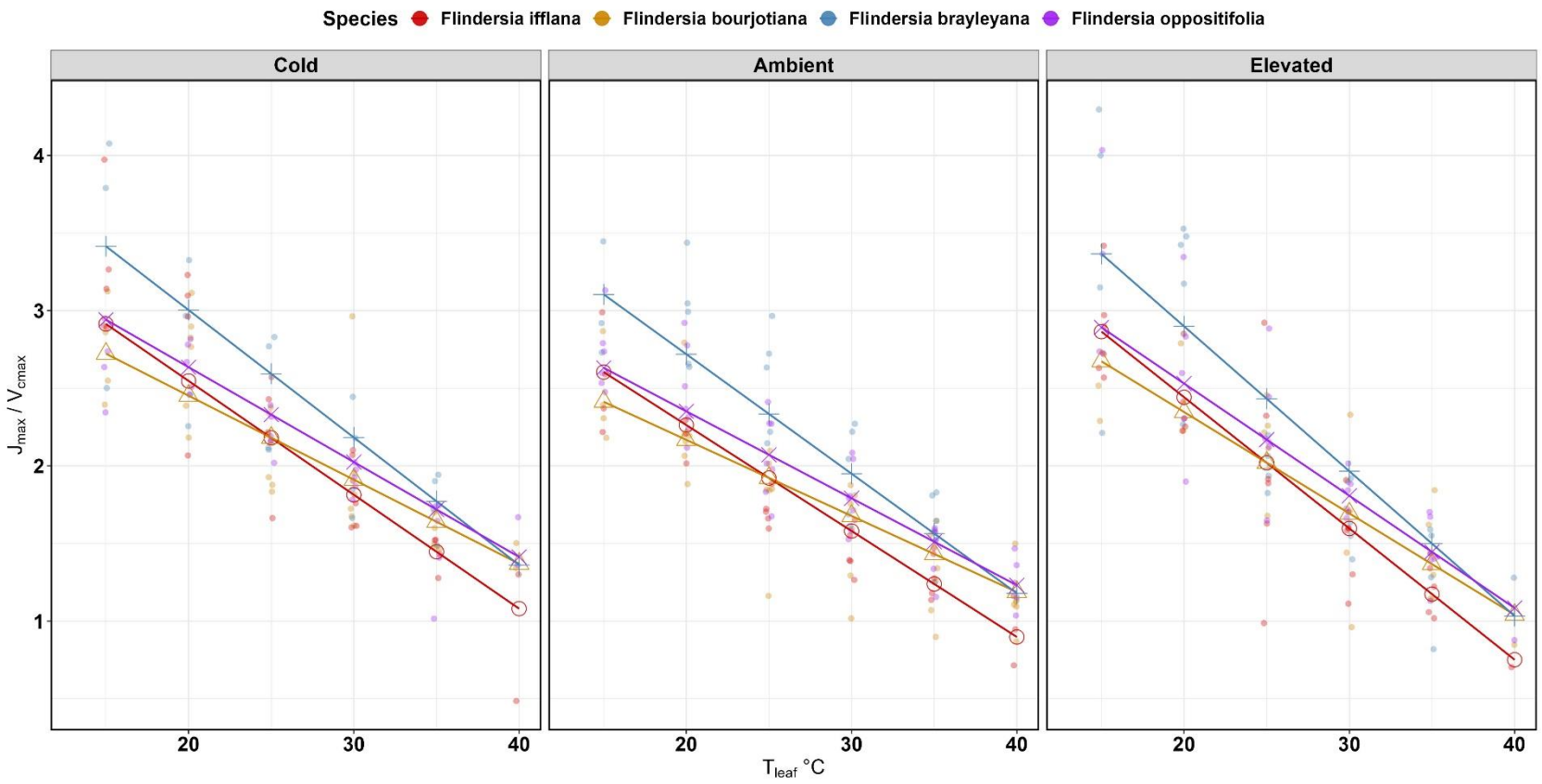

Figure 4.1. A plot of temperature response for the ratio of maximum rate of electron transport to maximum carboxylation rate of RuBisCO (J_{max}/V_{cmax}) against leaf temperatures (T_{leaf} –15, 20, 25, 30, 35, 40°C) from individual pots. Linear regression with predicted values and regression lines for each species are shown, faceted for each of the growth chambers (T_{growth}– Cold, lowland Ambient and Elevated temperatures). Species are shown as Red- lowland tree species, *F. ifflana*; light Orange- mid-elevation tree species, *F. bourjotiana*; Blue- upland tree species, *F. brayleyana*; and Purple- mountaintop restricted tree species, *F. oppositifolia*.

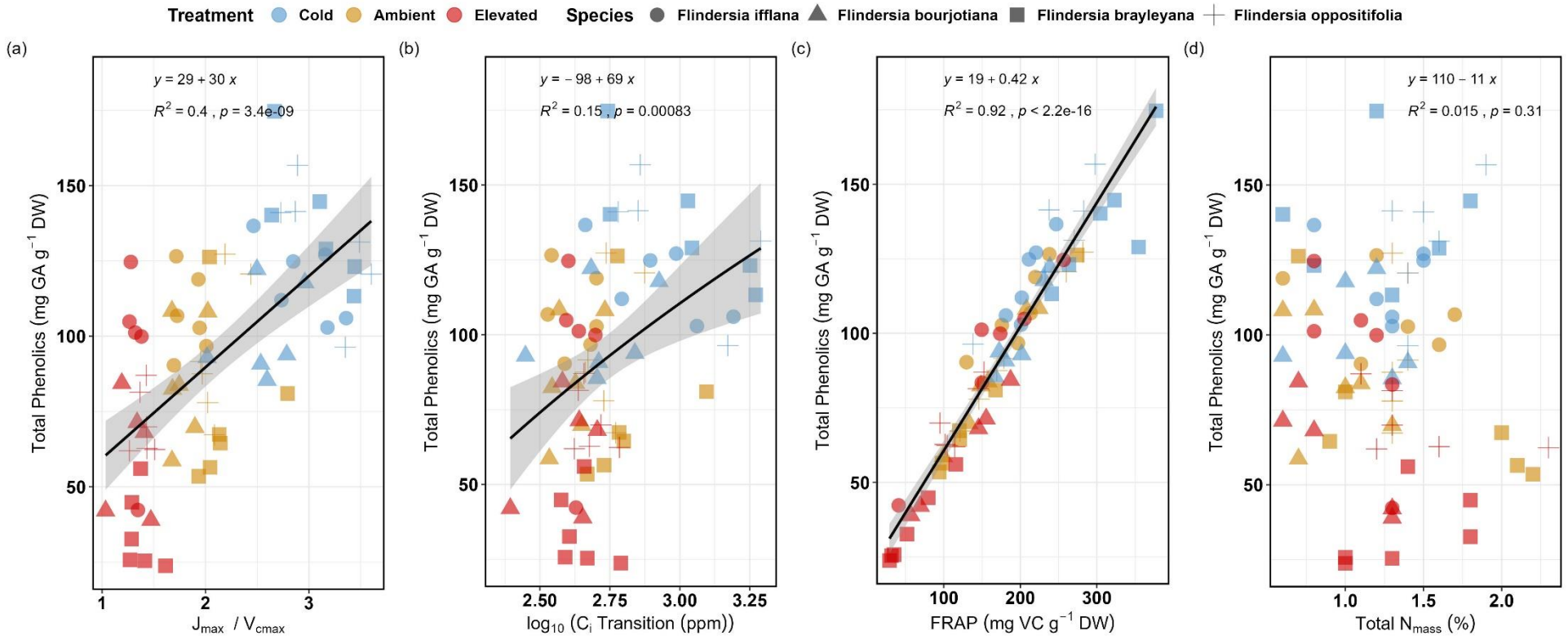

Figure 4.2. Total leaf phenolics concentration from experimental leaf samples plotted against the *Jmax/Vcmax* ratio (a); the intercellular carbon dioxide transition point (C_i–*Transition* on a $\log_{10}$-scale) (b); total leaf Ferric Reducing Ability of Plasma (FRAP) (expressed in mg of Vitamin–C per gram of leaf dry weight) (c); and total leaf nitrogen content (mass basis) (d). Linear regression is shown as a solid black line with 95% CI (light grey). Species are shown as symbols: circle– lowland tree *F. ifflana*; Solid triangle– mid-elevation *F. bourjotiana*; Solid square– upland *F. brayleyana;* and cross–mountaintop restricted *F. oppositifolia.* Each of the T_{growth} chambers are, Cold– Blue, lowland Ambient– light Orange and Elevated temperatures– Red.

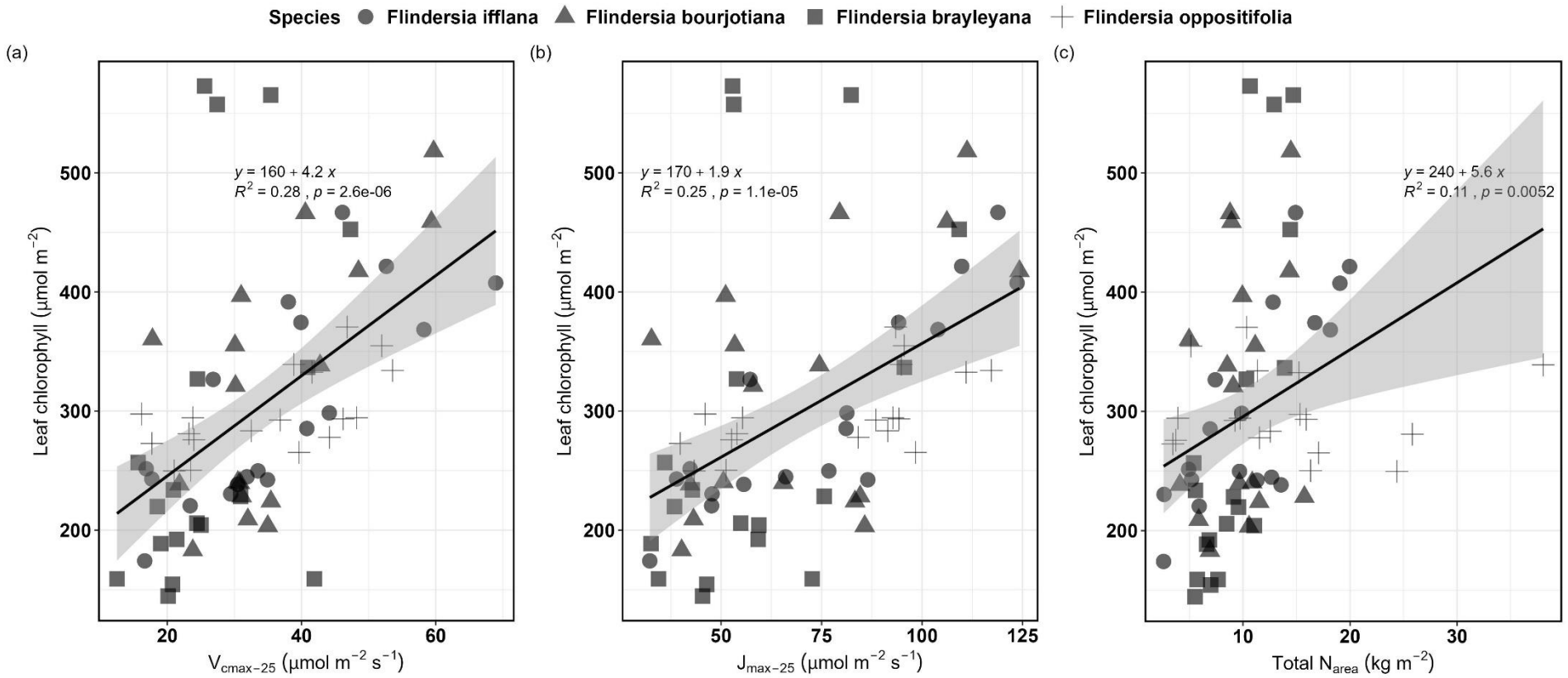

Figure 4.3. The leaf chlorophyll concentration plotted against maximum carboxylation capacity at 25° C (V_{cmax}-*25*) (a); maximum rates of electron transport at 25° C (J_{max}-*25*) (b); and total leaf N (on an area basis) (b). Linear regressions are shown as a solid black line with 95% CI (light grey). Species are shown as symbols: circle- lowland tree *F. ifflana*; Solid triangle- mid-elevation *F. bourjotiana*; Solid square- upland *F. brayleyana*; and cross- mountaintop restricted *F. oppositifolia*.

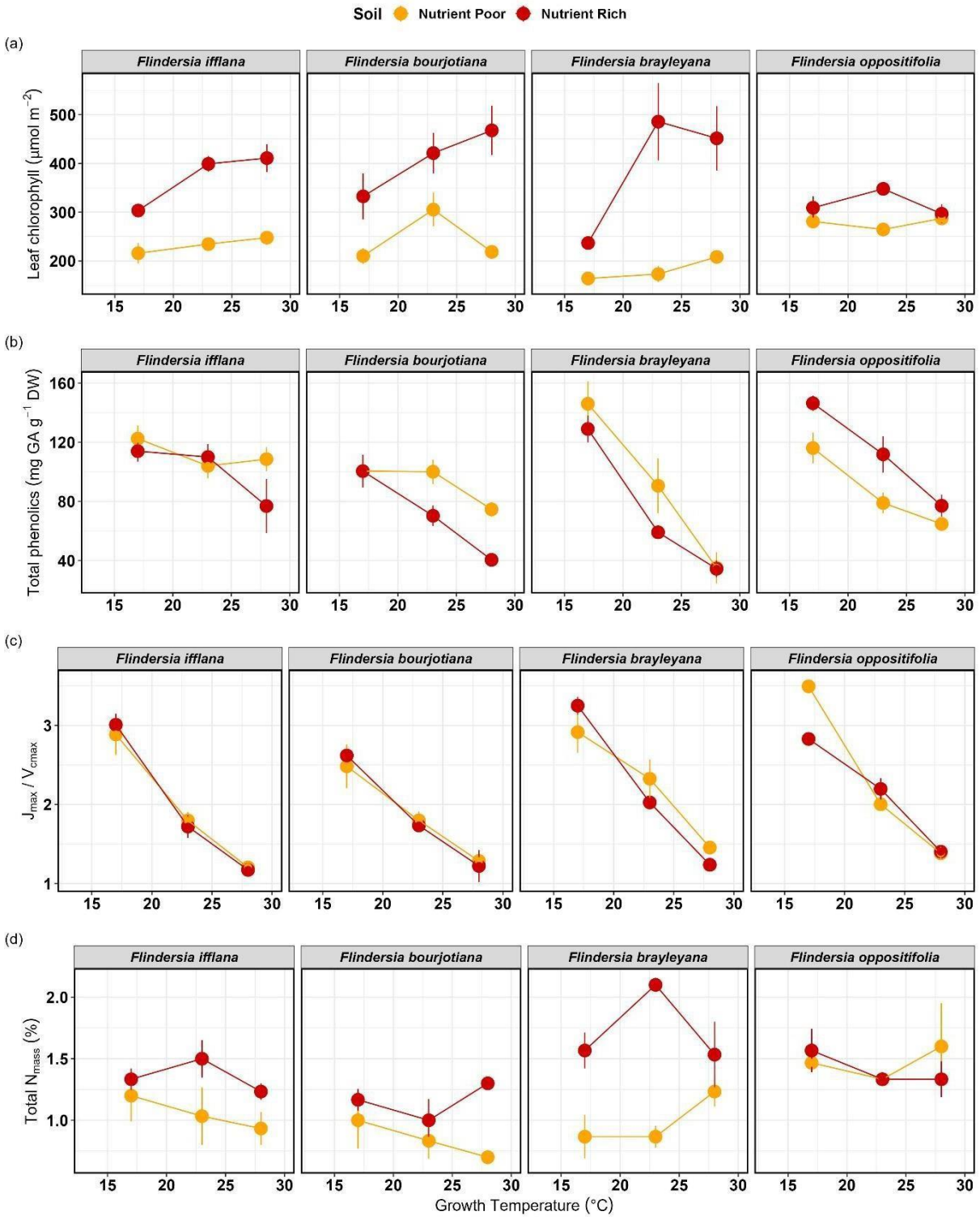

Figure 4.4 Variation in **(a)** leaf chlorophyll concentration; **(b)** leaf phenolics concentration; and **(c)** the J_{max}/V_{cmax} ratio across the experimental growth temperatures; and **(d)** total leaf N_{mass}. *Flindersia* species from left to right are arranged based on their provenance of collection: Lowland, Mid-elevation, Upland, Mountaintop. Data points shown here are from leaves (n=3, means ± SE) from each of the nutrient rich (Red) and nutrient poor soils (light Orange) (shown as a legend on top).

Supplementary Table 4.1. Summary table of means (±SD) rounded to its nearest whole number of total leaf chlorophyll and phenolics concentrations studied from experimental leaf samples (n= 2 - 3) for each species by growth temperature and soil nutrient type combination.

Species	Growth chamber	Soil type	Leaf Chlorophyll (μmol m^{-2})	Leaf Phenolics (mg GA g^{-1} DW)
F. ifflana (lowland) Thermal generalist	**Cold (~17° C)**	**Nutrient Rich**	303 (±21)	114 (±9)
		Nutrient Poor	215 (±36)	122 (±12)
	Lowland ambient (~23° C)	**Nutrient Rich**	399 (±27)	110 (±12)
		Nutrient Poor	234 (±12)	104 (±11)
	Elevated (~28° C)	**Nutrient Rich**	410 (±49)	76 (±25)
		Nutrient Poor	247 (±4)	108 (±11)
F. bourjotiana (mid-elevation) Thermal generalist	**Cold (~17° C)**	**Nutrient Rich**	332(±81)	100 (±12)
		Nutrient Poor	210 (±27)	100 (±15)
	Lowland ambient (~23° C)	**Nutrient Rich**	421 (±71)	70 (±9)
		Nutrient Poor	305 (±59)	100 (±11)
	Elevated (~28° C)	**Nutrient Rich**	467 (±71)	35 (±8)
		Nutrient Poor	218 (±13)	74 (±7)
F. brayleyana (upland) Thermal generalist	**Cold (~17° C)**	**Nutrient Rich**	236 (±18)	129 (±15)
		Nutrient Poor	164 (±22)	146 (±26)
	Lowland ambient (~23° C)	**Nutrient Rich**	485 (±137)	60 (±6)
		Nutrient Poor	173 (±28)	90 (±26)
	Elevated (~28° C)	**Nutrient Rich**	451 (±114)	34 (±8)
		Nutrient Poor	208 (±18)	35 (±15)
F. oppositifolia (mountaintop) Thermal specialist	**Cold (~17° C)**	**Nutrient Rich**	308 (±40)	146 (±8)
		Nutrient Poor	280 (±11)	116 (±15)
	Lowland ambient (~23° C)	**Nutrient Rich**	347 (±19)	111 (±18)
		Nutrient Poor	264 (±25)	78(±12)
	Elevated (~28° C)	**Nutrient Rich**	296 (±33)	77 (±11)
		Nutrient Poor	287 (±8)	65 (±4)

Supplementary Table 4.2. Summary table of means (±SD) of the photosynthetic CO_2 compensation point (Gamma star) and the Michaelis-Menten coefficient (Km) for Farquhar model obtained from each model fit from experimental leaf samples (*n*=3) for each species by growth temperature and soil nutrient type combination.

Species	Growth chamber	Soil type	Gamma Star (*ppm*)	Km (*ppm*)
F. ifflana (lowland) Thermal generalist	**Cold (~17° C)**	**Nutrient Rich**	30.19 (±0.79)	400.9 (±16.8)
		Nutrient Poor	30.43 (±0.46)	405.9 (±9.8)
	Lowland ambient (~23° C)	**Nutrient Rich**	44.04 (±0.05)	746.97 (±0.08)
		Nutrient Poor	30.43 (±0.30)	771.53 (±8.9)
	Elevated (~28° C)	**Nutrient Rich**	63.29 (±0.6)	1375 (±21.7)
		Nutrient Poor	62.64 (±0.30)	1400.31 (±23.8)
F. bourjotiana (mid-elevation) Thermal generalist	**Cold (~17° C)**	**Nutrient Rich**	29.98 (±0.5)	396.4 (±10.4)
		Nutrient Poor	30.4 (±0.24)	404.94 (±5.1)
	Lowland ambient (~23° C)	**Nutrient Rich**	44.22 (±0.5)	752 (±14.6)
		Nutrient Poor	45.02 (±0.7)	775.5 (±20.2)
	Elevated (~28° C)	**Nutrient Rich**	62.05 (±0.6)	1352 (±24.8)
		Nutrient Poor	63.98 (±0.9)	1427 (±36.7)
F. brayleyana (upland) Thermal generalist	**Cold (~17° C)**	**Nutrient Rich**	30.34 (±0.4)	403.94 (±8.3)
		Nutrient Poor	29.92 (±0.12)	395.05 (±2.6)
	Lowland ambient (~23° C)	**Nutrient Rich**	44.04 (±0.0)	746.97 (±0.08)
		Nutrient Poor	44.88 (±0.3)	771.53 (±8.9)
	Elevated (~28° C)	**Nutrient Rich**	62.42 (±0.31)	1366 (±12.0)
		Nutrient Poor	60.89 (±0.76)	1308 (±29.12)
F. oppositifolia (mountaintop) Thermal specialist	**Cold (~17° C)**	**Nutrient Rich**	30.5 (±0.25)	409.21 (±5.4)
		Nutrient Poor	29.80 (±0.2)	392.49 (±4.02)
	Lowland ambient (~23° C)	**Nutrient Rich**	42.92 (±0.21)	715.15 (±6.07)
		Nutrient Poor	42.94 (±0.6)	744.15(±11.42)
	Elevated (~28° C)	**Nutrient Rich**	61.95 (±0.9)	1348 (±34.6)
		Nutrient Poor	63.75 (±83)	1418 (±33.1)

Supplementary Figure 4.1 A. Fruit pods of *Flindersia spp.* – (L – R): *F. bourjotiana* (Mid-elevation), *F. oppositifolia* (Mountaintop), *F. brayleana* (Upland) and *F. ifflana* (Lowland); **B.** Seeds sown on a bed of NR soil; **C.** Seedlings germinated ca. ~2 months since sown; **D.** Glasshouse where temperature-controlled growth experiments were conducted. **E.** Pots containing seedlings of *Flindersia spp.* being studied from one of the growth chambers.

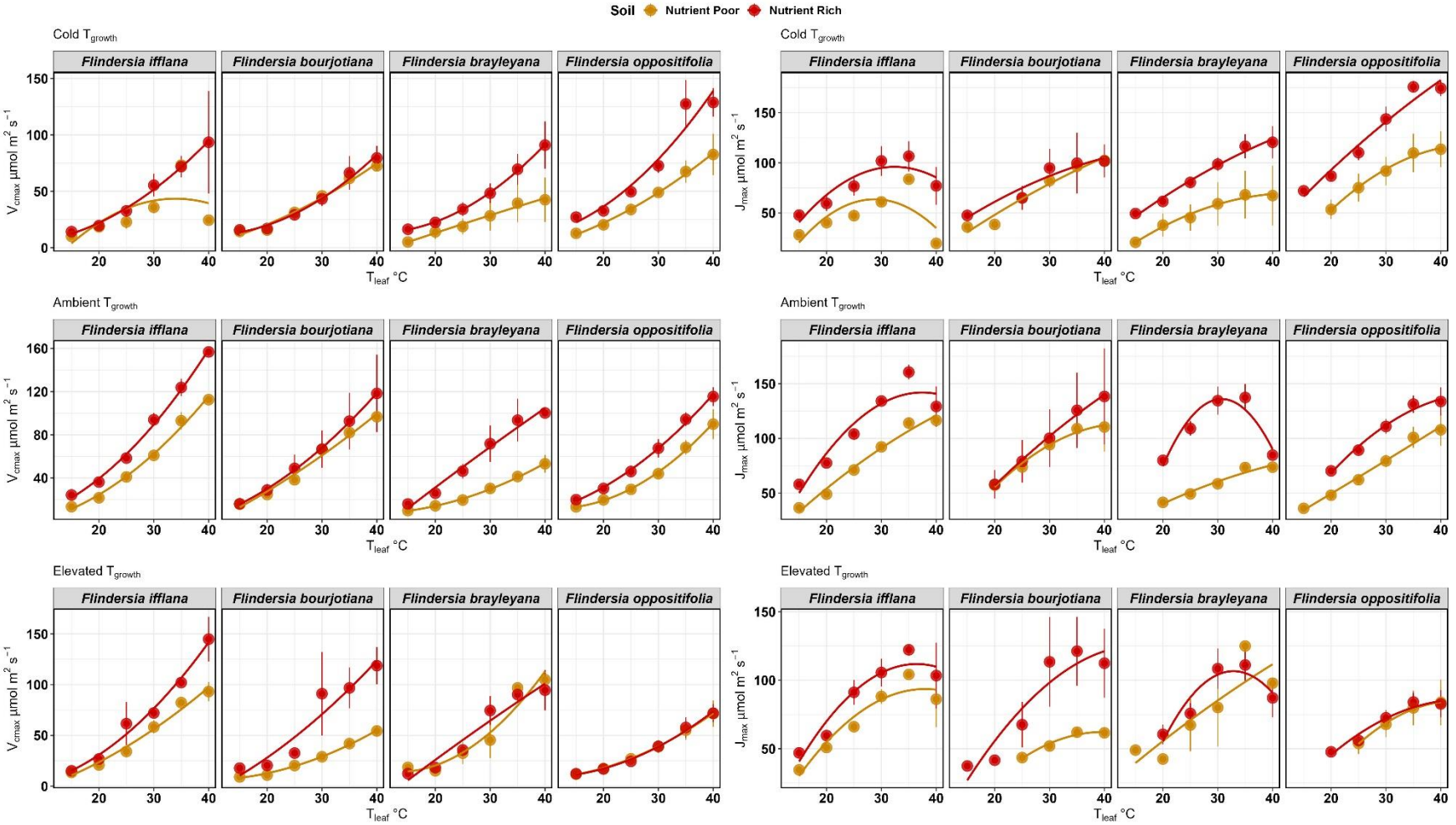

Supplementary Figure 4.2 Temperature response of leaf photosynthetic capacities of the four *Flindersia* spp. from experimental pots. Plots are for maximum carboxylation rate of RuBisCO (V_{cmax}) and maximum rate of electron transport (J_{max}) against leaf temperatures (15, 20, 25, 30, 35, 40°C) from individual pots containing Nutrient Rich (Red) and Nutrient Poor (Orange) soil, with second order polynomial regression lines fitted for each of the two-soil nutrient type. Data points are means (±1SE) from 2-3 pots for each soil nutrient type by growth temperature combination. Growth chambers are of the following order: Top-Cold; Middle-Lowland Ambient; and Bottom- Elevated temperatures. *Flindersia* species from L – R are, Lowland, Mid-elevation, Upland and Mountaintop restricted. Missing data points are for those treatments which showed poor response to leaf temperatures and have been removed from the figure.

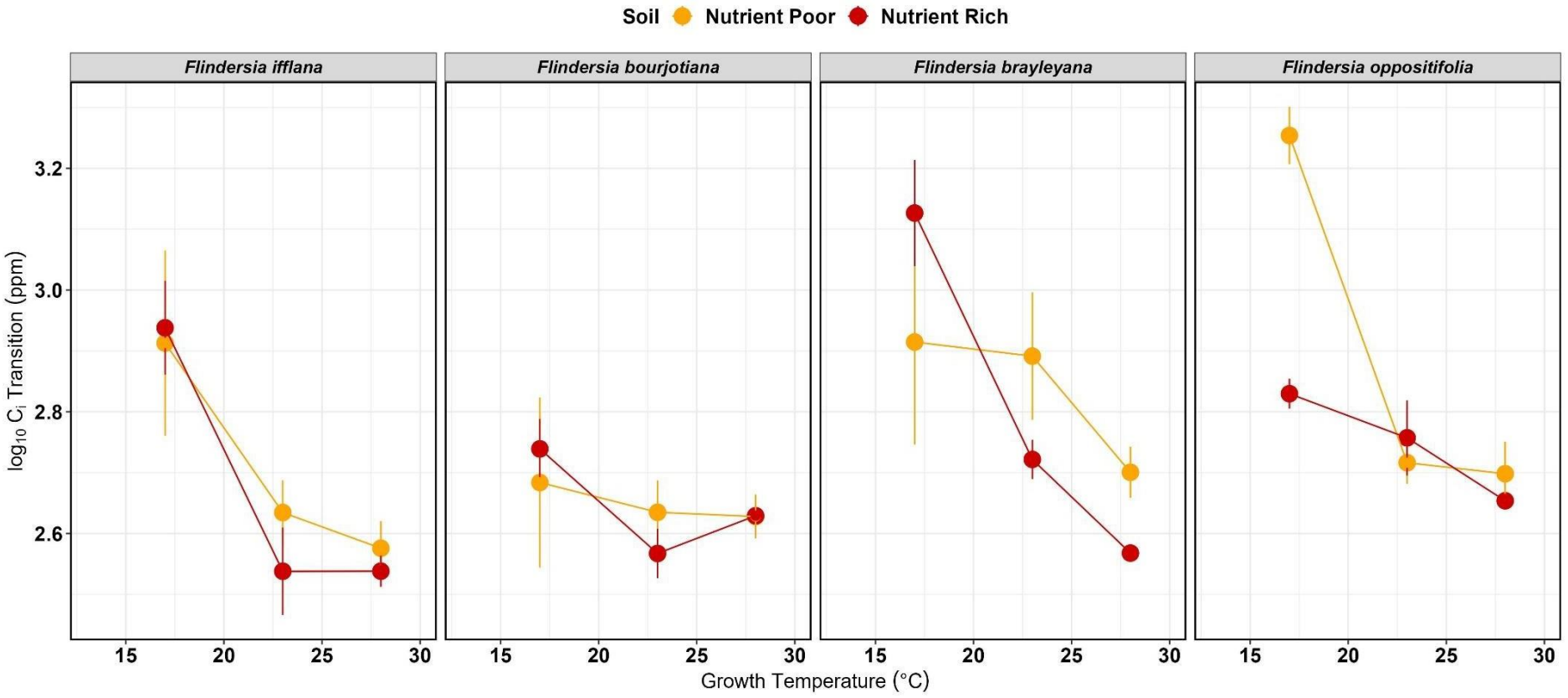

Supplementary Figure 4.3 The intercellular CO_2 transition point (log_{10} scale) obtained from the FvCB model of C_3 photosynthesis from experimental leaf samples plotted against the growth temperatures. Data points are means (±1SE) from 3 pots for each soil nutrient type- Nutrient Rich (Red) and Nutrient Poor (Orange). *Flindersia* species from L – R are, Lowland, Mid-elevation, Upland and Mountaintop restricted.

Chapter – 5: General discussion and concluding remarks

5.1 Study summary

My PhD thesis focused on understanding the effects of elevation, and by extension temperature and soil nutrient availability, on tree growth, physiology and biochemistry among closely related species across the Australian Wet Tropics (AWT) World Heritage Area. I pursued this thesis to understand, a) whether tropical mountaintop restricted tree species are constrained in their distributions by physiological limitations; and b) whether species display an ability to acclimate to climate warming. To test this, I first evaluated, 1) in-situ microclimate (soil, near surface air and above-ground air temperatures) and edaphic properties (soil C:N, pH, organic matter content) to understand how they co-vary with elevation; next 2) I tested how changes in some of these environmental variables (temperature and soil nutrient availability) affect tree growth and leaf functional traits among congeners of the genus *Flindersia* (Rutaceae) along an elevation gradient; and 3) I experimentally evaluated the effects of temperature and soil nutrient availability on plant growth, physiology and biochemistry among four species of *Flindersia*. I focused on tree species of the genus *Flindersia*, as the genus is often a dominant component of forests across the AWT (Bradford et al., 2014), as well as containing congeners that are both widespread and mountaintop restricted. Species such as *F. oppositifolia* occupy a narrow thermal niche space and are threatened by future climate change (Costion et al., 2015).

5.1.1 Microclimate and soil nutrient availability in the Australian Wet Tropics

In Chapter 2, I studied trends in long term microclimate and topsoil nutrients, soil organic matter content and soil $\delta^{15}N$ stable isotope composition from across an elevation gradient in the AWT. Here I found differences in the slopes of soil and above ground air temperatures with elevation such that air temperatures declined at a steeper rate with elevation. I observed that this decline resulted in a temperature difference between soil-to-air ($\Delta T_{soil-air}$) that also changed across elevation in a linear fashion. Soils in the lower elevation sites were cooler and soils in the upland and mountaintop sites were warmer than above-ground air. I then observed that the bioclimatic variables such as temperature seasonality and the diel and annual temperature ranges also increased along the elevation profile and were higher for air compared to soils. Finally, I found that soil pH and $\delta^{15}N$ declined with elevation, whereas soil C:N ratio and organic matter content increased with elevation.

It has been reported previously from studies involving global soil temperature datasets that unlike temperate forests, where soil temperatures are higher by several degrees than air temperature, tropical rainforest soils can track the air temperatures and are either marginally cooler or warmer depending on the landscape conditions (Lembrechts et al., 2021). Although the difference in mean $\Delta T_{soil-air}$ went from negative to positive with increasing elevation, they are not that large a difference in biological terms (a range from -0.25°C to *ca* +0.26°C). The DTR and ATR on the other hand are probably more important bioclimatic predictor variables because of their concerted effects on key ecophysiological processes (Goulden et al., 2004; Vargas and Allen, 2008). For instance, fluctuations in DTR and ATR can impact plant growth, phenology and affect the CO_2 exchange, i.e., by altering stomatal activity in response to VPD in the daytime and or by increasing the magnitude of night-time respiration rates (Goulden et al., 2004; Grossiord et al., 2020). Studies have also found evidence on how DTR affects the biological activity of other life forms (Vallejo-Vargas et al. 2022). Therefore, paired studies of these bioclimatic variables with key ecological processes such as photosynthesis, respiration and phenological changes will be necessary to better understand how biological systems would respond to climatic fluctuations in the long-term.

The temperature difference in soil and air along elevation in this study has not been reported previously from the AWT. In the first instance, I surmised that this trend may be related to a change in tree basal area with elevation (Figure 2.6F). It could be that the basal area increase may have influenced below canopy air temperatures (Pfeifer et al., 2018) causing the air temperatures at higher elevation sites to be sufficiently cooler. However, this did not explain why mountaintop soils were warmer than air. It could have been driven by higher light levels on tropical mountaintop sites. For example, in the lower elevation sites taller canopy can intercept light and limit excess light levels reaching the ground to warm-up the soils (Pfeifer et al., 2018), whereas vegetation at higher elevation sites are generally characterized by short-statured canopy, and often thinned due to higher wind allowing sufficient light to enter the ground (Fahey, 2015). One possible explanation for this was also observed based on the soil thermal properties, i.e., montane soils that had a higher organic matter content were sufficiently warmer (Supplementary Figure 2.B) and this may have influenced the soil heat flux in the system (Abu-Hamdeh and Reeder, 2000; Schjønning, 2021). These observations warrant detailed investigations involving paired microclimate data with tree canopy cover/architecture, light levels, soil texture, and other parameters

related to energy balance that are required to confirm the trends in microclimate with elevation.

I then observed that there are interactions in climate and edaphic variables such as soil pH, C:N ratio and organic matter content in a co-ordinate space on the PCA. It is important to consider these interactions moving forward, because they reflect key ecological processes at the land-atmosphere interface that have implications under future climate change (Wang et al., 2016; Misra, 2020). For instance, soil mineralization, organic carbon decomposition and nutrient cycling processes are sensitive to temperatures (Schuur and Matson, 2001; Salinas et al., 2011). This is partly because of its effects on microbial decomposer communities that are adapted to cooler temperatures and limited nitrogen soils in topical montane ecosystems (Nottingham et al. 2015; Salinas et al., 2011). Therefore, studies on how microbial communities change with increasing elevation in the AWT may be interesting – especially given the gradient in microclimate and soil nutrient availability that were observed in this thesis.

Overall, this chapter found that the microclimate and soil nutrient availability change with elevation, and it is important to consider the soil heterogeneity, the diel temperature ranges and the difference in $\Delta T_{soil-air}$ when studying below-canopy ecological process (e.g., seed dormancy, germination, sapling growth) in these sites. Lastly, the microclimate recorded from this chapter (Singh Ramesh et al., 2022) could potentially be used to improve species distribution models especially for tropical montane species given that they capture species' microclimatic niche at a much higher spatiotemporal resolution and can aid forecasting microclimate in the context of climate change.

5.1.2 Plant growth and biomass allocation strategies with warming

Given an understanding of trends in both microclimate and edaphic properties across elevation in the AWT, I sought to test the independent and combined effects of growth temperatures and soil nutrient availability on species' growth and leaf functional traits among closely related species in Chapter 3. Here, I first investigated trends in stem diameter growth rates (GR) and leaf traits such as the LMA, and foliar stable $\delta^{13}C$ and $\delta^{15}N$ from *Flindersia* species along an elevation gradient in the AWT. In the field I found that the GR and foliar $\delta^{15}N$ declined with elevation whereas LMA and $\delta^{13}C$ increased with elevation. Studies in tropical rainforests have observed related differences in tree growth and leaf functional traits among closely related species with elevation (Liu et al., 2007; Rapp et al., 2012); these trends could result from at least three important drivers: decreasing temperatures, decreasing soil nutrient availability, and changes in species composition along the gradient (Malhi et al.,

2010; Rapp, 2010).

I then conducted a glasshouse experiment on saplings of *Flindersia* species germinated from seeds sourced from various sites along the elevation gradient in the AWT (Supplementary Table 3.1) and tested the effects of growth temperature and soil nutrients on plant growth and leaf traits in isolation from other environmental variables. The experimental saplings displayed a stronger response in plant relative growth rates (RGR) for species with lowland habitat preference, i.e., RGR was higher in NR soils and increased with warmer growth temperatures, indicating the ability to utilize nutrients for growth with warming. On the other hand, upland and mountaintop restricted species displayed optimal growth under ambient growth temperatures, but then declined under Elevated (warmer) growth temperatures. Such observations align with previous studies in the Neotropics that have observed acclimation to warmer growth temperatures in lowland plants (Cheesman and Winter, 2013; Slot et al., 2018), but limited thermal acclimation has been reported in some mountaintop plants under warmer temperatures (Vårhammar et al., 2015; Dusenge et al., 2021). Although this suggests that mountaintop tree species may be negatively affected by warming, there could be potential for *ex-situ* conservation of tropical mountaintop plants under lowland growth temperatures given that their growth did not decline under those conditions. However, there are other environmental factors such as increasing atmospheric water stress (Bauman et al., 2022b) and biotic interactions that may negatively impact survival of such mountaintop endemic plants (Cheesman and Winter, 2013). Further studies that involve transplanting of montane species to lowland sites would be helpful to address these outstanding questions.

Next, I found differences in the biomass allocation among species across growth chambers. For example, the tropical mountaintop species displayed the highest root-to-shoot biomass ratio (R:S) under nutrient poor and cold growth temperatures – conditions approximating the tropical montane provenance. The relatively higher allocation of biomass to roots in mountaintop plants is indicative of an adaptive functional strategy towards shallow soils and physical support from strong winds, in addition to nutrient foraging (Körner, 2007; Girardin et al., 2010; Wu et al., 2013). These observations suggest that *F. oppositifolia* has an added advantage to compete successfully in the mountaintop environment, which was not observed in the lowland species in the glasshouse under similar growth conditions.

Foliar $\delta^{13}C$ isotopic composition of experimental plants compared with those observed in field showed a different relationship to that observed for temperature. The variation of foliar $\delta^{13}C$ in the experiments showed an increasing trend with VPD to suggest that this could be driven due to stomatal response to VPD (Grossiord et al., 2020), i.e., it may

have caused a lower c_i/c_a resulting in an enrichment in $\delta^{13}C$ with increasing VPD (Cernusak et al., 2013). However, the VPD in the field is lower at higher elevation sites, indicating that the effect of VPD may not be enough to overcome the response in foliar $\delta^{13}C$ driven by other factors that co-vary with elevation. Other driving factors in the field that did not occur in the glasshouse, such as the decrease in atmospheric pressure that accompanies an increase in elevation, could have resulted in enrichment in foliar $\delta^{13}C$ in the field. The ^{13}C discrimination is less mechanistically understood in relation to atmospheric pressure, but it is known that a decrease in oxygen partial pressure in the chloroplast can increase the efficiency of carboxylation (Farquhar and Wong, 1984), which may further decrease discrimination against ^{13}C.

For foliar $\delta^{15}N$ under glasshouse conditions I observed differences consistent with field-based trends, i.e., an increase with growth temperature. These trends are related in part to a decline in $\delta^{15}N$ of soil nitrogen with elevation (Wang et al., 2019) that was observed in Chapter 2, and I found some evidence of such a relationship in this Chapter (Supplementary Figure 3.5). It is important to note here that the experimental differences reflect just a snapshot of the plant nutrient acquisition strategy based on the available soil N, whereas the trends observed in the field reflect the ecosystem nitrogen pool that would have developed from nutrient cycling processes integrated over millennia (Craine et al., 2015). In the field, enrichment of $\delta^{15}N$ in leaves at warmer, lowland sites suggests that there is a more open nitrogen cycle, where nitrogen loss pathways discriminate against the heavier isotope. The decline in foliar $\delta^{15}N$ with elevation in the AWT suggests a slowing and tightening of the nitrogen cycle with increasing elevation. This could be a key driver of the decreasing tree growth rates with elevation that I observed in the field.

Finally, I observed that upland species displayed a steeper increase in foliar $\delta^{15}N$ with growth temperature compared to the lowland species. The upland species could have also evolved to function in conditions of relatively low nitrogen availability and lacked the capacity to utilize nitrogen to the same extent as lowland ones in response to the warmer growth temperatures. There could also be soil microbes controlling $\delta^{15}N$ soil transformations that can lead to nitrogen isotope fractionations (Houlton et al., 2006; Pajares and Bohannan, 2016; Hestrin et al., 2019) and these observations may warrant investigations on the soil microbiome in the AWT.

Overall, in this chapter I found new insights into how temperature and soil nutrient availability alter species-specific growth and leaf trait responses in response to elevation. I found that the functional strategy of *Flindersia oppositifolia* in mountaintop sites is probably based on the proportionally larger investment in root biomass allocation which may be

adaptive in the nutrient poor soils and high wind loads typical of these landscapes (Körner, 2003). In addition to the above observations, I found that some of the variation in leaf traits, related to foliar $\delta^{13}C$, is probably driven by other environmental factors, such as atmospheric pressure, that were not replicated in the glasshouse.

5.1.3 Leaf photosynthetic capacities and foliar chemistry with warming

In Chapter 4, I evaluated the temperature response of leaf photosynthetic capacities and studied its relationship with foliar chemistry, i.e., leaf chlorophyll and phenolics concentrations. I used the same experimental set-up and *Flindersia* species as in Chapter-3. For discussion purposes here I refer to the three *Flindersia* species with wide elevational ranges as thermal generalists, and the mountaintop restricted species (*F. oppositifolia*) as a thermal specialist.

I first studied the leaf temperature response of photosynthetic capacities, i.e., the maximum carboxylation capacity of the enzyme RuBisCO (V_{cmax}), and the maximum rates of electron transport (J_{max}), by fitting the FvCB model of C_3 photosynthesis to net photosynthesis (A_n) and carbon dioxide concentration (C_i) curves. I observed that the ratio of J_{max}/V_{cmax} declined with increasing leaf temperature and with differences in the slopes for plants grown at warmer temperatures. There were also differences among *Flindersia* species observed in this response.

Next, I quantified leaf chlorophyll and soluble phenolics concentration on those experimental leaves. I found that the temperature response of J_{max}/V_{cmax} and the intercellular carbon dioxide transition point (C_i–T) from V_{cmax} limitation to J_{max} limitation was positively related to foliar phenolics concentration. There was no response of phenolics to leaf nitrogen concentration. On the other hand, I observed that the leaf chlorophyll concentrations were positively related to the $V_{cmax\text{-}25}$ and $J_{max\text{-}25}$ at 25°C and increased with leaf N_{area}. Finally, under experimental growth temperature conditions I found that the chlorophyll increased with increasing nutrient availability and displayed plasticity in its allocation for thermal generalists, whereas it showed limited plasticity in the mountaintop restricted thermal specialist. The response of phenolic concentrations to experimental growth temperatures went in the opposite direction, i.e., declined strongly with warming for all species. The J_{max}/V_{cmax} ratio across chamber growth temperatures followed a similar response as the phenolic concentrations.

The J_{max} and V_{cmax} each respond rather differently to temperatures (Supplementary Table 4.3); V_{cmax} has a steeper response to temperature compared to J_{max} and is possibly driven by the constraints of carboxylation capacity to low temperatures, i.e., due to the

activity of the enzyme RuBisCO (Sage and Kubien, 2007). The relation of phenolics with both temperature and leaf photosynthetic capacities could be a result of abiotic stress from excess electrons. The theory behind this response is related to the co-ordination in the investment in J_{max} and V_{cmax}, such that resources have been optimally shared between them (Maire et al., 2012). In this case a higher C_i–T would indicate an overinvestment in J_{max} and this could have resulted in excess electrons in the system that has triggered secondary metabolic pathways to produce higher leaf phenolic concentrations, which function as antioxidants, to deal with reactive oxygen species caused by excess electrons (Piluzza and Bullitta, 2011; Karabourniotis et al., 2014). This was further confirmed by the strong correlations in the response of foliar phenolics and antioxidant capacity (Figure 4.2c).

Studies have argued that increase in foliar phenolics could be driven by abiotic stress in species' ecological niches, such as cooler growth temperatures, increased light (UV-B radiation), low soil nutrients and increased herbivory (Coley et al., 2002; Alonso-Amelot et al., 2007; Chen et al., 2013; Abdala-Roberts et al., 2016; Schneider et al., 2019). Since there was no response to soil nutrients or leaf N in foliar phenolics, the results of this study are not consistent with the carbon-nutrient balance hypothesis (CNB) (Coley et al., 2002), which would predict an increase in phenolics under nutrient poor conditions. We can safely disregard the popular CNB hypothesis and move on to a more mechanistic approach as emphasized in some studies (Hamilton et al., 2001). For instance, I found that the leaf photosynthetic capacities (J_{max}/V_{cmax}) followed a similar decline to phenolics with warmer growth temperatures. As discussed above, this could be due to the influence of J_{max} in driving higher phenolics allocation because of the increase in electron transport rates at cooler growth temperatures triggering production of secondary metabolites, such as phenolics (Piluzza and Bullitta, 2011; Karabourniotis et al., 2014). Such observations on the allocation of foliar phenolics with plant biochemistry and its effects on temperature and soil nutrient availability have not been reported previously from tropical rainforest trees in the AWT, although independent effects of phenolics as defense compounds have been established (Parsons et al., 2014).

Overall, some of the empirical observations in this chapter suggest that in the tropics, plants growing at higher elevations invest more in phenolics as defense compounds primarily against abiotic stress (as antioxidants as seen in my study), and secondarily against biotic stressors (such as against herbivory), as has been documented in the literature (Coley et al., 2002). If these results are extrapolated to native rainforest trees in the AWT, I would expect leaf herbivory to increase with temperature, making mountaintop restricted species potentially more vulnerable to climate warming.

5.2 Future research

My thesis has tested the effects of temperature and soil nutrients on the response on tropical mountaintop tree species, *F. oppositifolia* and found how they are limited in their growth and physiology that may restrict them to these narrow environmental gradients.

Future research should focus on whether this type of response holds true to other co-occurring taxa in the montane ecosystem. And, if so, what is the extent of adaptation and acclimation of these taxa in relation to these environmental cues. Next, it would be useful to understand in-situ responses of plant growth, physiology and biochemistry by conducting transplant experiments of mountaintop restricted and widely distributed *Flindersia* species across various sites along the elevation profile to evaluate the effects of other environmental drivers that could not be reproduced in the glasshouse (such as sunlight, atmospheric pressure, water availability, and biotic interactions). For example, the AWT bioregion has been forecasted to experience rising VPD, which would lead to increased drought. Under such weather conditions, what are the functionally important plants that can tolerate drought should be a major focus. Finally, a study focusing on soil microbial communities and paired warming experiments with tree species will be useful to better evaluate plant-soil interactions along the gradient. This kind of approach will be useful to unravel functionally important species that can be of potential use for future conservation planning of the tropical mountaintops and will open further opportunities on the limited knowledge on tropical tree responses to elevation in these fragile ecosystems.

5.3 Concluding remarks

Tropical montane ecosystems are highly vulnerable to climate change and species restricted to the wet tropical mountaintops are thought to be at risk under projected warming (Costion et al., 2015).

My thesis has shown how variation in microclimate and soil nutrient availability is important in the AWT. I showed in this thesis that there are differences in the temperature trends such as diel and annual temperature ranges and temperature seasonality and differences in the soil-to-air temperatures with elevation. I also found that the soil pH, C:N and organic matter content co-vary with elevation and that there are interactions among climate and edaphic properties that are important to consider in future studies when using elevation as a proxy in the AWT.

My investigation of the effects of temperature and soil nutrient availability on a regionally

important genus, *Flindersia*, has revealed differences in species' ecological strategies. I observed changes in plant growth, biomass allocation and leaf trait variation among closely related species that were not previously reported from the AWT. In addition, I found that there are other important factors that vary with elevation (VPD, atmospheric pressure) that have effects on plant growth and leaf traits and need be considered while using elevation as a proxy for climate change experiments.

Next, I was able to bridge the gap in understanding the temperature response of plant physiological limitations in tropical mountaintop restricted species in AWT, by evaluating its

leaf photosynthetic capacity using the FvCB model that was not well established in previous literature. In addition to the above, I found evidence of its relationship with foliar chemistry – an important feature that has not been recognized in previous literature and opens new opportunities in developing climate change effects on tree responses in tropics. Finally, the limited growth and plasticity in allocation of foliar chemistry that I observed adds to the body of evidence indicating that tropical mountaintop species are at heightened risk from climate change impacts and require urgent conservation efforts.

Bibliography

Abdala-Roberts, L., Rasmann, S., Berny-Mier Y Terán, J.C., Covelo, F., Glauser, G., and Moreira, X. (2016). Biotic and abiotic factors associated with altitudinal variation in plant traits and herbivory in a dominant oak species. *American Journal of Botany* 103**,** 2070-2078.

Abu-Hamdeh, N., and Reeder, R. (2000). Soil thermal conductivity effects of density, moisture, salt concentration, and organic matter. *Soil Science Society of America Journal* 64**,** 1285-1290.

Alonso-Amelot, M.E. (2008). High altitude plants, chemistry of acclimation and adaptation. *Studies in Natural Products Chemistry* 34**,** 883-982.

Alonso-Amelot, M.E., Oliveros-Bastidas, A., and Calcagno-Pisarelli, M.P. (2007). Phenolics and condensed tannins of high altitude *Pteridium arachnoideum* in relation to sunlight exposure, elevation, and rain regime. *Biochemical Systematics and Ecology* 35**,** 1-10.

Alonso-Rodríguez, A.M., Wood, T.E., Torres-Díaz, J., Cavaleri, M.A., Reed, S.C., and Bachelot, B. (2022). Understory plant communities show resistance to drought, hurricanes, and experimental warming in a wet tropical forest. *Frontiers in Forests and Global Change***,** 142.

Amundson, R., Austin, A.T., Schuur, E.A., Yoo, K., Matzek, V., Kendall, C., Uebersax, A., Brenner, D., and Baisden, W.T. (2003). Global patterns of the isotopic composition of soil and plant nitrogen. *Global Biogeochemical Cycles* 17**,** 1-5.

Apgaua, D.M., Tng, D.Y., Forbes, S.J., Ishida, Y.F., Vogado, N.O., Cernusak, L.A., and Laurance, S.G. (2019). Elevated temperature and CO_2 cause differential growth stimulation and drought survival responses in eucalypt species from contrasting habitats. *Tree Physiology* 39**,** 1806-1820.

Ashton, L., Odell, E., Burwell, C., Maunsell, S., Nakamura, A., McDonald, W., and Kitching, R. (2016). Altitudinal patterns of moth diversity in tropical and subtropical Australian rainforests. *Austral Ecology* 41**,** 197-208.

Aspinwall, M.J., Vårhammar, A., Blackman, C.J., Tjoelker, M.G., Ahrens, C., Byrne, M., Tissue, D.T., and Rymer, P.D. (2017). Adaptation and acclimation both influence photosynthetic and respiratory temperature responses in *Corymbia calophylla*. *Tree Physiology* 37**,** 1095-1112.

Bader, M.Y., Rietkerk, M., and Bregt, A.K. (2007). Vegetation structure and temperature regimes of tropical alpine treelines. *Arctic, Antarctic, and Alpine Research* 39**,** 353- 364.

Bahar, N.H.A., Ishida, F.Y., Weerasinghe, L.K., Guerrieri, R., O'sullivan, O.S., Bloomfield, K.J., Asner, G.P., Martin, R.E., Lloyd, J., Malhi, Y., Phillips, O.L., Meir, P., Salinas, N., Cosio, E.G., Domingues, T.F., Quesada, C.A., Sinca, F., Vega, A.E., Ccorimanya, P.P.Z., Aguila-Pasquel, J., Huaypar, K.Q., Torres, I.C., Loayza, R.B., Tapia, Y.P., Ovalle, J.H., Long, B.M.,

Evans, J.R., and Atkin, O.K. (2017). Leaf-level photosynthetic capacity in lowland Amazonian and high-elevation Andean tropical moist forests of Peru. *New Phytologist* 214**,** 1002-1018.

Baltzer, J.L., Thomas, S.C., Nilus, R., and Burslem, D.F.R.P. (2005). Edaphic specialization in tropical trees: physiological correlates and responses to reciprocal transplantation. *Ecology* 86**,** 3063-3077.

Bauman, D., Fortunel, C., Cernusak, L.A., Bentley, L.P., Mcmahon, S.M., Rifai, S.W., Aguirre-Gutiérrez, J., Oliveras, I., Bradford, M., and Laurance, S.G. (2022a). Tropical tree growth sensitivity to climate is driven by species intrinsic growth rate and leaf traits. *Global Change Biology* 28**,** 1414-1432.

Bauman, D., Fortunel, C., Delhaye, G., Malhi, Y., Cernusak, L.A., Bentley, L.P., Rifai, S.W., Aguirre-Gutiérrez, J., Menor, I.O., Phillips, O.L., Mcnellis, B.E., Bradford, M., Laurance, S.G.W., Hutchinson, M.F., Dempsey, R., Santos-Andrade, P.E., Ninantay-Rivera, H.R., Chambi Paucar, J.R., and McMahon, S.M. (2022b). Tropical tree mortality has increased with rising atmospheric water stress. *Nature* 608**,** 528–533.

Baumgartner, S., Bauters, M., Barthel, M., Drake, T.W., Ntaboba, L.C., Bazirake, B.M., Six, J., Boeckx, P., and Van Oost, K. (2021). Stable isotope signatures of soil nitrogen on an environmental–geomorphic gradient within the Congo Basin. *SOIL* 7**,** 83-94.

Bellingham, P.J., and Tanner, E.V.J. (2000). The influence of topography on tree growth, mortality, and recruitment in a tropical montane forest. *Biotropica* 32**,** 378-384.

Ben-Shachar, M.S., Makowski, D., Lüdecke, D., Kelley, K., and Stanley, D. (2021). "Package 'effectsize'" in R.

Bendix, J., Homeier, J., Cueva Ortiz, E., Emck, P., Breckle, S.W., Richter, M., and Beck, E. (2006). Seasonality of weather and tree phenology in a tropical evergreen mountain rain forest. *International Journal of Biometeorology* 50**,** 370-384.

Benzie, I.F.F., and Strain, J.J. (1996). The Ferric Reducing Ability of Plasma (FRAP) as a Measure of "Antioxidant Power": The FRAP Assay. *Analytical Biochemistry* 239**,** 70- 76.

Booth, T.H. (2018). Why understanding the pioneering and continuing contributions of BIOCLIM to species distribution modelling is important. *Austral Ecology* 43**,** 852-860.

Borowiak, K., Gąsecka, M., Mleczek, M., Dąbrowski, J., Chadzinikolau, T., Magdziak, Z., Goliński, P., Rutkowski, P., and Kozubik, T. (2015). Photosynthetic activity in relation to chlorophylls, carbohydrates, phenolics and growth of a hybrid *Salix purpurea× triandra× viminalis* 2 at various Zn concentrations. *Acta Physiologiae Plantarum* 37**,** 1-12.

Bowman, D.M.J.S., and Mcdonough, L. (1991). Tree species distribution across a seasonally flooded elevation gradient in the Australian monsoon tropics. *Journal of Biogeography* 18**,** 203-212.

Bradford, M.G., Metcalfe, D.J., Ford, A., Liddell, M.J., and McKeown, A. (2014). Floristics, stand structure and aboveground biomass of a 25-ha rainforest plot in the wet tropics of Australia. *Journal of Tropical Forest Science* 26**,** 543-553.

Bruijnzeel, L.A., Kappelle, M., Mulligan, M., and Scatena, F.N. (2011). "Tropical montane cloud forests: state of knowledge and sustainability perspectives in a changing world," in *Tropical Montane Cloud Forests: Science for Conservation and Management,* eds. F.N. Scatena, L.A. Bruijnzeel & L.S. Hamilton. (Cambridge: Cambridge University Press), 691-740.

Bryant, J.P., Chapin I., F.S., and Klein, D.R. (1983). Carbon-nutrient balance of boreal plants in relation to vertebrate herbivory. *Oikos***,** 357-368.

Bunyan, M., Bardhan, S., Singh, A., and Jose, S. (2015). Effect of topography on the distribution on the distribution of tropical montane forest fragments: a predictive modelling approach. *Journal of Tropical Forest Science* 27**,** 30-38.

Burke, K.D., Williams, J.W., Chandler, M.A., Haywood, A.M., Lunt, D.J., and Otto-Bliesner, B.L. (2018). Pliocene and Eocene provide best analogs for near-future climates. *Proceedings of the National Academy of Sciences* 115**,** 13288-13293.

Bush, A., Catullo, R.A., Mokany, K., Thornhill, A.H., Miller, J.T., Ferrier, S., and Grytnes, J.A. (2018). Truncation of thermal tolerance niches among Australian plants. *Global Ecology and Biogeography* 27**,** 22-31.

Cavaleri, M.A., Reed, S.C., Smith, W.K., and Wood, T.E. (2015). Urgent need for warming experiments in tropical forests. *Global Change Biology* 21**,** 2111-2121.

Cavelier, J., Tanner, E., and Santamaría, J. (2000). Effect of water, temperature and fertilizers on soil nitrogen net transformations and tree growth in an elfin cloud forest of Colombia. *Journal of Tropical Ecology* 16**,** 83-99.

Cernusak, L.A., Ubierna, N., Winter, K., Holtum, J.A.M., Marshall, J.D., and Farquhar, G.D. (2013). Environmental and physiological determinants of carbon isotope discrimination in terrestrial plants. *New Phytologist* 200**,** 950-965.

Cheesman, A.W., and Winter, K. (2013). Growth response and acclimation of CO_2 exchange characteristics to elevated temperatures in tropical tree seedlings. *Journal of Experimental Botany* 64**,** 3817-3828.

Chen, L., Niu, K., Wu, Y., Geng, Y., Mi, Z., Flynn, D.F., and He, J.-S. (2013). UV radiation is the primary factor driving the variation in leaf phenolics across Chinese grasslands. *Ecology and Evolution* 3**,** 4696-4710.

Close, D.C., and Mcarthur, C. (2002). Rethinking the role of many plant phenolics: protection from photodamage not herbivores? *Oikos* 99**,** 166-172.

Coley, P., Massa, M., Lovelock, C., and Winter, K. (2002). Effects of elevated CO_2 on foliar chemistry of saplings of nine species of tropical tree. *Oecologia* 133**,** 62-69.

Coley, P.D., and Barone, J.A. (1996). Herbivory and plant defenses in tropical forests. *Annual Review of Ecology and Systematics* 27**,** 305-335.

Coley, P.D., Bryant, J.P., and Chapin, F.S., 3rd (1985). Resource availability and plant antiherbivore defense. *Science* 230**,** 895-899.

Colwell, R.K., Brehm, G., Cardelus, C.L., Gilman, A.C., and Longino, J.T. (2008). Global warming, elevational range shifts, and lowland biotic attrition in the wet tropics. *Science* 322**,** 258-261.

Condit, R., Engelbrecht, B.M.J., Pino, D., Pérez, R., and Turner, B.L. (2013). Species distributions in response to individual soil nutrients and seasonal drought across a community of tropical trees. *Proceedings of the National Academy of Sciences* 110**,** 5064-5068.

Cork, S.J., and Krockenberger, A.K. (1991). Methods and pitfalls of extracting condensed tannins and other phenolics from plants: Insights from investigations on *Eucalyptus* leaves. *Journal of Chemical Ecology* 17**,** 123-134.

Costion, C.M., Simpson, L., Pert, P.L., Carlsen, M.M., John Kress, W., and Crayn, D. (2015). Will tropical mountaintop plant species survive climate change? Identifying key knowledge gaps using species distribution modelling in Australia. *Biological Conservation* 191**,** 322-330.

Crafts-Brandner, S. J., and Salvucci, M. E. (2000). Rubisco activase constrains the photosynthetic potential of leaves at high temperature and CO_2. *Proceedings of the National Academy of Sciences*, 97(24), 13430-13435.

Craine, J.M., Brookshire, E.N.J., Cramer, M.D., Hasselquist, N.J., Koba, K., Marin-Spiotta, E., and Wang, L. (2015). Ecological interpretations of nitrogen isotope ratios of terrestrial plants and soils. *Plant and Soil* 396**,** 1-26.

Crayn, D.M., Costion, C., and Harrington, M.G. (2015). The Sahul–Sunda floristic exchange: dated molecular phylogenies document Cenozoic intercontinental dispersal dynamics. *Journal of Biogeography* 42**,** 11-24.

Crous, K.Y., Drake, J.E., Aspinwall, M.J., Sharwood, R.E., Tjoelker, M.G., and Ghannoum, O. (2018). Photosynthetic capacity and leaf nitrogen decline along a controlled climate gradient in provenances of two widely distributed Eucalyptus species. *Global Change Biology* 24**,** 4626-4644.

Crous, K.Y., Uddling, J., and De Kauwe, M.G. (2022). Temperature responses of photosynthesis and respiration in evergreen trees from boreal to tropical latitudes. *New Phytologist* 234**,** 353-374.

Curtin, D., Campbell, C.A., and Jalil, A. (1998). Effects of acidity on mineralization: pH- dependence of organic matter mineralization in weakly acidic soils. *Soil Biology and Biochemistry* 30**,** 57-64.

Dai, L., Fu, R., Guo, X., Du, Y., Zhang, F., and Cao, G. (2022). Soil moisture variations in response to precipitation across different vegetation types on the northeastern Qinghai- Tibet plateau. *Frontiers in Plant Science* 13.

Doughty, C.E., and Goulden, M.L. (2008). Are tropical forests near a high temperature threshold? *Journal of Geophysical Research: Biogeosciences* 113**,** G00B07.

Dusenge, M.E., Wittemann, M., Mujawamariya, M., Ntawuhiganayo, E.B., Zibera, E., Ntirugulirwa, B., Way, D.A., Nsabimana, D., Uddling, J., and Wallin, G. (2021). Limited thermal acclimation of photosynthesis in tropical montane tree species. *Global Change Biology* 27**,** 4860-4878.

Duursma, R.A. (2015). Plantecophys- an R package for analysing and modelling leaf gas exchange data. *PLoS ONE* 10**,** e0143346.

Elsen, P.R., and Tingley, M.W. (2015). Global mountain topography and the fate of montane species under climate change. *Nature Climate Change* 5**,** 772.

Ensslin, A., Mollel, N.P., Hemp, A., Fischer, M., and Laliberté, E. (2018). Elevational transplantation suggests different responses of African submontane and savanna plants to climate warming. *Journal of Ecology* 106**,** 296-305.

Evans, J.R. (1989). Photosynthesis and nitrogen relationships in leaves of C_3 plants. *Oecologia* 78**,** 9-19.

Evans, J.R., and von Caemmerer, S. (1996). Carbon dioxide diffusion inside leaves. *Plant Physiology* 110**,** 339-346.

Evans, T.G., Diamond, S.E., and Kelly, M.W. (2015). Mechanistic species distribution modelling as a link between physiology and conservation. *Conservation Physiology* 3**,** cov056.

Ewers, R.M., and Banks-Leite, C. (2013). Fragmentation impairs the microclimate buffering effect of tropical forests. *PLoS ONE* 8**,** e58093.

Fahey, T.J., Sherman, R.E., and Tanner, E.V.J. (2016). Tropical montane cloud forest: environmental drivers of vegetation structure and ecosystem function. *Journal of Tropical Ecology* 32**,** 355-367.

Farouki, O.T. (1981). "Thermal properties of soils series on rock and soil mechanics". (Trans. Tech. Pub.: Cold Regions Research and Engineering Lab Hanover, NH).

Farquhar, G., and Wong, S. (1984). An empirical model of stomatal conductance. *Functional Plant Biology* 11**,** 191-210.

Farquhar, G.D., Von Caemmerer, S., and Berry, J.A. (1980). A biochemical model of photosynthetic CO_2 assimilation in leaves of C_3 species. *Planta* 149**,** 78-90.

Fick, S.E., and Hijmans, R.J. (2017). WorldClim 2: new 1-km spatial resolution climate surfaces for global land areas. *International Journal of Climatology* 37**,** 4302-4315.

Freeman, B.G., Lee-Yaw, J.A., Sunday, J.M., and Hargreaves, A.L. (2018). Expanding, shifting and shrinking: The impact of global warming on species' elevational distributions. *Global Ecology and Biogeography* 27, 1268-1276.

Frenne, P., Zellweger, F., Rodríguez-Sánchez, F., Scheffers, B., Hylander, K., Luoto, M., Vellend, M., Verheyen, K., and Lenoir, J. (2019). Global buffering of temperatures under forest canopies. *Nature Ecology & Evolution* 3**,** 744-749.

Gao, J.M., Zhang, Y., Yu, G.R., Song, Q., Yang, Z., Sun, X., and Zhao, S.J. (2008). Characteristics of soil temperature in tropical seasonal rain forest in Xishuangbanna, southwest China. *Chinese Journal of Ecology* 27**,** 880-887.

Gardner, A.S., Maclean, I.M.D., and Gaston, K.J. (2019). Climatic predictors of species distributions neglect biophysiologically meaningful variables. *Diversity and Distributions* 25**,** 1318-1333.

Girardin, C.A.J., Malhi, Y., Aragao, L.E.O.C., Mamani, M., Huasco, W.H., Durand, L., Feeley, K.J., Rapp, J., Silva-Espejo, J.E., Silman, M., Salinas, N., and Whittaker, R.J. (2010). Net primary productivity allocation and cycling of carbon along a tropical forest elevational transect in the Peruvian Andes. *Global Change Biology* 16**,** 3176-3192.

Robinson, D. (2001). d15N as an integrator of the nitrogen cycle. *Trends in Ecology & Evolution* 16(3): 153-162.

Gleason, S.M., Read, J., Ares, A., and Metcalfe, D.J. (2010). Species-soil associations, disturbance, and nutrient cycling in an Australian tropical rainforest. *Oecologia* 162**,** 1047-1058.

Gonçalves, J.F., Júnior, U., and Silva, E. (2008). Evaluation of a portable chlorophyll meter to estimate chlorophyll concentrations in leaves of tropical wood species from Amazonian Forest. *Hoehnea* 35**,** 185-188.

Gong, H., Li, Y., Yu, T., Zhang, S., Gao, J., Zhang, S., and Sun, D. (2020). Soil and climate effects on leaf nitrogen and phosphorus stoichiometry along elevational gradients. *Global Ecology and Conservation* 23**,** e01138.

Goudberg, N.J. (1990). *The feeding ecology of three species of north Queensland upland rainforest ringtail possums, Hemibelideus lemuroides, Pseudocheirus herbertensis and Pseudocheirus archeri (Marsupialia: Petauridae).* James Cook University.

Goulden, M. L., Miller, S. D., da Rocha, H. R., Mary C. Menton, de Freitas, H. C., Adelaine Michelae Silva Figueira, & Cleilim Albert Dias de Sousa. (2004). Diel and seasonal patterns of tropical forest CO_2 exchange. *Ecological Applications*, *14*(4), S42–S54. http://www.jstor.org/stable/4493629

Grossiord, C., Buckley, T.N., Cernusak, L.A., Novick, K.A., Poulter, B., Siegwolf, R.T.W., Sperry, J.S., and Mcdowell, N.G. (2020). Plant responses to rising vapor pressure deficit. *New Phytologist* 226**,** 1550-1566.

Hamilton, J.G., Zangerl, A.R., Delucia, E.H., and Berenbaum, M.R. (2001). The carbon–nutrient balance hypothesis: its rise and fall. *Ecology Letters* 4**,** 86-95.

Hamilton, L.S., Juvik, J.O., and Scatena, F.N. (2012). *Tropical Montane Cloud Forests.* Springer Science & Business Media.

Haskell, D., Flaspohler, D., Webster, C., and Meyer, M. (2010). Variation in soil temperature, moisture, and plant growth with the addition of downed woody material on lakeshore restoration sites. *Restoration Ecology* 20**,** 113-121.

He, X., Hou, E., Liu, Y., and Wen, D. (2016). Altitudinal patterns and controls of plant and soil nutrient concentrations and stoichiometry in subtropical China. *Scientific Reports* 6**,** 24261.

Herwitz, S.R. (1986). Episodic stemflow inputs of magnesium and potassium to a tropical forest floor during heavy rainfall events. *Oecologia* 70**,** 423-425.

Herwitz, S.R. (1991). Aboveground adventitious roots and stemflow chemistry of *Ceratopetalum virchowii* in an Australian montane tropical rain forest. *Biotropica* 23**,** 210-218.

Hestrin, R., Hammer, E.C., Mueller, C.W., and Lehmann, J. (2019). Synergies between mycorrhizal fungi and soil microbial communities increase plant nitrogen acquisition. *Communications Biology* 2**,** 233.

Hikosaka, K., Ishikawa, K., Borjigidai, A., Muller, O., and Onoda, Y. (2005). Temperature acclimation of photosynthesis: mechanisms involved in the changes in temperature dependence of photosynthetic rate. *Journal of Experimental Botany* 57**,** 291-302.

Ho, L.T., Schneider, R., and Thomas, F.M. (2019). Growth of the tropical *Pinus kesiya* as influenced by climate and nutrient availability along an elevational gradient. *Journal of Plant Ecology* 13**,** 97-106.

Holopainen, J.K., Virjamo, V., Ghimire, R.P., Blande, J.D., Julkunen-Tiitto, R., and Kivimäenpää, M. (2018). Climate change effects on secondary compounds of forest trees in the northern hemisphere. *Frontiers in Plant Science* 9:1445.

Houlton, B.Z., Sigman, D.M., and Hedin, L.O. (2006). Isotopic evidence for large gaseous nitrogen losses from tropical rainforests. *Proceedings of the National Academy of Sciences* 103**,** 8745-8750.

Huber, M., and Caballero, R. (2011). The early Eocene equable climate problem revisited. *Clim. Past* 7**,** 603-633.

Hursh, A., Ballantyne, A., Cooper, L., Maneta, M., Kimball, J., and Watts, J. (2017). The sensitivity of soil respiration to soil temperature, moisture, and carbon supply at the global scale. *Global Change Biology* 23**,** 2090-2103.

Jackson, L.S., and Forster, P.M. (2010). An empirical study of geographic and seasonal variations in diurnal temperature range. *Journal of Climate* 23**,** 3205-3221.

Jaganathan GK and Biddick M (2021) Experimental warming hastens physical dormancy break and germination in tropical Fabaceae. *Front. Plant Sci*. 12:782706. doi: 10.3389/fpls.2021.782706

Jang, Y.S., Shen, S.F., Juang, J.Y., Huang, C.Y., and Lo, M.H. (2022). Discontinuity of diurnal temperature range along elevated regions. *Geophysical Research Letters* 49**,** e2021GL097551.

Jaramillo, C., Ochoa, D., Contreras, L., Pagani, M., Carvajal-Ortiz, H., Pratt, L.M., Krishnan, S., Cardona, A., Romero, M., and Quiroz, L. (2010). Effects of rapid global warming at the Paleocene-Eocene boundary on neotropical vegetation. *Science* 330**,** 957-961.

Jarvis, A., and Mulligan, M. (2011). The climate of cloud forests. *Hydrological Processes* 25**,** 327-343.

Jiang, Y., Zang, R., Lu, X., Huang, Y., Ding, Y., Liu, W., Long, W., Zhang, J., and Zhang, Z. (2015). Effects of soil and microclimatic conditions on the community-level plant functional traits across different tropical forest types. *Plant and Soil* 390**,** 351-367.

Jones, C. G., & Hartley, S. E. (1999). A protein competition model of phenolic allocation. *Oikos*, *86*(1), 27-44.

Jones, H. (2013). *Plants and Microclimate: A quantitative approach to environmental plant physiology* (3rd ed.). Cambridge: Cambridge University Press. doi:10.1017/CBO9780511845727

Joyce, E.M., Thiele, K.R., Slik, F.J.W., and Crayn, D.M. (2020). Checklist of the vascular flora of the Sunda-Sahul Convergence Zone. *Biodivers Data J* 8**,** e51094.

Karabourniotis, G., Liakopoulos, G., Nikolopoulos, D., Bresta, P., Stavroulaki, V., and Sumbele, S. (2014). "Carbon gain vs. water saving, growth vs. defence": two dilemmas with soluble phenolics as a joker. *Plant Science* 227**,** 21-27.

Kassambara, A., and Mundt, F. (2017). Package 'factoextra' in R. Extract and visualize the results of multivariate data analyses. 76, 2.

Kauffman, S., Sombroek, W., and Mantel, S. (1998). "Soils of rainforests characterization and major constraints of dominant forest soils in the humid tropics". In: Schulte, A., Ruhiyat, D. (eds) *Soils of Tropical Forest Ecosystems*. Springer Berlin Heidelberg, 9-20.

Kearney, M.R. (2018). MicroclimOz – A microclimate data set for Australia, with example applications. *Austral Ecology* 44**,** 533-534.

Kiese, R., & Butterbach-Bahl, K. (2002). N_2O and CO_2 emissions from three different tropical forest sites in the wet tropics of Queensland, Australia. *Soil Biology and Biochemistry*, *34*(7), 975-987.

Körner, C. (2003). "Plant ecology at high elevations". In: *Alpine Plant Life: Functional Plant Ecology of High Mountain Ecosystems*. (Springer Berlin Heidelberg), 1-7.

Körner, C. (2007). The use of 'altitude' in ecological research. *Trends in Ecology & Evolution* 22**,** 569-574.

Körner, C., and Paulsen, J. (2004). A world-wide study of high-altitude treeline temperatures. *Journal of Biogeography* 31**,** 713-732.

Kuznetsova, A., Brockhoff, P.B., and Christensen, R.H. (2017). lmerTest package: tests in linear mixed effects models. *Journal of Statistical Software* 82**,** 1-26.

Laurance, W.F., Carolina Useche, D., Shoo, L.P., Herzog, S.K., Kessler, M., Escobar, F., Brehm, G., Axmacher, J.C., Chen, I.C., Gámez, L.A., Hietz, P., Fiedler, K., Pyrcz, T., Wolf, J., Merkord, C.L., Cardelus, C., Marshall, A.R., Ah-Peng, C., Aplet, G.H., Del Coro Arizmendi, M., Baker, W.J., Barone, J., Brühl, C.A., Bussmann, R.W., Cicuzza, D., Eilu, G., Favila, M.E., Hemp, A., Hemp, C., Homeier, J., Hurtado, J., Jankowski, J., Kattán, G., Kluge, J., Krömer, T., Lees, D.C., Lehnert, M., Longino, J.T., Lovett, J., Martin, P.H., Patterson, B.D., Pearson, R.G., Peh, K.S.H., Richardson, B., Richardson, M., Samways, M.J., Senbeta, F., Smith, T.B., Utteridge, T.M.A., Watkins, J.E., Wilson, R., Williams, S.E., and Thomas, C.D. (2011). Global warming, elevational ranges, and the vulnerability of tropical biota. *Biological Conservation* 144**,** 548-557.

Leahy, L., Scheffers, B.R., Andersen, A.N., Hirsch, B.T., and Williams, S.E. (2021). Vertical niche

and elevation range size in tropical ants: implications for climate resilience. *Diversity and Distributions* 27**,** 485-496.

Lembrechts, J., Nijs, I., and Lenoir, J. (2018). Incorporating microclimate into species distribution models. *Ecography* 42**,** 1267-1279.Lembrechts, J.J., Van Den Hoogen, J., Aalto, J., Ashcroft, M.B., De Frenne, P., Kemppinen, J., Kopecký, M., Luoto, M., Maclean, I.M.D., Crowther, T.W., Bailey, J.J., Haesen, S., Klinges, D.H., Niittynen, P., Scheffers, B.R., Van Meerbeek, K., Aartsma, P., Abdalaze, O., Abedi, M., Aerts, R., Ahmadian, N., Ahrends, A., Alatalo, J.M., Alexander, J.M., Allonsius, C.N., Altman, J., Ammann, C., Andres, C., Andrews, C., Ardö, J., Arriga, N., Arzac, A., Aschero, V., Assis, R.L., Assmann, J.J., Bader, M.Y., Bahalkeh, K., Barančok, P., Barrio, I.C., Barros, A., Barthel, M., Basham, E.W., Bauters, M., Bazzichetto, M., Marchesini, L.B., Bell, M.C., Benavides, J.C., Benito Alonso, J.L., Berauer, B.J., Bjerke, J.W., Björk, R.G., Björkman, M.P., Björnsdóttir, K., Blonder, B., Boeckx, P., Boike, J., Bokhorst, S., Brum, B.N.S., Brůna, J., Buchmann, N., Buysse, P., Camargo, J.L., Campoe, O.C., Candan, O., Canessa, R., Cannone, N., Carbognani, M., Carnicer, J., Casanova-Katny, A., Cesarz, S., Chojnicki, B., Choler, P., Chown, S.L., Cifuentes, E.F., Čiliak, M., Contador, T., Convey, P., Cooper, E.J., Cremonese, E., Curasi, S.R., Curtis, R., Cutini, M., Dahlberg, C.J., Daskalova, G.N., De Pablo, M.A., Della Chiesa, S., Dengler, J., Deronde, B., Descombes, P., Di Cecco, V., Di Musciano, M., Dick, J., Dimarco, R.D., Dolezal, J., Dorrepaal, E., Dušek, J., Eisenhauer, N.,Eklundh, L., Erickson, T.E., Erschbamer, B., et al. (2021). Global maps of soil temperature.

Global Change Biology 28**,** 3110-3144.

Li, R., Zhao, L., Wu, T., Wang, Q., Ding, Y., Yao, J., Wu, X., Hu, G., Xiao, Y., Du, Y., Zhu, X., Qin, Y., Yang, S., Bai, R., Du, E., Liu, G., Zou, D., Qiao, Y., and Shi, J. (2019). Soil thermal conductivity and its influencing factors at the Tanggula permafrost region on the Qinghai– Tibet Plateau. *Agricultural and Forest Meteorology* 264**,** 235-246.

Lima-Melo, Y., Alencar, V.T., Lobo, A.K., Sousa, R.H., Tikkanen, M., Aro, E.-M., Silveira, J.A., and Gollan, P.J. (2019). Photoinhibition of photosystem I provides oxidative protection during imbalanced photosynthetic electron transport in *Arabidopsis thaliana*. *Frontiers in Plant Science* 10**,** 916.

Liu, X., Zhao, L., Gasaw, M., Gao, D., Qin, D., and Ren, J. (2007). Foliar $\delta^{13}C$ and $\delta^{15}N$ values of C_3 plants in the Ethiopia Rift Valley and their environmental controls. *Chinese Science Bulletin* 52**,** 1265-1273.

Liu, X., and Luo, T. (2011). Spatiotemporal variability of soil temperature and moisture across two contrasting timberline ecotones in the Sergyemla mountains, southeast Tibet. *Arctic, Antarctic, and Alpine Research* 43**,** 229-238.

Lüdecke, D., Ben-Shachar, M.S., Patil, I., Waggoner, P., and Makowski, D. (2021). performance: An R package for assessment, comparison and testing of statistical models. *Journal of Open Source Software* 6.

Liyanage, G., Offord, C., Crayn, D., Guja, L., Worboys, S., and Sommerville, K. (2022). Understanding seed dormancy and germination aids conservation of rainforest species from tropical montane cloud forest: A case study confirming morphophysiological dormancy in the genus Tasmannia. *Aust. J. Bot.* 70, 399–408. doi: 10.1071/BT22011

Ma, J.-Y., Sun, W., Liu, X.-N., and Chen, F.-H. (2012). Variation in the stable carbon and nitrogen isotope composition of plants and soil along a precipitation gradient in northern China. *PLoS ONE* 7**,** e51894.

Maire, V., Martre, P., Kattge, J., Gastal, F., Esser, G., Fontaine, S., and Soussana, J.-F. (2012). The Coordination of leaf photosynthesis links C and N Fluxes in C_3 plant species. *PLoS ONE* 7**,** e38345.

Malhi, Y. (2012). "Extinction Risk from Climate Change in Tropical Forests," in *Saving a Million Species: Extinction Risk from Climate Change,* ed. L. Hannah. (Washington, DC: Island Press/Center for Resource Economics), 239-259.

Malhi, Y., and Grace, J. (2000). Tropical forests and atmospheric carbon dioxide. *Trends in Ecology & Evolution* 15**,** 332-337.

Malhi, Y., Silman, M., Salinas, N., Bush, M., Meir, P., and Saatchi, S. (2010). Introduction: elevation gradients in the tropics: laboratories for ecosystem ecology and global change research. *Global Change Biology* 16**,** 3171-3175.

Malizia, A., Blundo, C., Carilla, J., Osinaga Acosta, O., Cuesta, F., Duque, A., Aguirre, N., Aguirre, Z., Ataroff, M., Baez, S., Calderón-Loor, M., Cayola, L., Cayuela, L., Ceballos, S., Cedillo, H., Farfán Ríos, W., Feeley, K.J., Fuentes, A.F., Gámez Álvarez, L.E., Grau, R., Homeier, J., Jadan, O., Llambi, L.D., Loza Rivera, M.I., Macía, M.J., Malhi, Y., Malizia, L., Peralvo, M., Pinto, E., Tello, S., Silman, M., and Young, K.R. (2020). Elevation and latitude drives structure and tree species composition in Andean forests: Results from a large-scale plot network. *PLoS ONE* 15**,** e0231553.

Martinelli, L.A., Piccolo, M.C., Townsend, A.R., Vitousek, P.M., Cuevas, E., McDowell, W., Robertson, G.P., Santos, O.C., and Treseder, K. (1999). Nitrogen stable isotopic composition of leaves and soil: tropical versus temperate forests. *Biogeochemistry* 46**,** 45-65.

McInnes, K., Abbs, D., Jonas, B., Chiew, F., Church, J., Ekström, M., Kirono, D., Lenton, A., Lucas, C., Moise, A., Monselesan, D., Mpelasoka, F., Leanne, W., and Penny, W. (2015). "Climate Change in Australia Projections for Australia's Natural Resource Management Regions: Cluster Reports", (eds.) M. Ekström, P. Whetton, C. Gerbing, M. Grose, L. Webb & J. Risbey. CSIRO).

McJannet, D., Wallace, J., Fitch, P., Disher, M., and Reddell, P. (2006). *Water balance measurements in Australia's Wet Tropics: sites, methods and results.* CSIRO Land and Water, Canberra.

McJannet, D., Wallace, J., and Reddell, P. (2007). Precipitation interception in Australian tropical rainforests: II. Altitudinal gradients of cloud interception, stemflow, throughfall and

interception. *Hydrological Processes* 21**,** 1703-1718.

Medlyn, B., Dreyer, E., Ellsworth, D., Forstreuter, M., Harley, P., Kirschbaum, M., Le Roux, X., Montpied, P., Strassemeyer, J., and Walcroft, A. (2002). Temperature response of parameters of a biochemically based model of photosynthesis. II. A review of experimental data. *Plant, Cell & Environment* 25**,** 1167-1179.

Mercado, L.M., Medlyn, B.E., Huntingford, C., Oliver, R.J., Clark, D.B., Sitch, S., Zelazowski, P., Kattge, J., Harper, A.B., and Cox, P.M. (2018). Large sensitivity in land carbon storage due to geographical and temporal variation in the thermal response of photosynthetic capacity. *New Phytologist* 218**,** 1462-1477.

Metcalfe, D.J.F., A. J. (2009). "Floristics and plant biodiversity of the rainforests of the wet tropics," in *Living in a Dynamic Tropical Forest Landscape*. eds N.E. Stork and S.M. Turton.

Misra, V. (2020). "Chapter 2 - Land–atmosphere interactions," in *Regionalizing Global Climate Variations,* ed. V. Misra. Elsevier, 17-46.

Moore, B.D., Wallis, I.R., Marsh, K.J., and Foley, W.J. (2004). "The role of nutrition in the conservation of the marsupial folivores of eucalypt forests", in in *Conservation of Australia's Forest Fauna,* (eds.) D. Lunney. Royal Zoological Society of New South Wales.

Moreira, X., Abdala-Roberts, L., Hidalgo-Galvez, M.D., Vázquez-González, C., and Pérez- Ramos, I.M. (2020). Micro-climatic effects on plant phenolics at the community level in a Mediterranean savanna. *Scientific Reports* 10**,** 14757.

Noce, S., Caporaso, L., and Santini, M. (2020). A new global dataset of bioclimatic indicators. *Scientific Data* 7**,** 398.

Nottingham, A.T., Whitaker, J., Turner, B.L., Salinas, N., Zimmermann, M., Malhi, Y., and Meir, P. (2015). Climate warming and soil carbon in tropical forests: insights from an elevation gradient in the Peruvian Andes. *Bioscience* 65**,** 906-921.

Oliveira, R.S., Eller, C.B., Bittencourt, P.R.L., and Mulligan, M. (2014). The hydroclimatic and ecophysiological basis of cloud forest distributions under current and projected climates. *Annals of Botany* 113**,** 909-920.

Pajares, S., and Bohannan, B.J.M. (2016). Ecology of nitrogen fixing, nitrifying, and denitrifying microorganisms in tropical forest soils. *Frontiers in Microbiology* 7:1045

Panwar, A., Renner, M., and Kleidon, A. (2020). Imprints of evaporative conditions and vegetation type in diurnal temperature variations. *Hydrology and Earth System Sciences* 24**,** 4923-4942.

Parry, C., Blonquist Jr, J.M., and Bugbee, B. (2014). In situ measurement of leaf chlorophyll concentration: analysis of the optical/absolute relationship. *Plant, Cell & Environment* 37**,** 2508-2520.

Parsons, S.A., Congdon, R.A., Shoo, L.P., Valdez-Ramirez, V., and Williams, S.E. (2014a). Spatial variability in litterfall, litter standing crop and litter quality in a tropical rain forest region. *Biotropica* 46**,** 378-386.

Parsons, S.A., Valdez-Ramirez, V., Congdon, R.A., and Williams, S.E. (2014b). Contrasting patterns

of litterfall seasonality and seasonal changes in litter decomposability in a tropical rainforest region. *Biogeosciences* 11**,** 5047-5056.

Pfeifer, M., Gonsamo, A., Woodgate, W., Cayuela, L., Marshall, A.R., Ledo, A., Paine, T.C.E., Marchant, R., Burt, A., Calders, K., Courtney-Mustaphi, C., Cuni-Sanchez, A., Deere, N.J., Denu, D., De Tanago, J.G., Hayward, R., Lau, A., Macía, M.J., Olivier, P.I., Pellikka, P., Seki, H., Shirima, D., Trevithick, R., Wedeux, B., Wheeler, C., Munishi, P.K.T., Martin, T., Mustari, A., and Platts, P.J. (2018). Tropical forest canopies and their relationships with climate and disturbance: results from a global dataset of consistent field-based measurements. *Forest Ecosystems* 5**,** 7.

Piluzza, G., and Bullitta, S. (2011). Correlations between phenolic content and antioxidant properties in twenty-four plant species of traditional ethnoveterinary use in the Mediterranean area. *Pharmaceutical biology* 49**,** 240-247.

Prentice, I.C., Dong, N., Gleason, S.M., Maire, V., and Wright, I.J. (2014). Balancing the costs of carbon gain and water transport: testing a new theoretical framework for plant functional ecology. *Ecology Letters* 17**,** 82-91.

Rapp, J., Silman, M., Clark, J., Girardin, C., Galiano, D., and Tito, R. (2012). Intra- and interspecific tree growth across a long altitudinal gradient in the Peruvian Andes. *Ecology* 93**,** 2061-2072.

Rapp, J.M. (2010). *Climate control on plant performance across an Andean altitudinal gradient.* Wake Forest University.

Ratier Backes, A., Frey, L., Arévalo, J.R., and Haider, S. (2021). Effects of soil properties, temperature and disturbance on diversity and functional composition of plant communities along a steep elevational gradient on Tenerife. *Frontiers in Ecology and Evolution* 9:758160

Rehm, E.M., and Feeley, K.J. (2015). The inability of tropical cloud forest species to invade grasslands above treeline during climate change: potential explanations and consequences. *Ecography* 38**,** 1167-1175.

Ritmejerytė, E., Boughton, B.A., Bayly, M.J., and Miller, R.E. (2019). Divergent responses of above- and below-ground chemical defence to nitrogen and phosphorus supply in waratahs (*Telopea speciosissima*). *Functional Plant Biology* 46**,** 1134-1145.

Roeble, E.E. (2018). *Modelling the vulnerability of endemic montane flora to climate change in the Australian Wet Tropics.* Master of Science, Masters thesis, Imperial College London.

Ross, S. M. (1993). Organic matter in tropical soils: current conditions, concerns and prospects for conservation. Progress in Physical Geography: Earth and Environment, 17(3), 265–305. https://doi.org/10.1177/030913339301700301

Saatchi, S.S., Harris, N.L., Brown, S., Lefsky, M., Mitchard, E.T., Salas, W., Zutta, B.R., Buermann, W., Lewis, S.L., and Hagen, S. (2011). Benchmark map of forest carbon stocks in tropical regions across three continents. *Proceedings of the National Academy of Sciences* 108**,** 9899-9904.

Sage, R.F., and Kubien, D.S. (2007). The temperature response of C_3 and C_4 photosynthesis.

Plant, Cell & Environment 30**,** 1086-1106.

Sah, S., and Brumme, R. (2003). Altitudinal gradients of natural abundance of stable isotopes of nitrogen and carbon in the needles and soil of a pine forest in Nepal. *Journal of Forest Science* 49, 19-26.

Salazar, D., Lokvam, J., Mesones, I., Vásquez Pilco, M., Ayarza Zuñiga, J.M., De Valpine, P., and Fine, P.V.A. (2018). Origin and maintenance of chemical diversity in a species- rich tropical tree lineage. *Nature Ecology & Evolution* 2**,** 983-990.

Salinas, N., Malhi, Y., Meir, P., Silman, M., Roman Cuesta, R., Huaman, J., Salinas, D., Huaman, V., Gibaja, A., Mamani, M., and Farfan, F. (2011). The sensitivity of tropical leaf litter decomposition to temperature: results from a large-scale leaf translocation experiment along an elevation gradient in Peruvian forests. *New Phytologist* 189**,** 967- 977.

Schemske, D.W., Mittelbach, G.G., Cornell, H.V., Sobel, J.M., and Roy, K. (2009). Is there a latitudinal gradient in the importance of biotic interactions? *Annual Review of Ecology, Evolution, and Systematics* 40**,** 245-269.

Schjønning, P. (2021). Thermal conductivity of undisturbed soil – measurements and predictions. *Geoderma* 402**,** 115188.

Schmitt, C.B., Senbeta, F., Woldemariam, T., Rudner, M., and Denich, M. (2013). Importance of regional climates for plant species distribution patterns in moist Afromontane forest. *Journal of Vegetation Science* 24**,** 553-568.

Schneider, G.F., Coley, P.D., Younkin, G.C., Forrister, D.L., Mills, A.G., and Kursar, T.A. (2019). Phenolics lie at the centre of functional versatility in the responses of two phytochemically diverse tropical trees to canopy thinning. *Journal of Experimental Botany* 70**,** 5853-5864.

Schulte, E.E., and Hopkins, B.G. (1996). "Estimation of soil organic matter by weight loss-on-ignition," in *Soil Organic Matter: Analysis and Interpretation*.), 21-31.

Schuur, E.A., and Matson, P.A. (2001). Net primary productivity and nutrient cycling across a mesic to wet precipitation gradient in Hawaiian montane forest. *Oecologia* 128**,** 431- 442.

Shamloo, M., Babawale, E.A., Furtado, A., Henry, R.J., Eck, P.K., and Jones, P.J.H. (2017). Effects of genotype and temperature on accumulation of plant secondary metabolites in Canadian and Australian wheat grown under controlled environments. *Scientific reports* 7**,** 9133-9133.

Sharkey, T.D. (2005). Effects of moderate heat stress on photosynthesis: importance of thylakoid reactions, rubisco deactivation, reactive oxygen species, and thermotolerance provided by isoprene. *Plant, Cell & Environment* 28**,** 269-277.

Sharkey, T.D., Bernacchi, C.J., Farquhar, G.D., and Singsaas, E.L. (2007). Fitting photosynthetic carbon dioxide response curves for C_3 leaves. *Plant, Cell & Environment* 30**,** 1035-1040.

Sharwood, R.E., Crous, K.Y., Whitney, S.M., Ellsworth, D.S., and Ghannoum, O. (2017). Linking photosynthesis and leaf N allocation under future elevated CO_2 and climate warming in *Eucalyptus globulus*. *Journal of Experimental Botany* 68**,** 1157-1167.

Shoo, L.P., Williams, S.E., and Hero, J.-M. (2005). Climate warming and the rainforest birds of the Australian Wet Tropics: Using abundance data as a sensitive predictor of change in total population size. *Biological Conservation* 125**,** 335-343.

Singh Ramesh, A., Cheesman, A.W., and Cernusak, L.A. (2022). "Far North Queensland microclimate data". 1.0.0 ed. (https://portal.tern.org.au/far-north-queensland-microclimate/23482: Terrestrial Ecosystem Research Network).

Singh Ramesh, A., Cheesman, A.W., Flores-Moreno, H., Preece, N.D., Crayn, D.M., and Cernusak, L.A. (2023). Temperature, nutrient availability, and species traits interact to shape elevation responses of Australian tropical trees. *Frontiers in Forests and Global Change* 6**,** 2.

Singh, R.K., and Sharma, R.V. (2017). Numerical analysis for ground temperature variation. *Geothermal Energy* 5**,** 22.

Slot, M., and Winter, K. (2016). "The Effects of Rising Temperature on the Ecophysiology of Tropical Forest Trees.", 385-412.

Slot, M., Winter, K., and Paine, C.E.T. (2018). High tolerance of tropical sapling growth and gas exchange to moderate warming. *Functional Ecology* 32**,** 599-611.

Soethe, N., Lehmann, J., and Engels, C. (2008). Nutrient availability at different altitudes in a tropical montane forest in Ecuador. *Journal of Tropical Ecology* 24**,** 397-406.

Strong, C., Boulter, S., Laidlaw, M., Maunsell, S., Putland, D., and Kitching, R. (2011). The physical environment of an altitudinal gradient in the rainforest of Lamington National Park, southeast Queensland. *Memoirs of the Queensland Museum - Nature* 55**,** 251-270.

Sumbele, S., Fotelli, M.N., Nikolopoulos, D., Tooulakou, G., Liakoura, V., Liakopoulos, G., Bresta, P., Dotsika, E., Adams, M.A., and Karabourniotis, G. (2012). Photosynthetic capacity is negatively correlated with the concentration of leaf phenolic compounds across a range of different species. *AoB Plants* 2012: pls025.

Tanner, E.V.J., Vitousek, P.M., and Cuevas, E. (1998). Experimental investigation of nutrient limitation of forest growth on wet tropical mountains. *Ecology* 79**,** 10-22.

Team, R.C. (2021). "R: a language and environment for statistical computing. R Foundation for Statistical Computing. Published 2018".

Thornhill, A.H., Mishler, B.D., Knerr, N.J., González-Orozco, C.E., Costion, C.M., Crayn, D.M., Laffan, S.W., and Miller, J.T. (2016). Continental-scale spatial phylogenetics of Australian angiosperms provides insights into ecology, evolution, and conservation. *Journal of Biogeography* 43**,** 2085-2098.

Tito, R., Vasconcelos, H.L., and Feeley, K.J. (2020). Mountain ecosystems as natural laboratories for climate change experiments. *Frontiers in Forests and Global Change* 3, 38.

Torello Raventos, M. (2014). *Environmental controls on wood density in tropical forests.* PhD thesis, James Cook University.

Unger, M., Homeier, J., and Leuschner, C. (2013). Relationships among leaf area index, below-canopy

light availability and tree diversity along a transect from tropical lowland to montane forests in NE Ecuador. *Tropical Ecology* 54**,** 33-45.

Usowicz, B., Łukowski, M., Marczewski, W., Usowicz, J.B., Lipiec, J., and Stankiewicz, K. (Year). "Thermal properties of peat, marshy and mineral soils in relation to soil moisture status in Polesie and Biebrza wetlands", in: *EGU General Assembly Conference Abstracts*, EGU2013-8534.

Vallejo-Vargas, A.F., Sheil, D., Semper-Pascual, A. *et al.* Consistent diel activity patterns of forest mammals among tropical regions. *Nat Commun* **13**, 7102 (2022). https://doi.org/10.1038/s41467-022-34825-1

Vargas, R. and Allen, M.F. (2008) Diel Patterns of Soil Respiration in a Tropical Forest after Hurricane Wilma. *Journal of Geophysical Research, 113,* G000620.

Vårhammar, A., Wallin, G., Mclean, C.M., Dusenge, M.E., Medlyn, B.E., Hasper, T.B., Nsabimana, D., and Uddling, J. (2015). Photosynthetic temperature responses of tree species in Rwanda: evidence of pronounced negative effects of high temperature in montane rainforest climax species. *New Phytologist* 206**,** 1000-1012.

Venter, M., Dwyer, J., Dieleman, W., Ramachandra, A., Gillieson, D., Laurance, S., Cernusak, L.A., Beehler, B., Jensen, R., and Bird, M.I. (2017). Optimal climate for large trees at high elevations drives patterns of biomass in remote forests of Papua New Guinea. *Global Change Biology* 23**,** 4873-4883.

Vitousek, P.M. (1984). Litterfall, nutrient cycling, and nutrient limitation in tropical forests. *Ecology* 65**,** 285-298.

Vitousek, P.M. (1998). The structure and functioning of montane tropical forests: control by climate, soils, and disturbance. *Ecology* 79**,** 1-2.

Vitousek, P.M., Gosz, J.R., Grier, C.C., Melillo, J.M., and Reiners, W.A. (1982). A comparative analysis of potential nitrification and nitrate mobility in forest ecosystems. *Ecological Monographs* 52**,** 155-177.

Walker, A.P., Beckerman, A.P., Gu, L., Kattge, J., Cernusak, L.A., Domingues, T.F., Scales, J.C., Wohlfahrt, G., Wullschleger, S.D., and Woodward, F.I. (2014). The relationship of leaf photosynthetic traits – Vcmax and Jmax – to leaf nitrogen, leaf phosphorus, and specific leaf area: a meta-analysis and modeling study. *Ecology and Evolution* 4**,** 3218- 3235.

Wallace, J., and McJannet, D. (2013). How might Australian rainforest cloud interception respond to climate change? *Journal of Hydrology* 481**,** 85-95.

Wang, D., He, N., Wang, Q., Lü, Y., Wang, Q., Xu, Z., and Zhu, J. (2016). Effects of temperature and moisture on soil organic matter decomposition along elevation gradients on the Changbai mountains, Northeast China. *Pedosphere* 26**,** 399-407.

Wang, H., Prentice, I.C., Davis, T.W., Keenan, T.F., Wright, I.J., and Peng, C. (2017). Photosynthetic responses to altitude: an explanation based on optimality principles. *New Phytologist* 213**,** 976-982.

Wang, X., Jiang, Y., Ren, H., Yu, F.-H., and Li, M.-H. (2019). Leaf and soil $\delta^{15}N$ patterns along elevational gradients at both treelines and shrublines in three different climate zones. *Forests* 10**,** 557.

Waterman, P.G. (1994). *Analysis of phenolic plant metabolites.* Oxford: Blackwell Scientific Publications.

Webb, L.J. (1959). A physiognomic classification of Australian rain forests. *Journal of Ecology* 47**,** 551-570.

Weber, E.T., Catterall, C.P., Locke, J., Ota, L.S., Prideaux, B., Shirreffs, L., Talbot, L., and Gordon, I.J. (2021). Managing a world heritage site in the face of climate change: a case study of the wet tropics in northern Queensland. *Earth* 2**,** 248-271.

Werner, F.A., and Homeier, J. (2015). Is tropical montane forest heterogeneity promoted by a resource-driven feedback cycle? evidence from nutrient relations, herbivory and litter decomposition along a topographical gradient. *Functional Ecology* 29**,** 430-440.

Wild, J., Kopecký, M., Macek, M., Šanda, M., Jankovec, J., and Haase, T. (2019). Climate at ecologically relevant scales: a new temperature and soil moisture logger for long-term microclimate measurement. *Agricultural and Forest Meteorology* 268**,** 40-47.

Williams, S., Falconi, L., Moritz, C., and Fenker Antunes, J. (2016). State of Wet Tropics Report 2015-2016: ancient, endemic, rare, and threatened vertebrates of the wet tropics.

Williams, S.E., Bolitho, E.E., and Fox, S. (2003). Climate change in Australian tropical rainforests: an impending environmental catastrophe. *Proceedings of the Royal Society B: Biological Sciences* 270**,** 1887-1892.

Wu, G., Johnson, S.K., Bornman, J.F., Bennett, S.J., Clarke, M.W., Singh, V., and Fang, Z. (2016). Growth temperature and genotype both play important roles in sorghum grain phenolic composition. *Scientific Reports* 6**,** 21835.

Wu, J., Hong, J., Wang, X., Sun, J., Lu, X., Fan, J., and Cai, Y. (2013). Biomass partitioning and its relationship with the environmental factors at the alpine steppe in northern Tibet. *PLoS ONE* 8**,** e81986.

Yap, J.Y.S., Rossetto, M., Costion, C., Crayn, D., Kooyman, R.M., Richardson, J., and Henry, R. (2018). Filters of floristic exchange: How traits and climate shape the rain forest invasion of Sahul from Sunda. *Journal of Biogeography* 45**,** 838-847.

Zimmermann, M., Davies, K., Zimmermann, V., and Bird, M. (2015). Impact of temperature and moisture on heterotrophic soil respiration along a moist tropical forest gradient in Australia. *Soil Research* 53**,** 286-297.